



Revolutionizing Turbine Cooling with Micro-Architectures Enabled by Direct Metal Laser Sintering

**The Ohio State University
Aerospace Research Center**

J.P. Bons, A. Ameri, J. Gregory,
A. Hossain, L. Agricola, E. Asar
(1 Nov 2017 – NETL UTSR Workshop)



Research Team

TEAM LEAD

Dr. Jeffrey Bons

Focus: Experimental
Fluid Mechanics and
Heat Transfer



Co-PI

Dr. Ali Ameri

Focus: Computational
Fluid Dynamics and
Heat Transfer



Co-PI

Dr. Jim Gregory

Focus: Experimental
Fluid Mechanics,
Fluidic Oscillator
Development



Arif Hossain

Graduate student



Lucas Agricola

Graduate student



Elif Asar

Graduate student



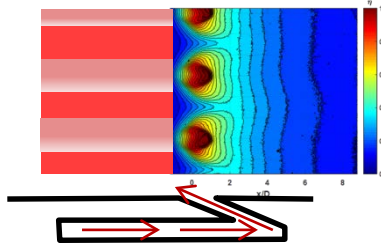
Objectives

- **Explore innovative cooling architectures** enabled by additive manufacturing techniques for improved cooling performance and reduced coolant waste.
- Leverage **DMLS** to better distribute coolant through **microchannels**, as well as to integrate **inherently unstable flow** devices to enhance internal and external heat transfer.
- **Demonstrate** these technologies
 1. at large scale and low speed.
 2. at relevant Mach numbers in a **high-speed cascade**.
 3. finally, at high speed and **high temperature**.
- Complement experiments with **CFD modeling** to explore a broader design space and extrapolate to more complex operating conditions.

Integration of Promising Designs in NGV

Reverse Cooling on PS:

- Fed by upstream microchannel
- Better surface coverage with lower massflow?

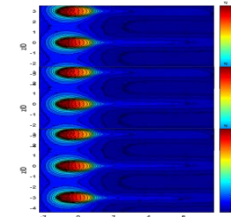


Microchannels in TE:

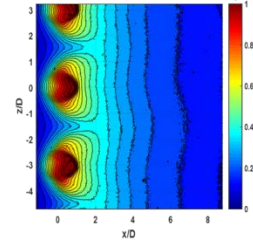
- Improved coverage with lower massflow required?
- Weight savings with skin cooling?

Sweeping Fluidic Oscillator Film Cooling:

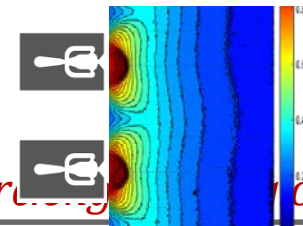
- Improved coverage with lower massflow required?



VS.

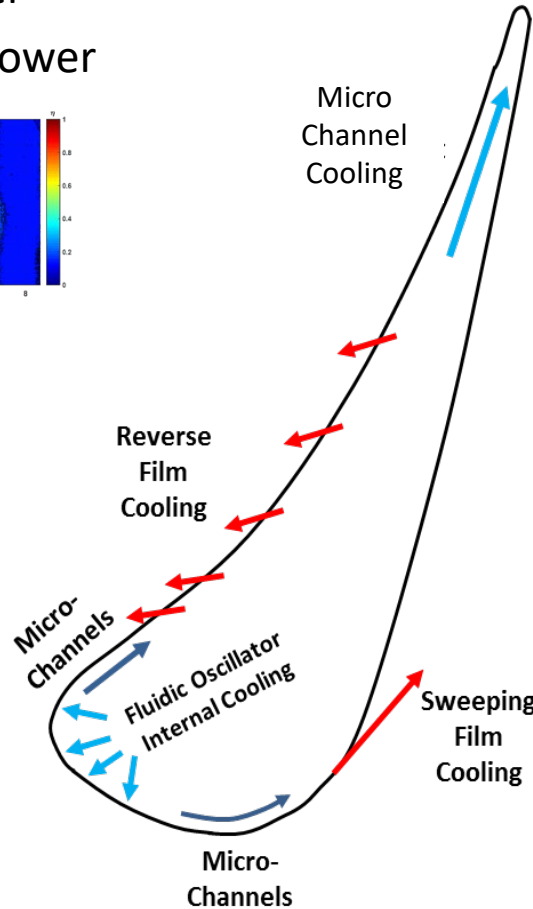
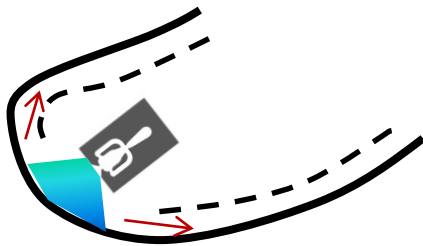


VS.



Fluidic Oscillator Impingement Cooling on LE:

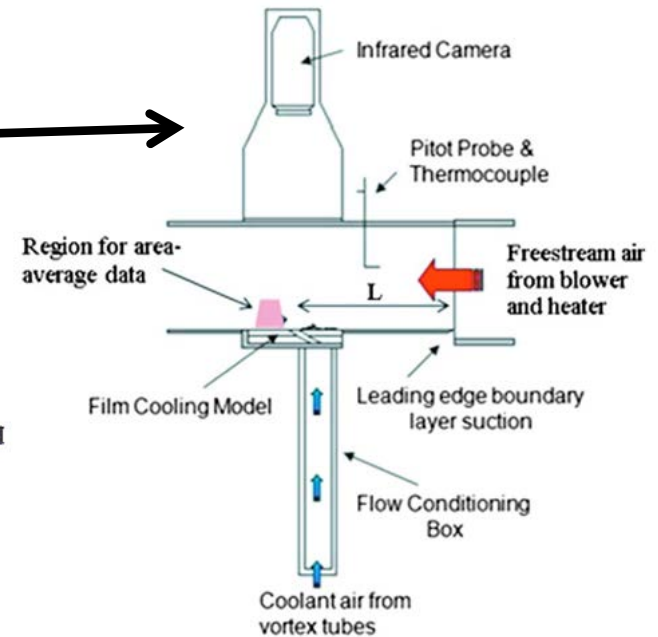
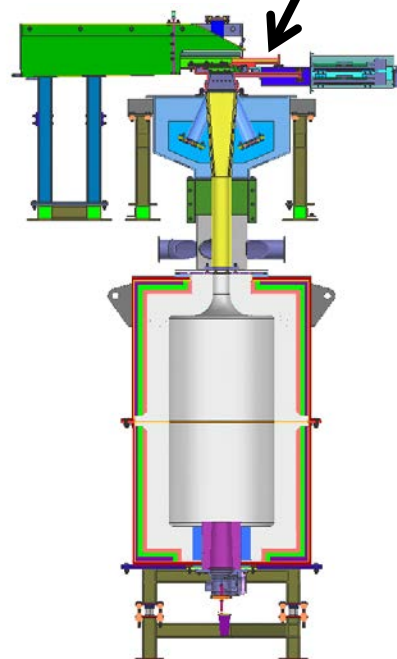
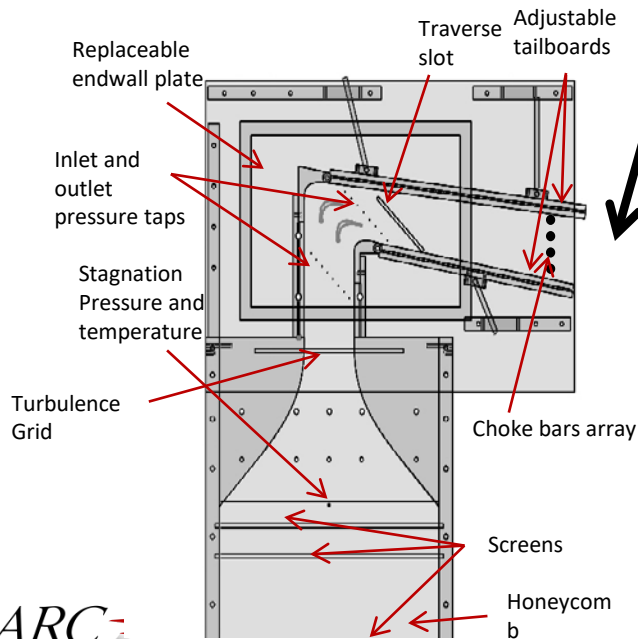
- Eliminate showerhead
- Lower massflow required?
- Microchannel exhaust





Turbine Heat Transfer Facilities

- For innovative concepts to be viable, must be vetted in facilities that simulate the real operating environment
- Graduated complexity
 - Low speed, large scale
 - High speed, smaller scale
 - High speed, high temp (T_w/T_b), small scale





Sweeping Jet Impingement Cooling

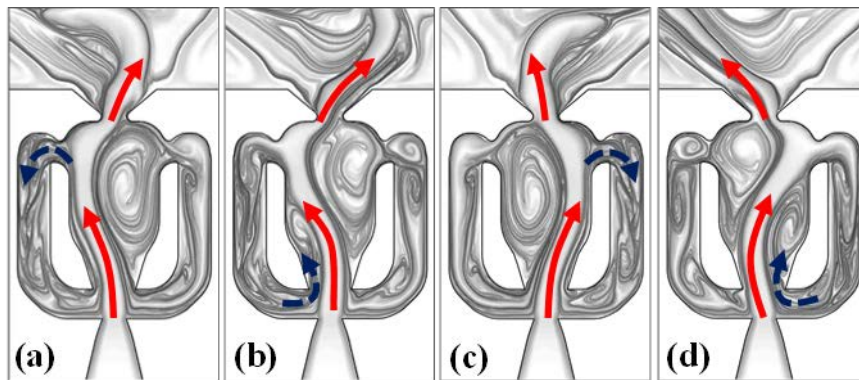
Design Variables

- Jet-to-wall spacing (H/D)
- Exit fan angle (ϕ)
- Aspect ratio (AR)
- Hole pitch (P/D)
- Reynolds number (Re)

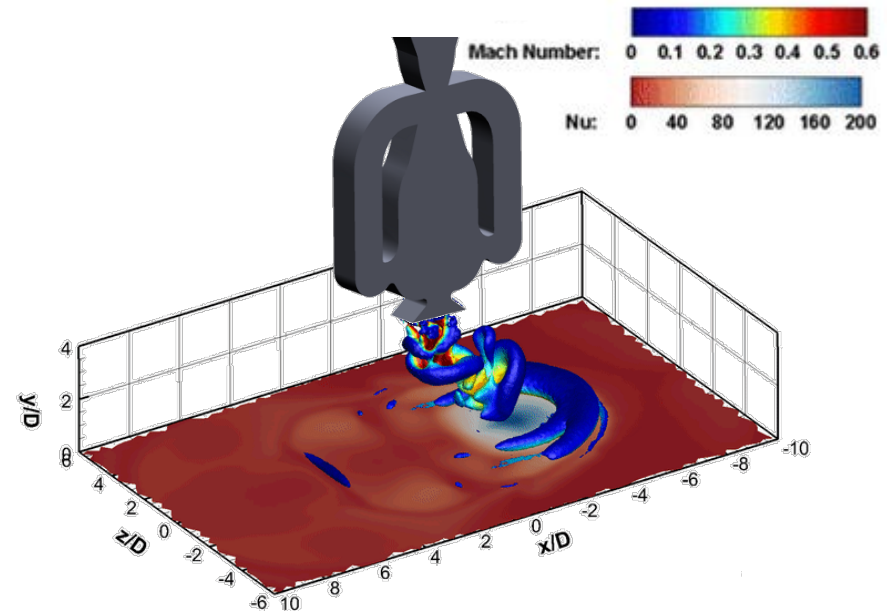


Overview

- ❑ **Goal:** Study the potential for using **sweeping jets for impingement** heat transfer in leading edge internal cooling applications.
- ❑ **Progression:**
 - ❑ **Flat plate** experiments to determine the effect of $Re, z/d_h$
 - ❑ **Computational studies** to determine the effect of exit nozzle angle, impingement surface curvature, and reduced frequency
 - ❑ **Low speed** wind tunnel experiments with engine-relevant Biot number
 - ❑ Array of sweeping jets in a **faired cylinder**
 - ❑ Array of sweeping jets in a linear cascade **nozzle guide vane**
 - ❑ **Transonic** cascade

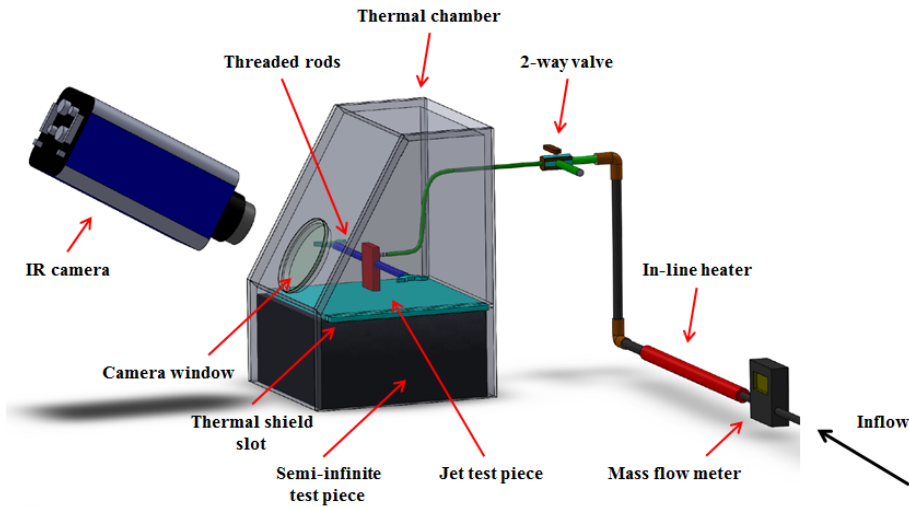


(Ostermann et al. 2015)





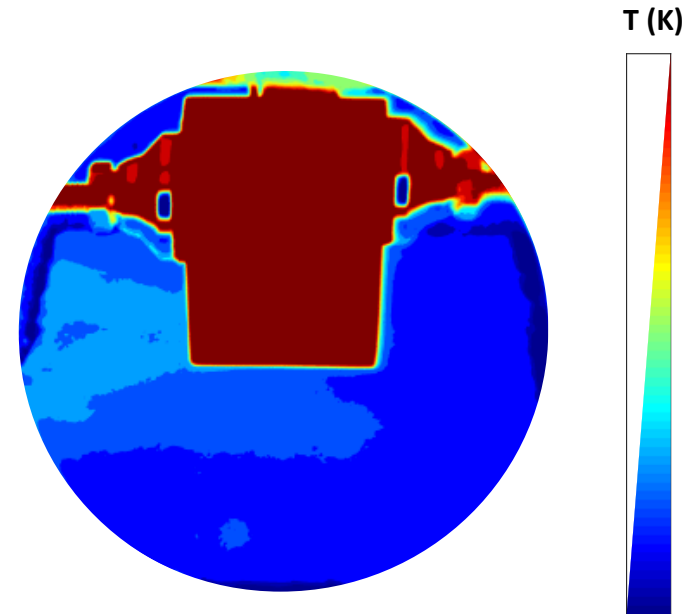
Flat Plate Impingement Experiments with Solo Fluidic Oscillator



- ❑ Test jets mounted in a temperature-controlled chamber for transient tests
- ❑ Results compared to a circular $L/D=1$ orifice jet at similar test conditions

- ❑ Surface temperature was measured with IR thermography, and heat flux was measured locally with heat flux gauges

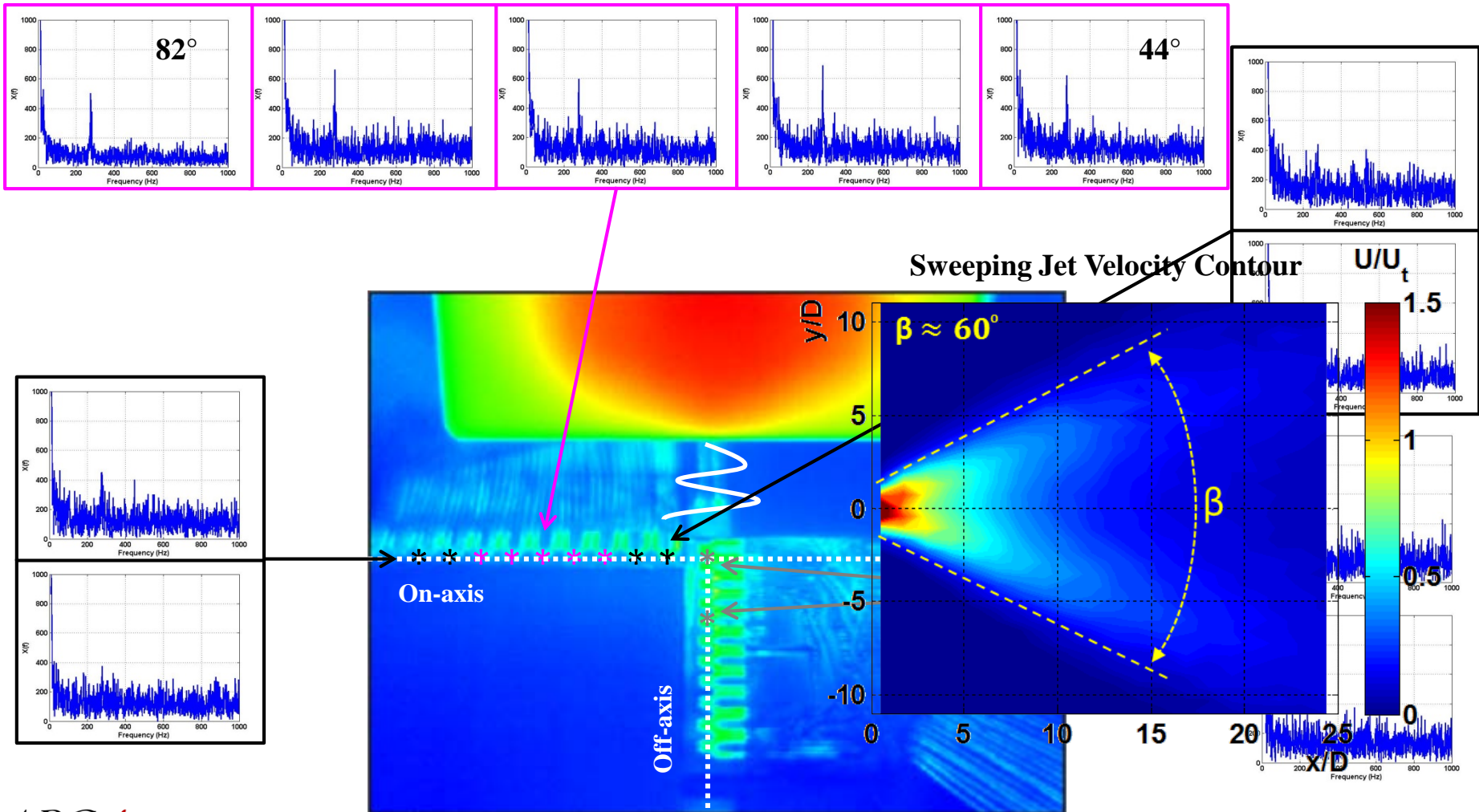
- ❑ Test matrix:
 - ❑ Reynolds numbers: 20,000 to 35,000
 - ❑ Jet-to-wall spacings: 5 to 7 (z/d_h)
 - ❑ Exit nozzle angles: 70° and 102°
 - ❑ Hydraulic diameter $d_h = 4.11$ mm
 - ❑ $AR = 1$ for all fluidic oscillators





Heat Flux Gauge Impingement Measurements

- ❑ Unsteadiness evident in local heat transfer (HFG power spectra and IR)
- ❑ Validation of **oscillation frequency** (to within 5%), **bi-stable flow field**, and **spreading angle**





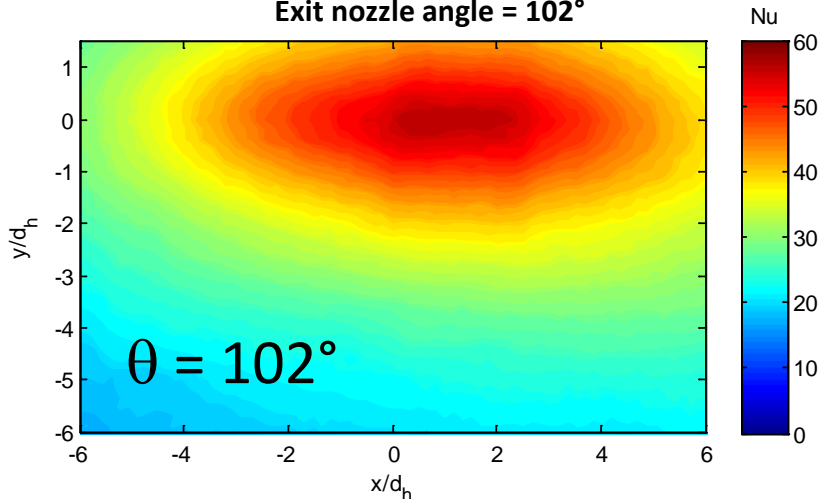
Results for Sweeping Impingement Jet

- ❑ Sweeping jet impingement **Nu depends on jet $Re^{0.5}$**
- ❑ Sweeping jet impingement heat transfer is **not symmetric** between lobes of high heat transfer
- ❑ Changing fluidic oscillator **exit angle** drastically **changes the sweeping jet** impingement heat transfer profile
- ❑ Heat transfer **on flat plate underperformed** compared to the circular jet

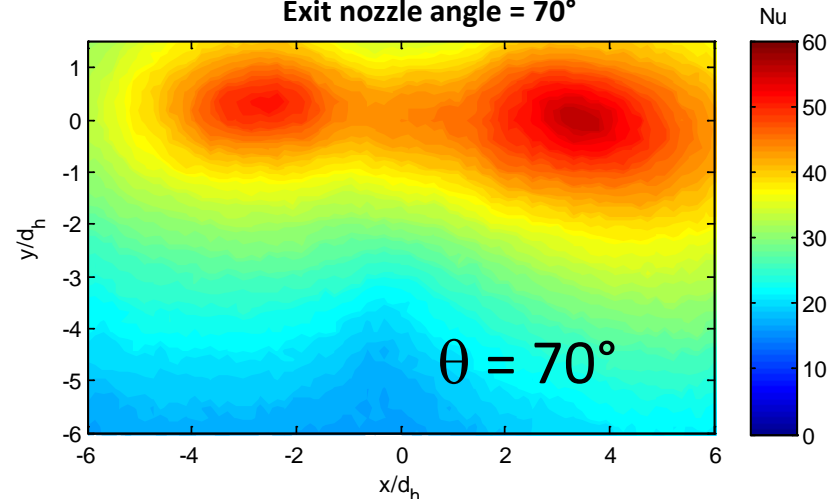


Opportunities for Design Optimization!!!

Sweeping Jet Nu Contour – Transient IR Measurement
Exit nozzle angle = 102°



Sweeping Jet Nu Contour – Transient IR Measurement
Exit nozzle angle = 70°

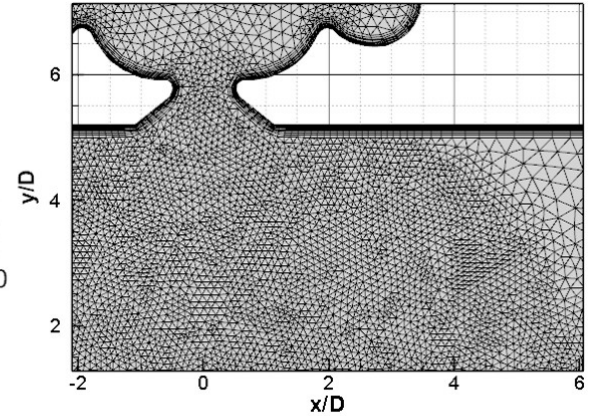
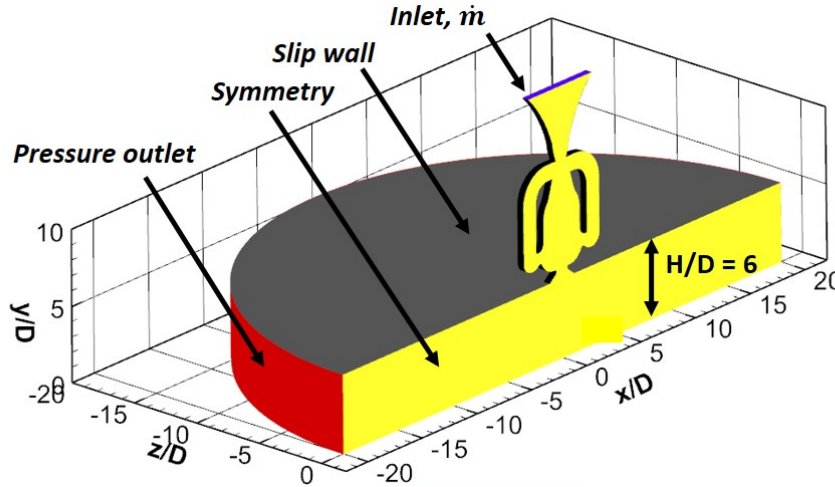




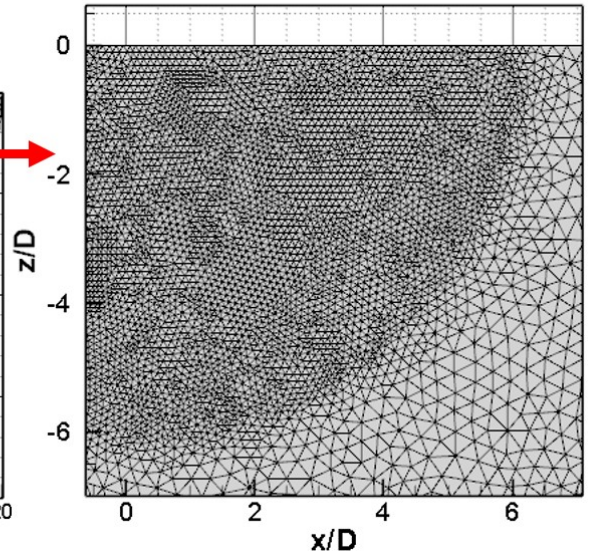
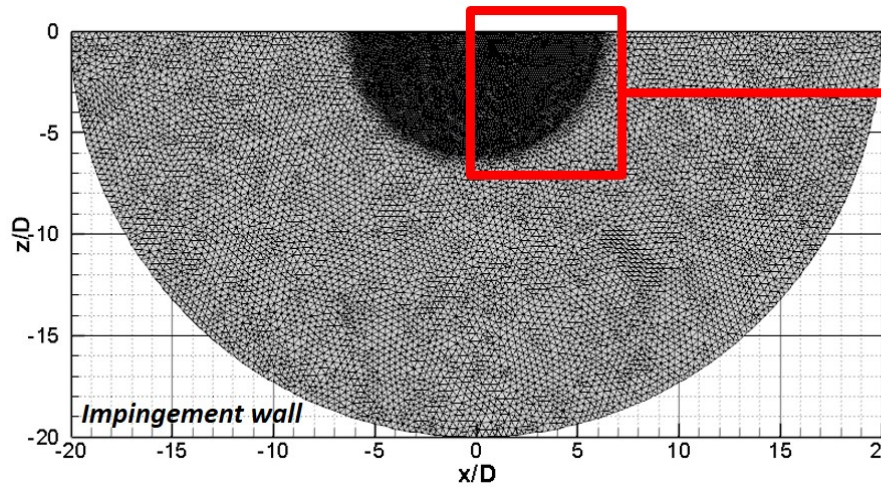
Impingement Study (CFD)

- CFD calculations performed with FO and round jet to investigate the external flow field and heat transfer parameters.
- Unsteady RANS** ($k - \omega$ SST model)
- Re = 35

CFD domain



CFD Grid

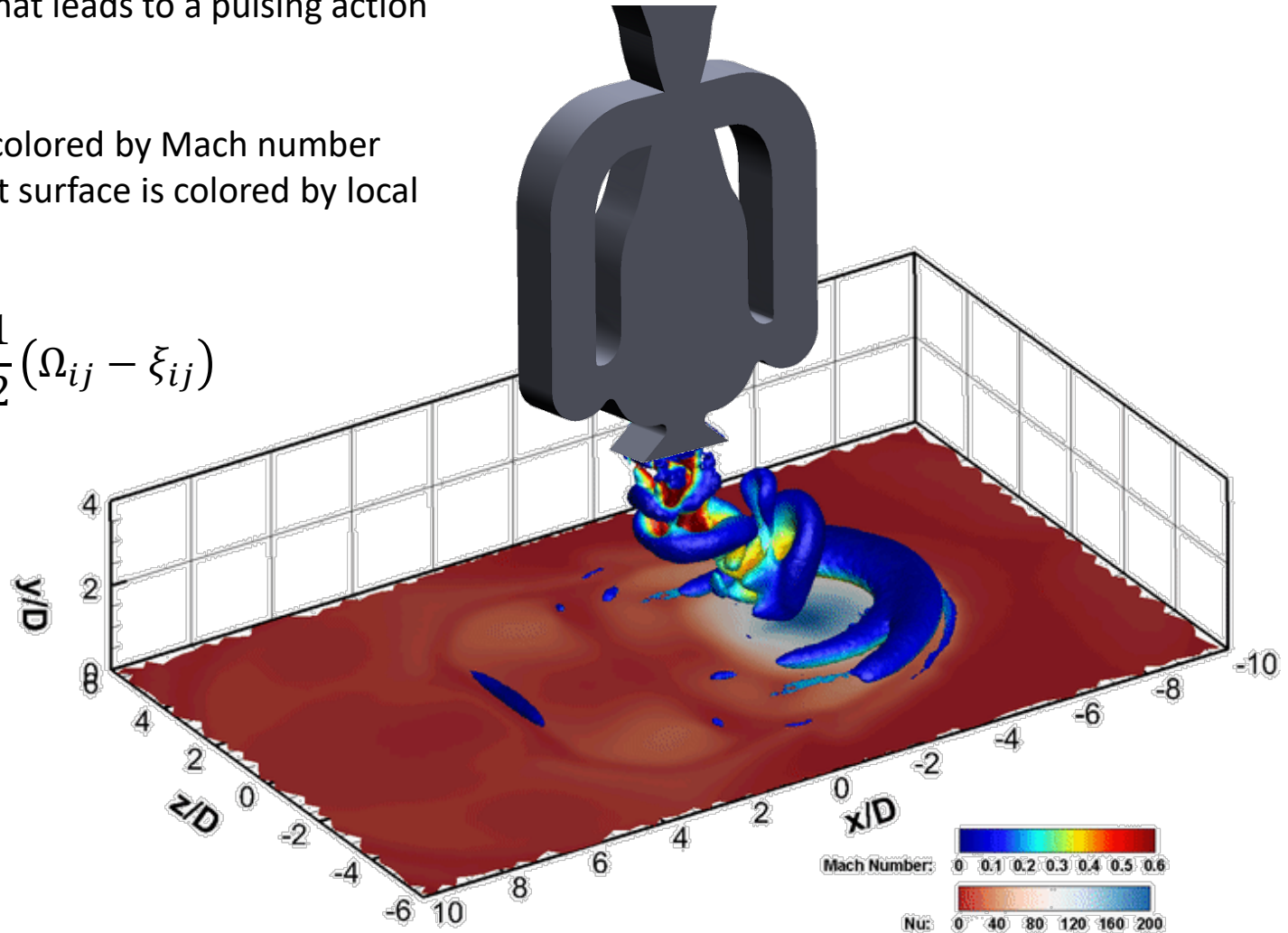




External Flow Field(Iso-surface of Q-criterion)

- ❑ CFD showed complicated flow structure due to entrainment that leads to a pulsing action of the jet.
- ❑ Iso-surfaces are colored by Mach number and impingement surface is colored by local Nu number.

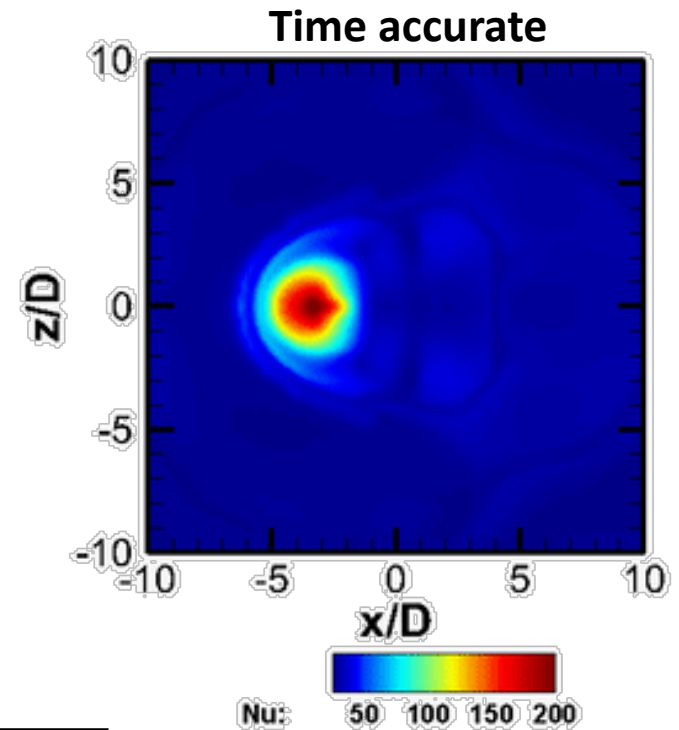
$$Q = \frac{1}{2}(\Omega_{ij} - \xi_{ij})$$



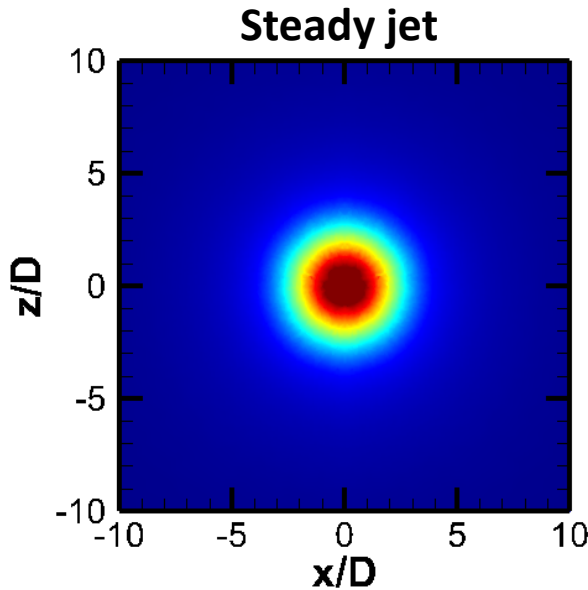
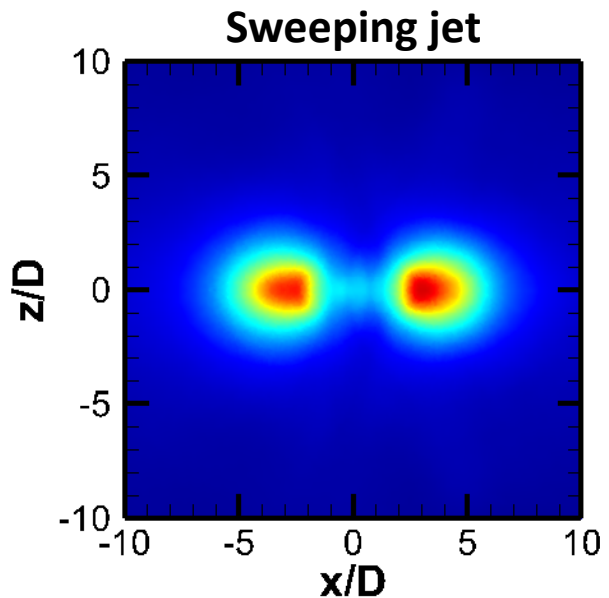


Surface Nusselt Number

- ❑ Sweeping action of the jet enhance cooling in the lateral direction.
- ❑ The time averaged Nu contour shows **two distinct lobe** of cold regions that were confirmed by heat flux gauge data.



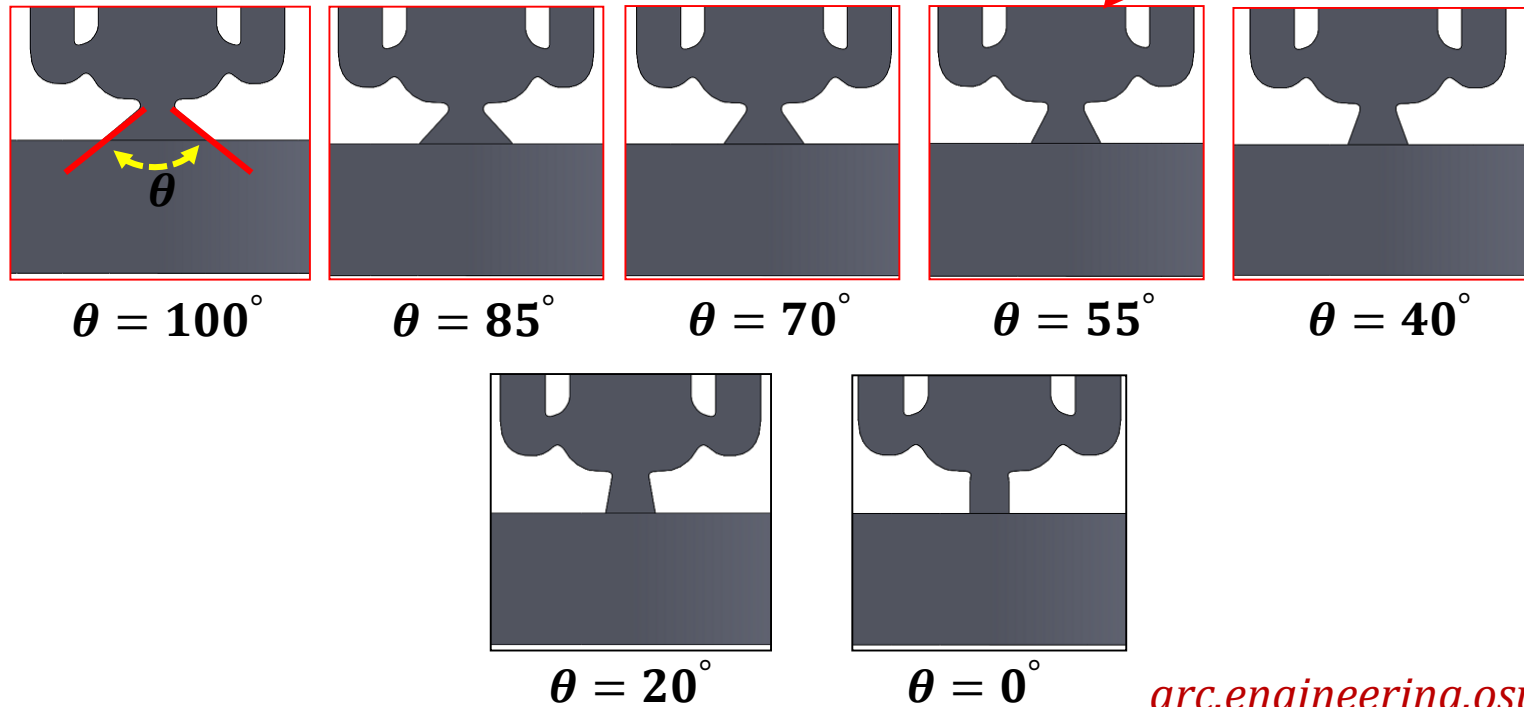
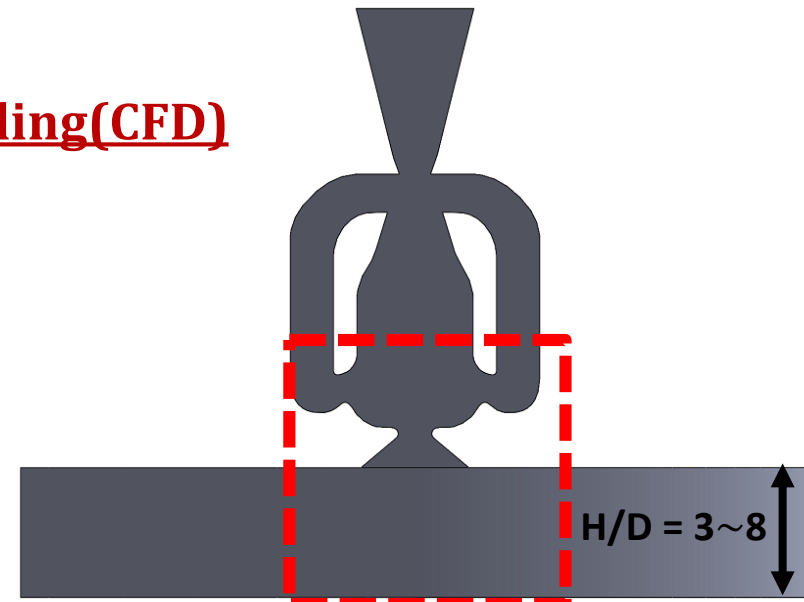
Time averaged





Effect of θ and H/D for Impingement Cooling(CFD)

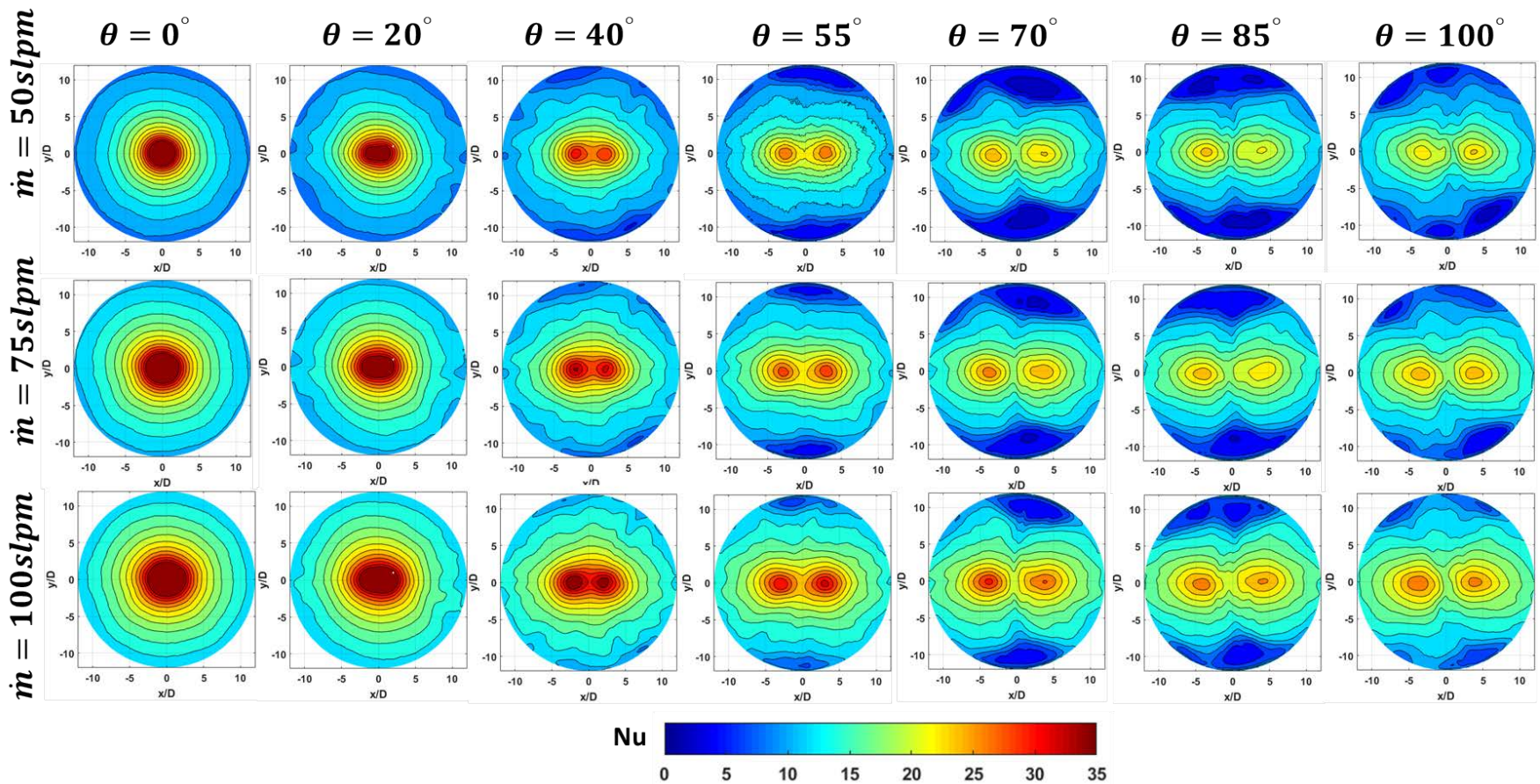
- ❑ 72 cases were examined.
- ❑ $\theta = 0^\circ, 20^\circ, 40^\circ, 55^\circ, 70^\circ, 85^\circ, 100^\circ, 130^\circ$.
- ❑ $\dot{m} = 50, 75, 100 \text{ slpm}$
- ❑ $H/D = 3, 5, 8$
- ❑ Unsteady RANS ($k - \omega$ SST turbulence)
- ❑ $Re_D \sim 17500, 26000, 35000$





Time Averaged Nu Distribution

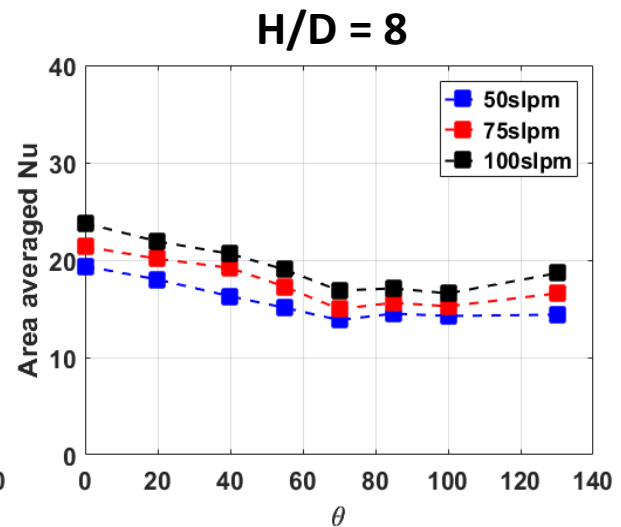
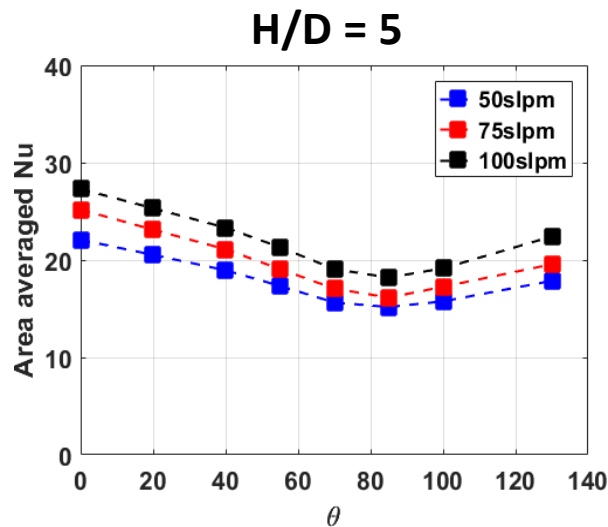
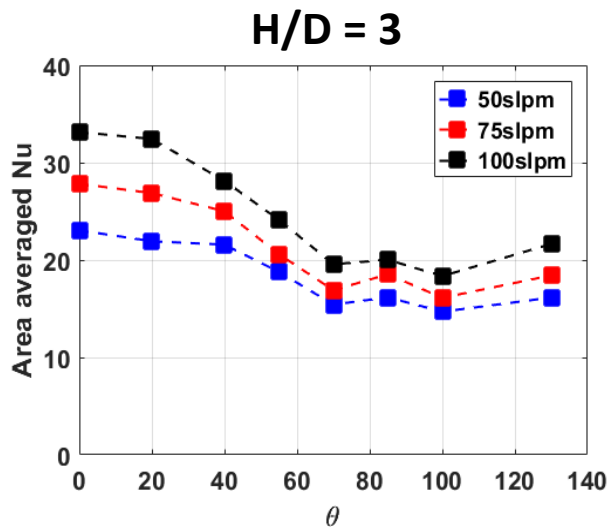
- ❑ Time averaged contours show the effect of exit fan angle on local Nu distribution.
- ❑ Large fan angle shows increased spreading of coolant. However, the peak value of Nu drops significantly due to mixing.





Area Averaged Nu Distribution

- ❑ Results are shown as a function of exit angle.
- ❑ Area averaged Nu drops linearly (up to $\theta = 85^\circ$) as the exit angle increases for all massflow rates for $H/D = 5$.
- ❑ Recall $\theta=0$ is essentially steady jet.



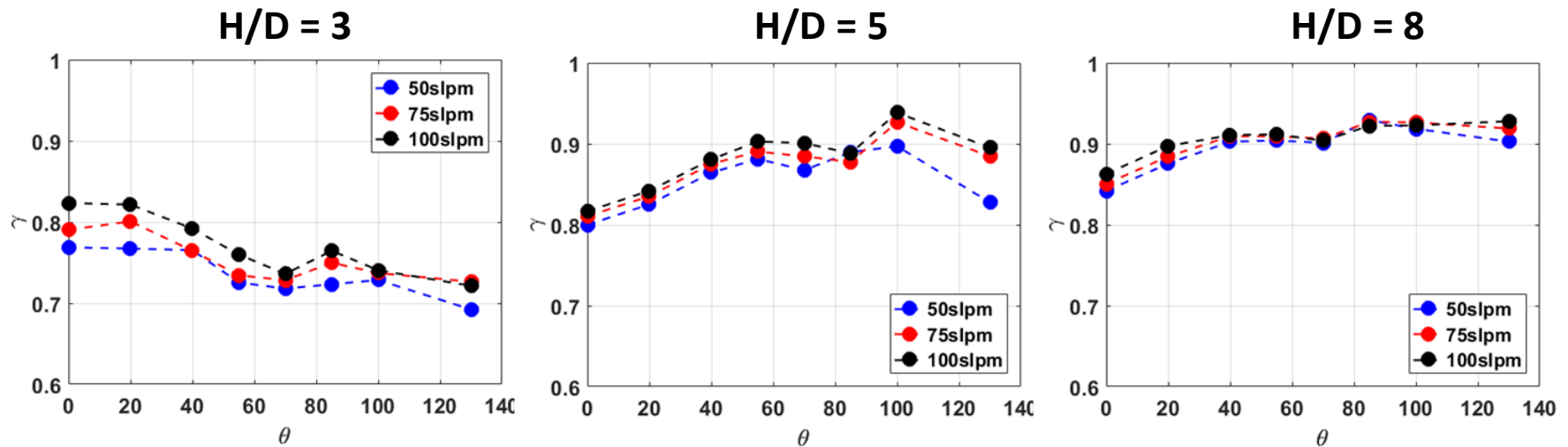
Oscillating jet always has lower area-averaged Nu compared to $\theta = 0$



Surface Uniformity Index

- ❑ The time averaged Nu distribution is not the whole story.
- ❑ In order to show the actual benefit of the sweeping action, a new parameter has been defined as ‘Surface Uniformity Index (γ)’
- ❑ $\gamma = 1$ indicates a perfectly uniform metal temperature.

$$\gamma = 1 - \frac{\sum_{i=1}^N \sqrt{(Nu_i - \overline{Nu_i}) \cdot A_i}}{\overline{NuA}}$$

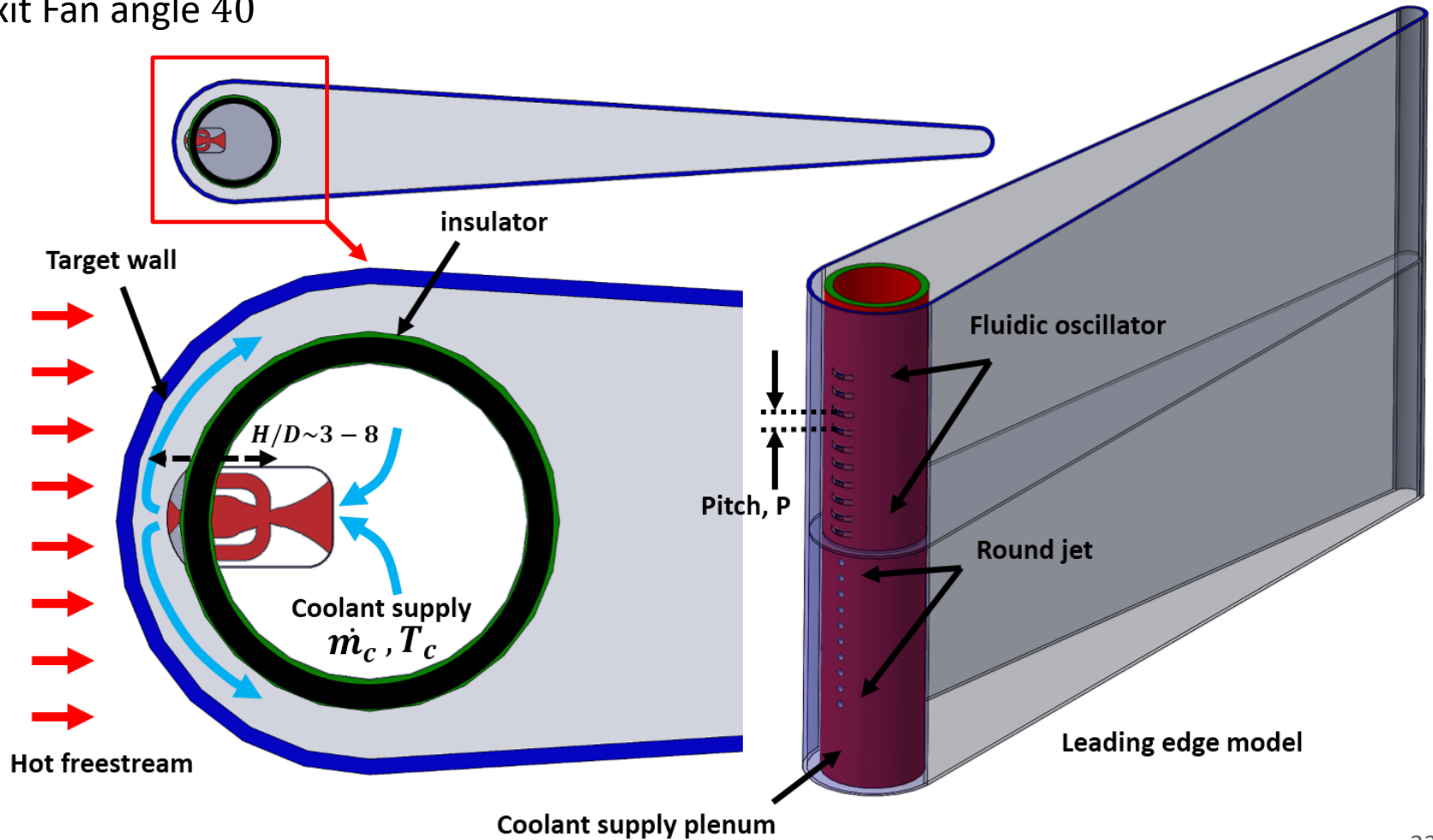


At H/D=5, oscillating jet **OUTPERFORMS** $\theta = 0$ for uniformity



Leading Edge Model

- ❑ Radius of curvature, $R_{LE} = 17D_h$
- ❑ Leading edge diameter, $D_{LE} = 101.6mm$
- ❑ Span, $S_{LE} = 380mm$
- ❑ LE wall thickness, $t_{LE} = 1.5mm$
- ❑ Exit Fan angle 40°





Leading Edge Wall Thickness (matched Bi number approach)

Adiabatic film effectiveness-

$$\eta = \frac{T_\infty - T_{aw}}{T_\infty - T_c}$$

Overall cooling effectiveness-

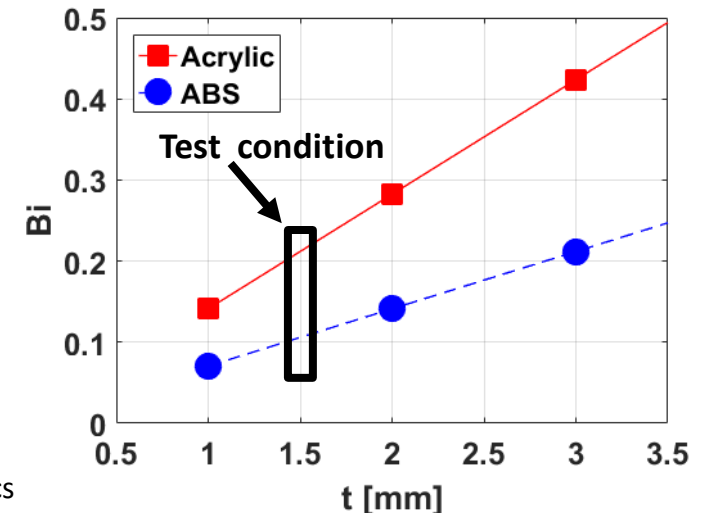
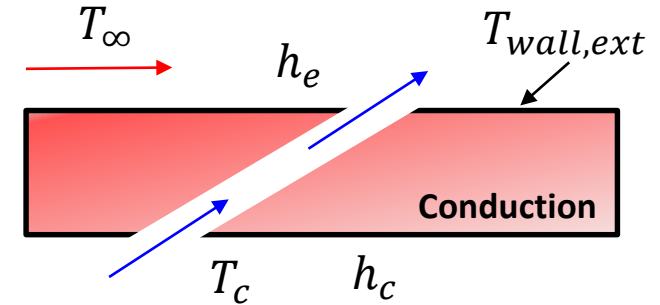
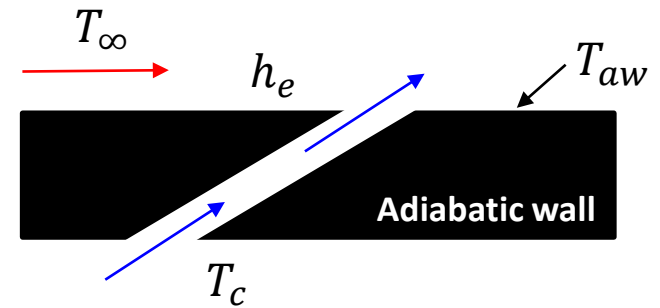
$$\phi = \frac{T_\infty - T_{wall,ext}}{T_\infty - T_c}$$

One dimensional heat transfer analysis-

$$\phi = \frac{1-\eta}{1+Bi+\frac{h_e}{h_c}} + \eta$$

$$Nu_D = 0.3 + \frac{0.62Re_D^{0.5}Pr^{0.33}}{\left(1+\left(\frac{0.4}{Pr}\right)^{0.66}\right)^{0.25}} \left[1 + \left(\frac{Re_D}{282000}\right)^{\frac{5}{8}}\right]^{\frac{4}{5}}$$

	Model	Engine
Bi	0.1	0.1-1.0
h_e/h_i	0.5	0.5
T_∞	310K	1680K [1]
T_c	275K	819K [1]



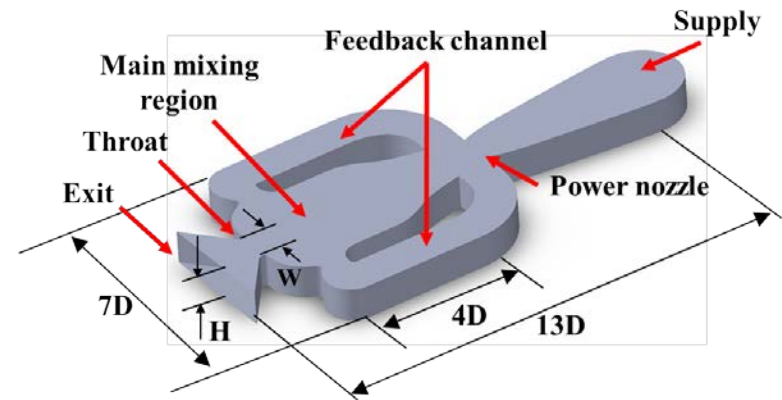


Leading Edge Model (Fluidic Oscillator)

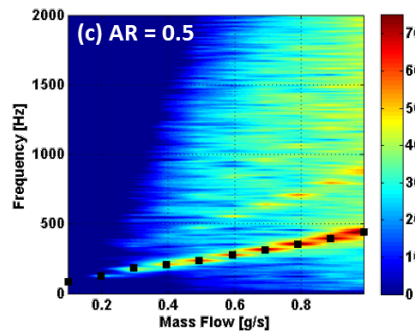
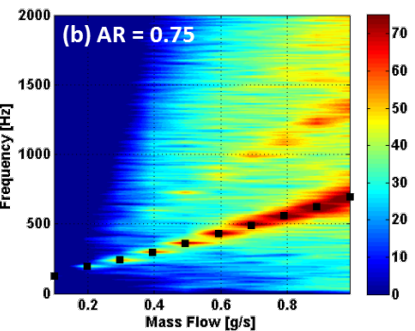
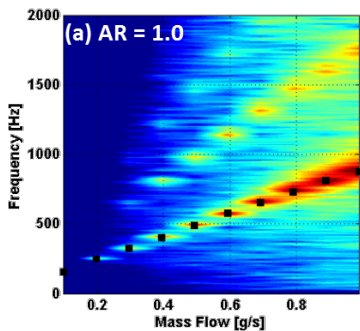
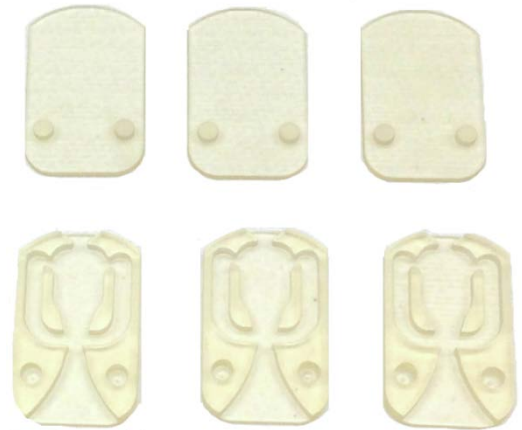
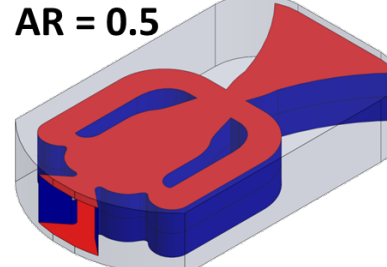
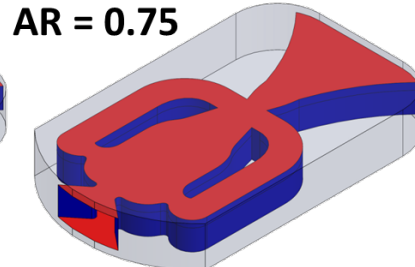
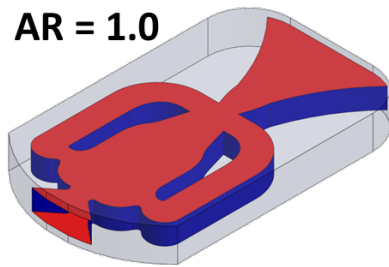
Geometric Parameter

$$\text{Aspect ratio (AR)} = \frac{\text{Throat width } (W_t)}{\text{Throat height } (H_t)}$$

Oscillator Characterization



3D printed FO



Frequency contour

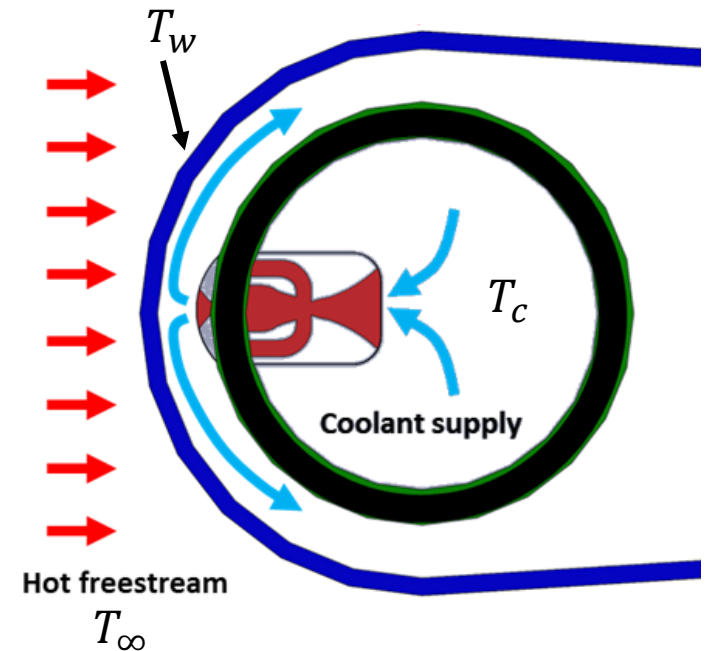
AR	D_h (mm)
1.00	2.50
0.75	2.85
0.50	3.33

Test Matrix

- ❑ 72 tests were conducted.
- ❑ Both heat transfer and pressure drop measurements were performed.
- ❑ Span averaged and area averaged cooling effectiveness were estimated.

$$\theta = \frac{T_{\infty} - T_w}{T_{\infty} - T_c}$$

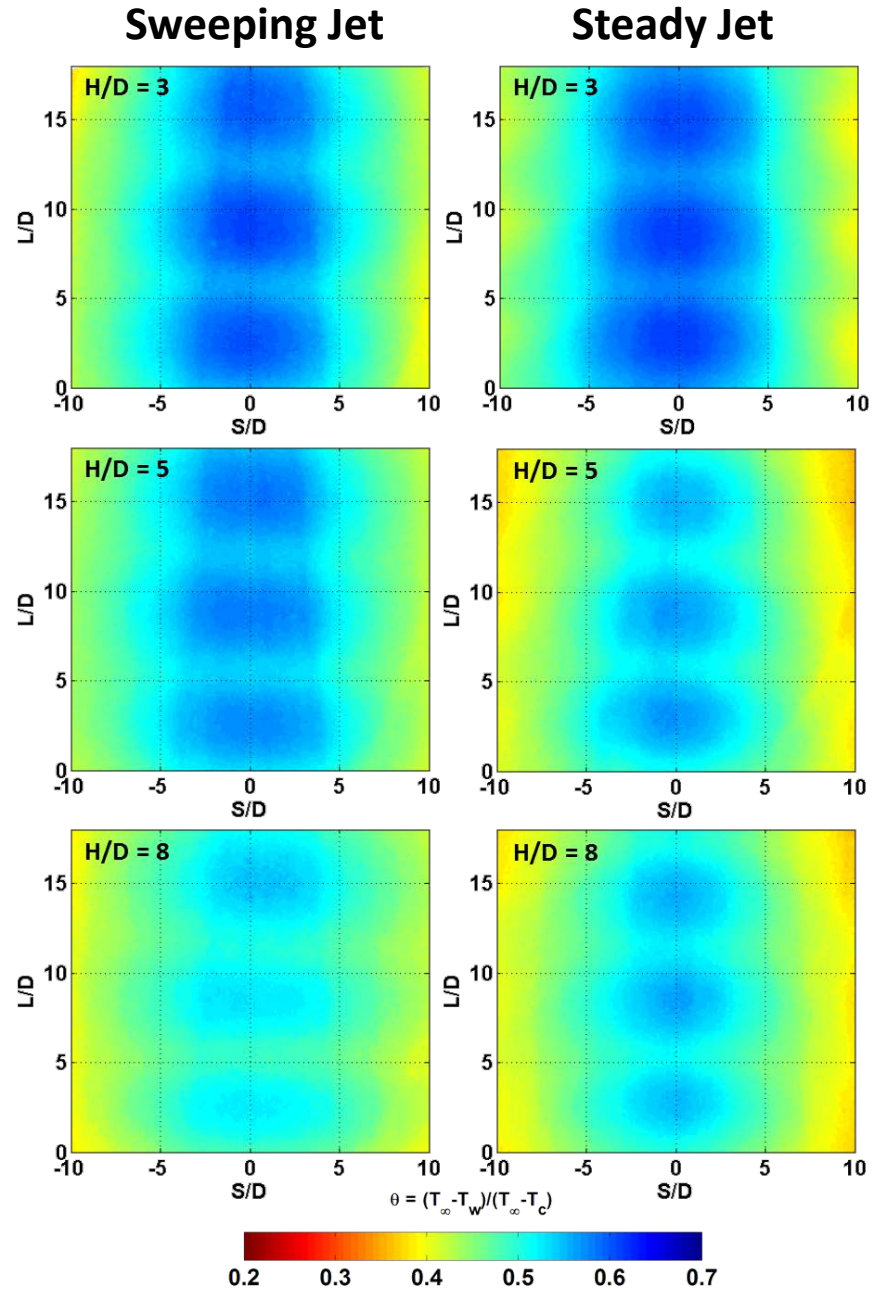
Aspect ratio	Pitch (P/D)	H/D	Tu
1	4,6	3,5,8	0.5%, 10.1%
0.75	4,6	3,5,8	0.5%, 10.1%
0.5	4,6	3,5,8	0.5%, 10.1%





Effect of H/D

- ❑ Span averaged cooling effectiveness are shown for AR = 1, P/D = 6
- ❑ Cooling effectiveness decreases with the increases of H/D and turbulence.
- ❑ At H/D = 5, sweeping jet shows promising performed compared to round jet.

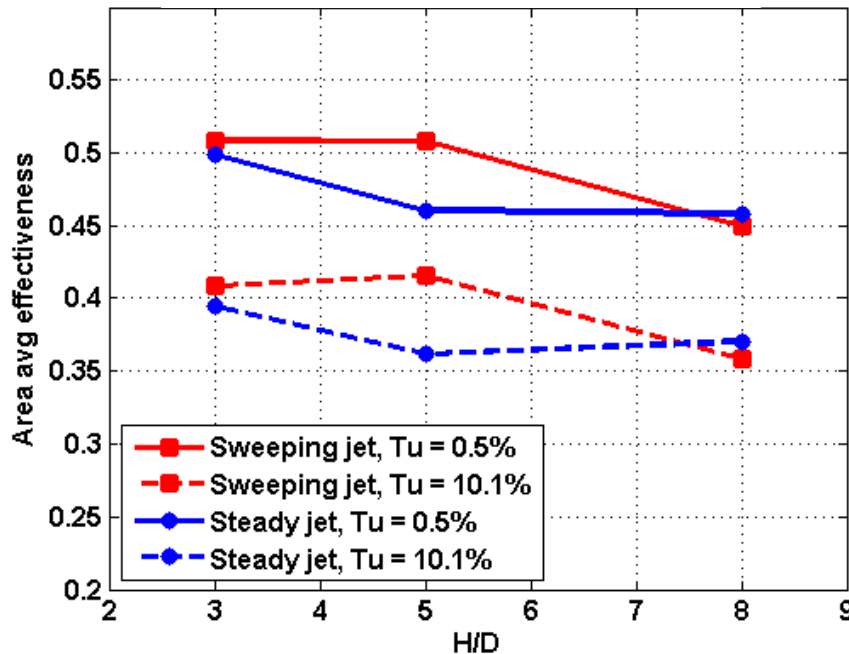




Effect of H/D

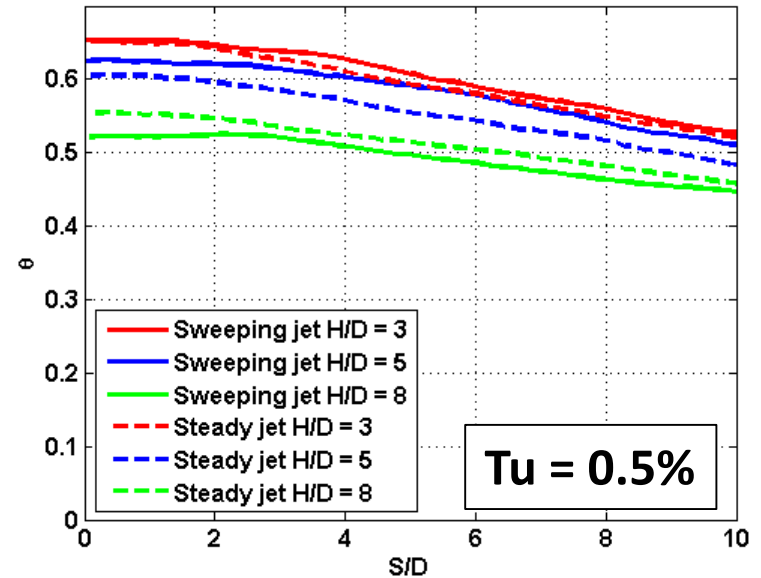
- Span averaged cooling effectiveness are shown for AR = 1, P/D = 4
- Area averaged cooling effectiveness shows the effect of turbulence at varying H/D.

Area averaged effectiveness

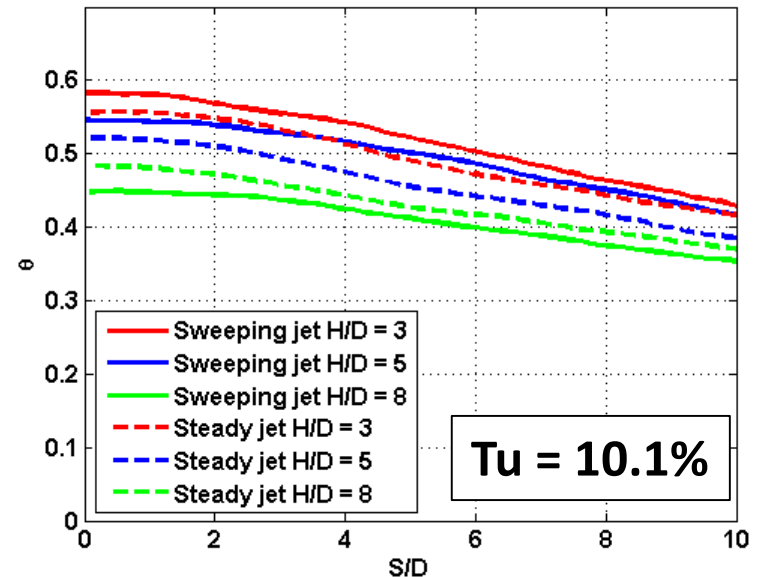


Span averaged effectiveness

AR = 1, P/D = 4, Tu = 0.5%



AR = 1, P/D = 4, Tu = 10.1%

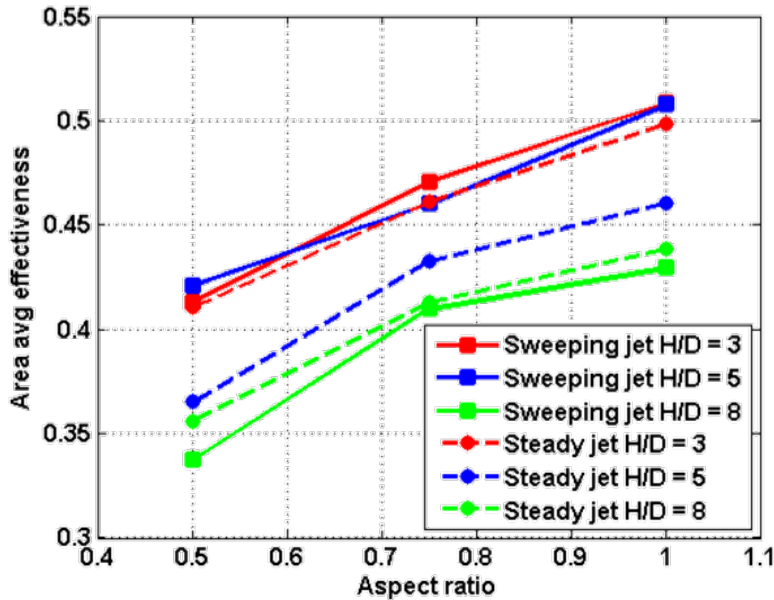




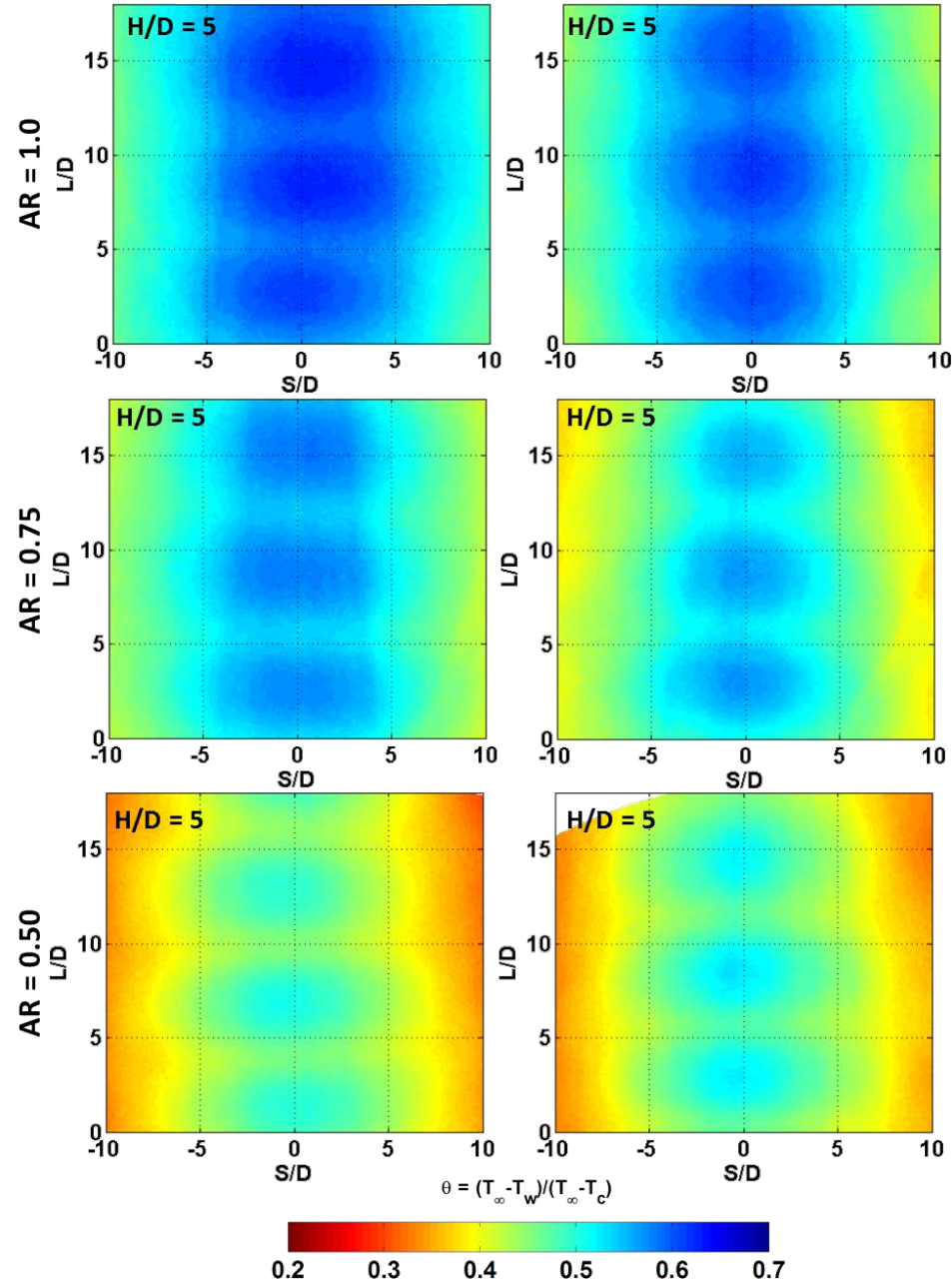
Effect of Aspect Ratio

- Overall cooling effectiveness contours are shown for sweeping jet and steady jet at three different aspect ratios.
- Area averaged effectiveness implies that **aspect ratio of AR = 1** has the **best cooling performance**.

Area averaged effectiveness



Overall cooling effectiveness

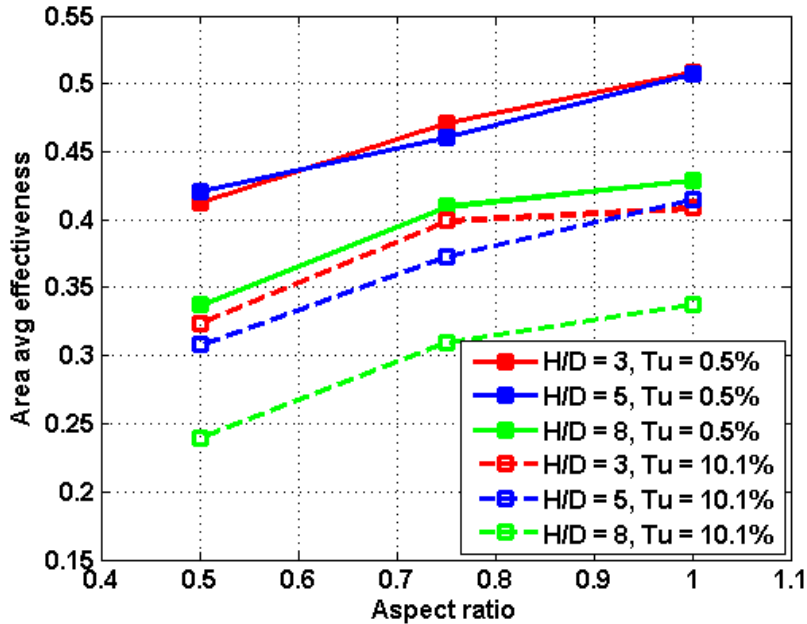




Effect of Freestream Turbulence

- Freestream turbulence augments external heat transfer thus a drop in overall cooling effectiveness has been observed.

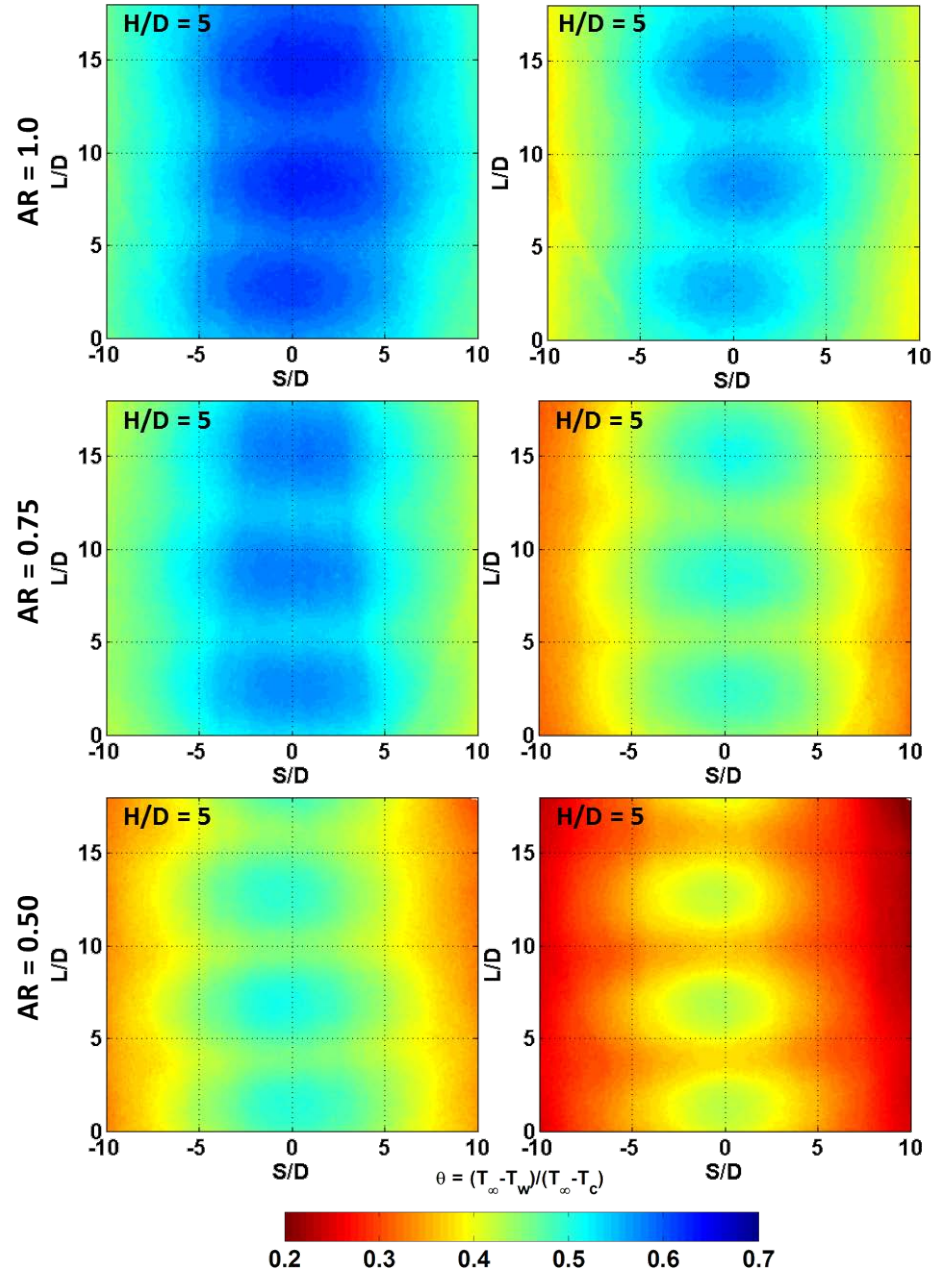
Area averaged effectiveness



Overall cooling effectiveness

Tu = 0.5%

Tu = 10.1%

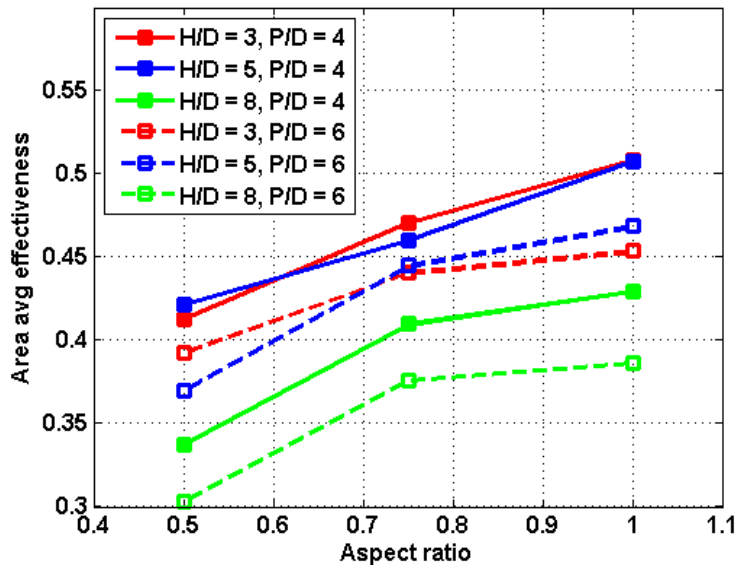




Effect of Pitch

At $P/D = 4$, the interaction between the adjacent jets augments internal heat transfer resulting in an increase in overall cooling effectiveness.

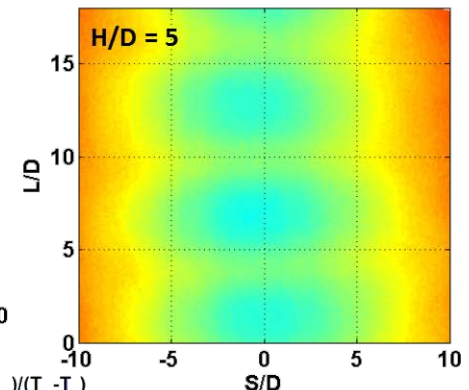
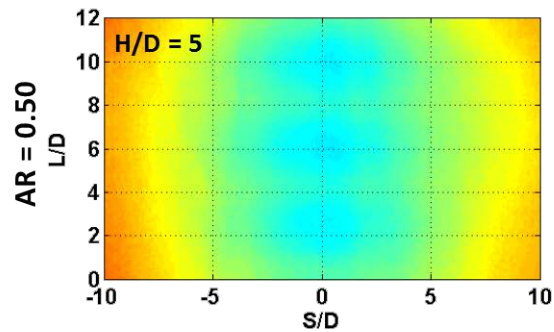
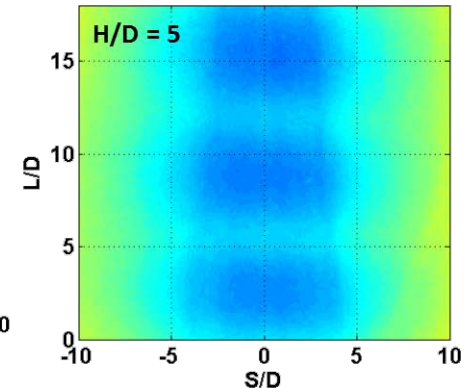
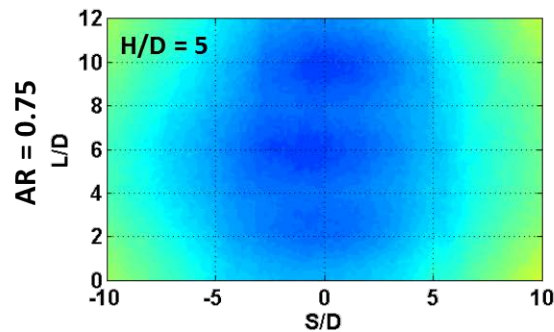
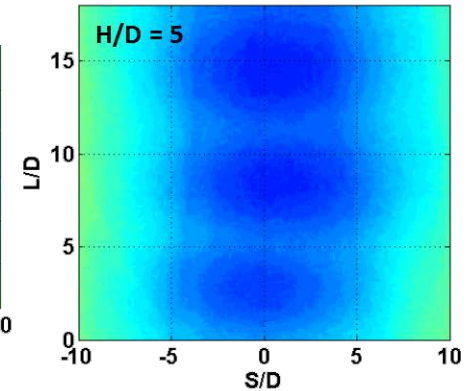
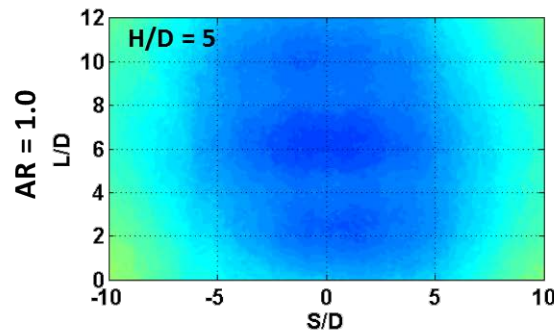
Area averaged effectiveness



Overall cooling effectiveness

$P/D = 4$

$P/D = 6$



$$\theta = (T_{\infty} - T_w) / (T_{\infty} - T_c)$$



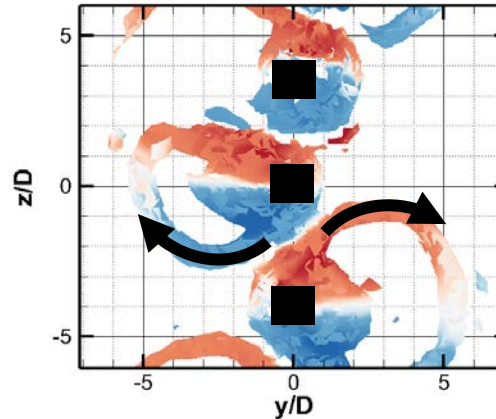


Internal flowfield (CDF)

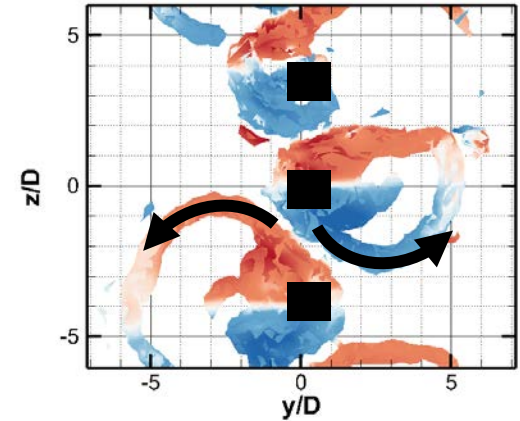
- ❑ CFD shows mutual interaction between adjacent jets over time that induce coolant flow in the spanwise direction.
- ❑ CFD also reveals that the jet oscillations are **not synchronized with adjacent jets**.

Iso-surface of Q-criterion colored by vorticity

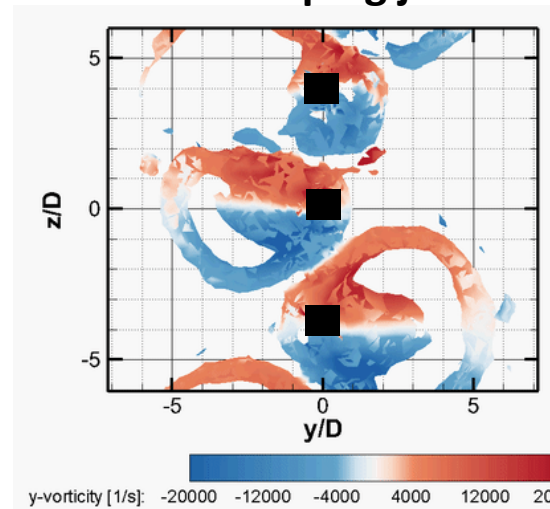
$\phi = 0^\circ$



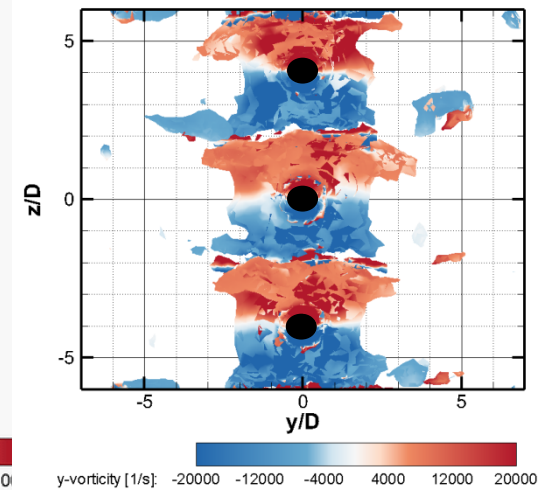
$\phi = 180^\circ$



Sweeping jet



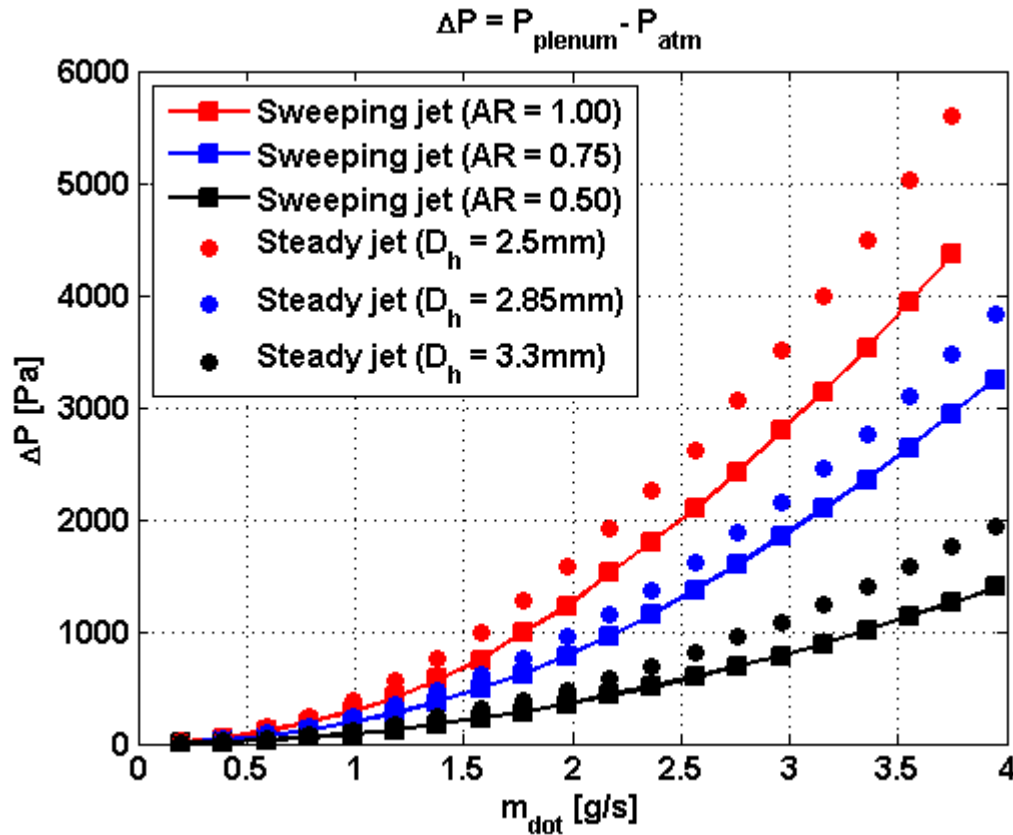
Steady jet





Pressure Drop Measurement

- Pressure drop across the device is lower for sweeping jet compared to steady jet for this particular plenum condition.

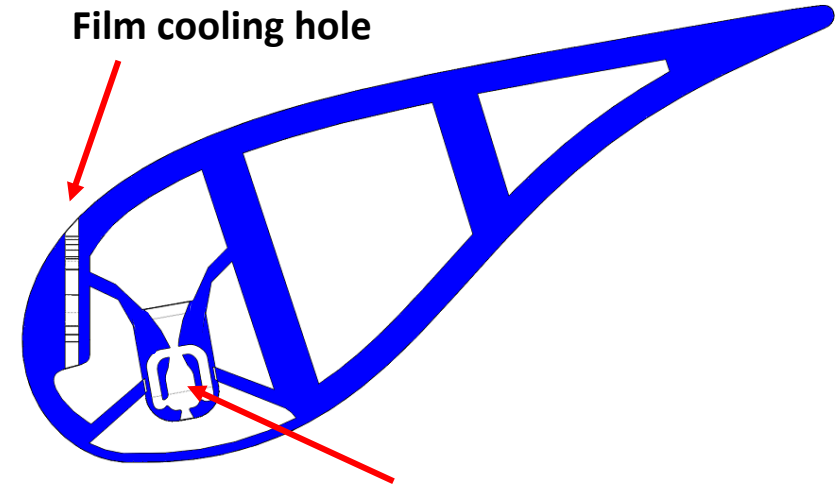




Vane Leading Edge Impingement

- ❑ Vane was designed at OSU as a research vane
- ❑ The vane has a large leading edge radius to facilitate surface temperature measurements
- ❑ Models were additively manufactured with stereolithography and fused deposition modeling
- ❑ Modular so that multiple impingement and film cooling geometries can be tested

OSU vane



Film cooling hole

Impingement hole



FDM



SLA

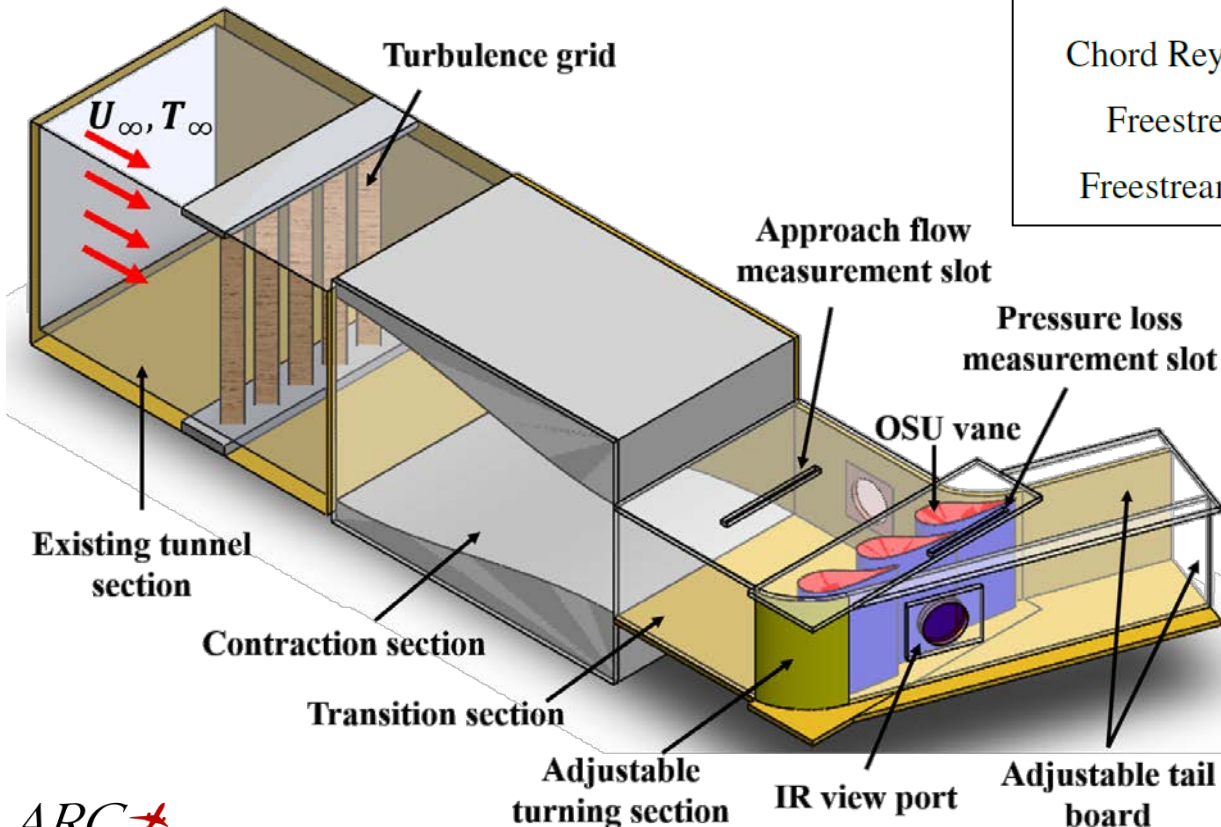


Cascade Design

- ❑ Tests performed in a linear cascade in an open-loop wind tunnel
- ❑ The linear cascade section consists of three-vanes, two passages.

Vane geometry and flow condition

Parameter	Value
True chord (C)	15.24cm(6in)
Axial chord (C_x)	8.33cm(3.28in)
Chord/pitch (C/P)	1.20
Span/chord (S/C)	1.25
Inlet and exit angles	0° and 70°
Chord Reynolds number (Re_{in})	9.5×10^4
Freestream velocity, (U_∞)	9.5m/s
Freestream temperature, (T_∞)	315K



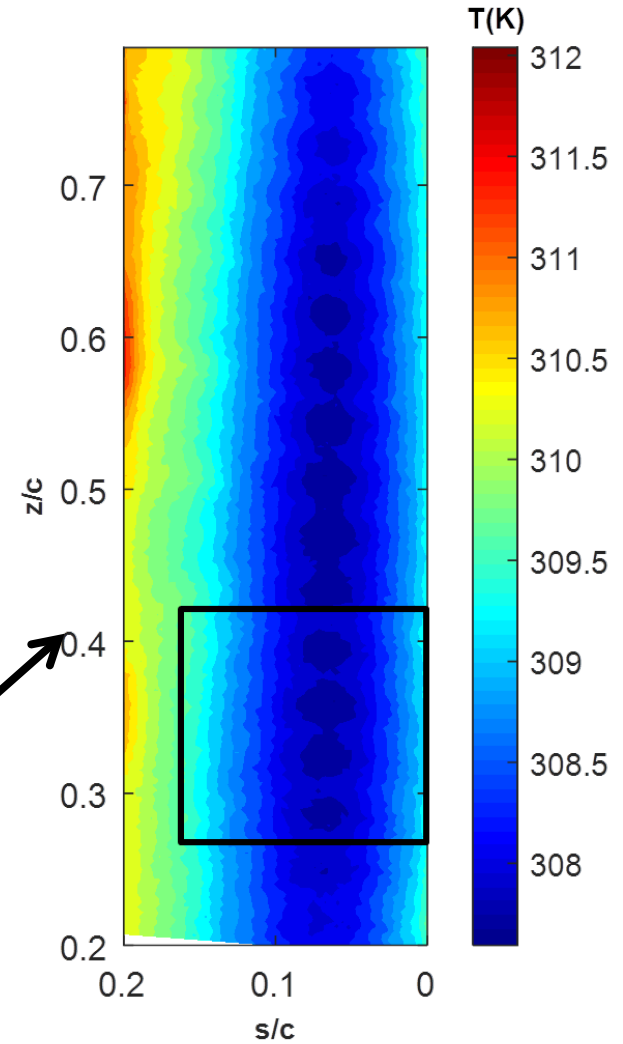
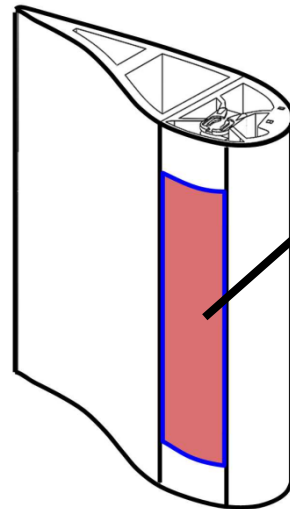
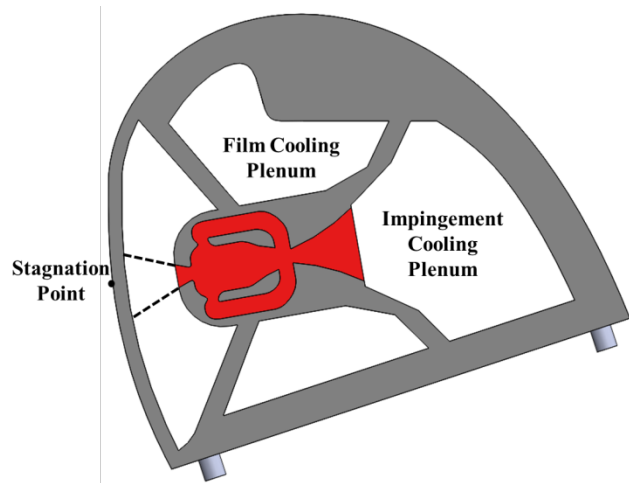


Vane Leading Edge Impingement

- ❑ Leading edge modules were manufactured by SLA for circular and sweeping jet configurations
- ❑ Leading edge thickness was designed to match engine-relevant Biot (0.1-0.3)
- ❑ Fluidic oscillator design parameters were taken from the leading edge model study
- ❑ Vane surface temperature was measured with IR thermography in the region indicated

Geometric parameters

d_h	P/d_h	H/d_h	AR	γ
1.5 mm	4	5	1	40°



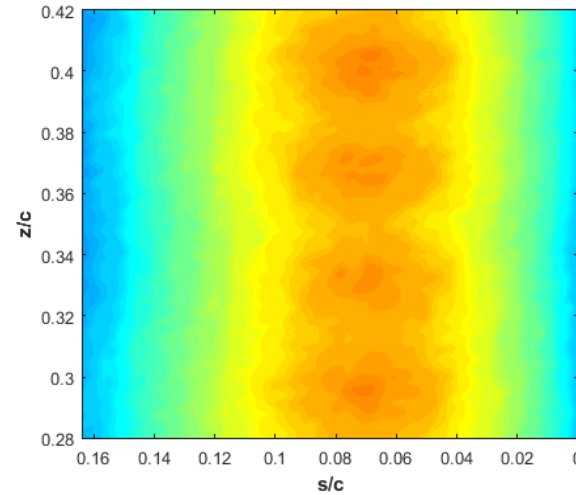
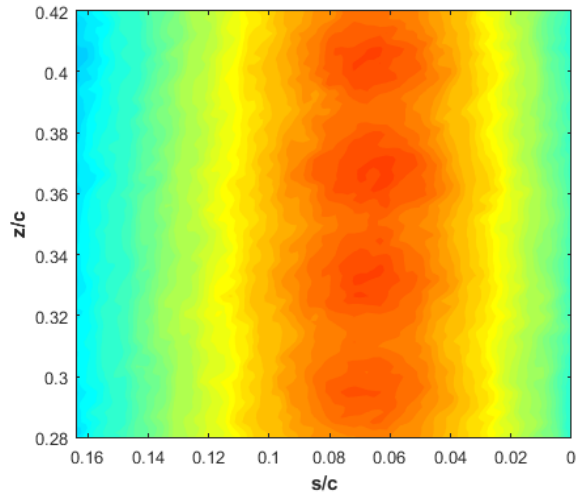


Overall Cooling Effectiveness

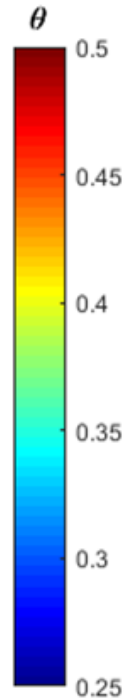
Circular Jet

Sweeping Jet

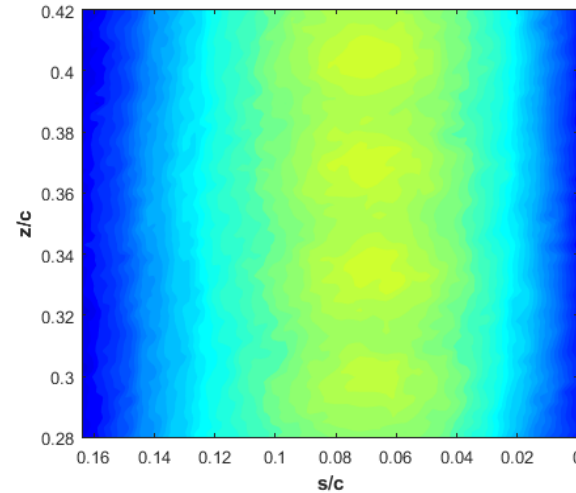
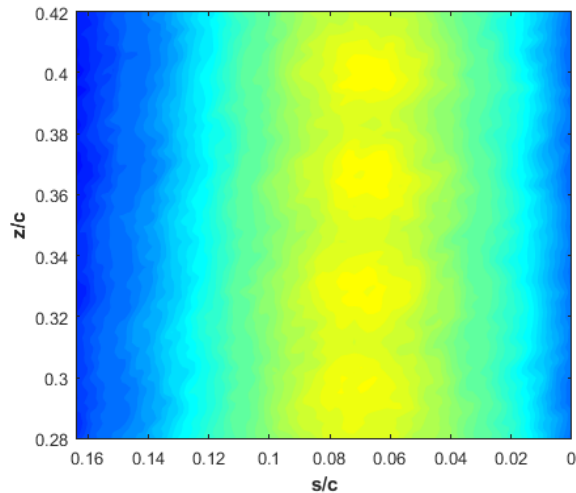
Low Tu (0.3%)



$$\theta = \frac{T_{\infty} - T_s}{T_{\infty} - T_{coolant}}$$



High Tu (6.1%)

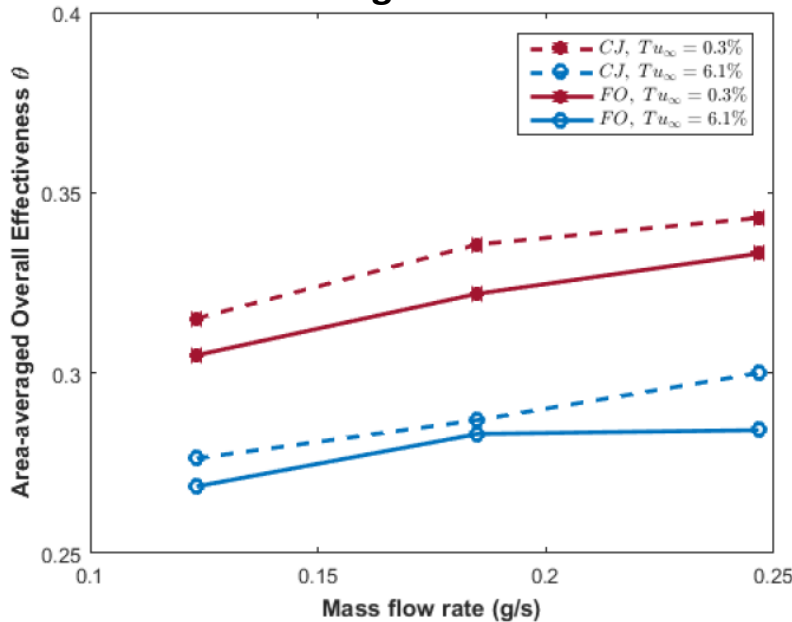




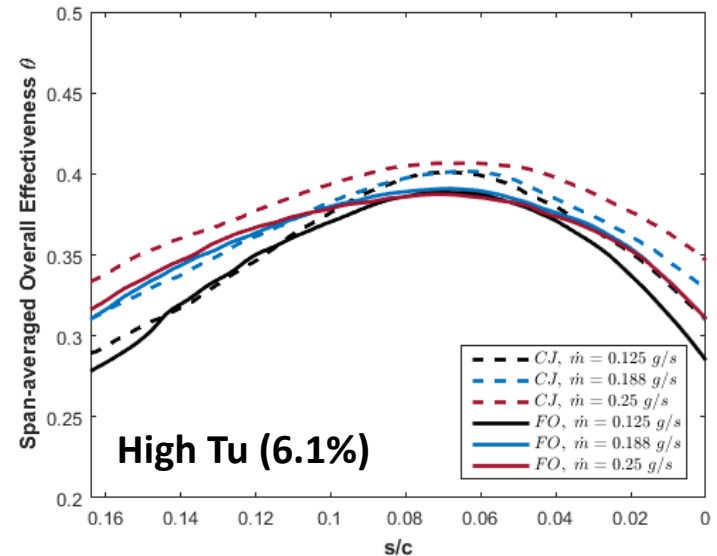
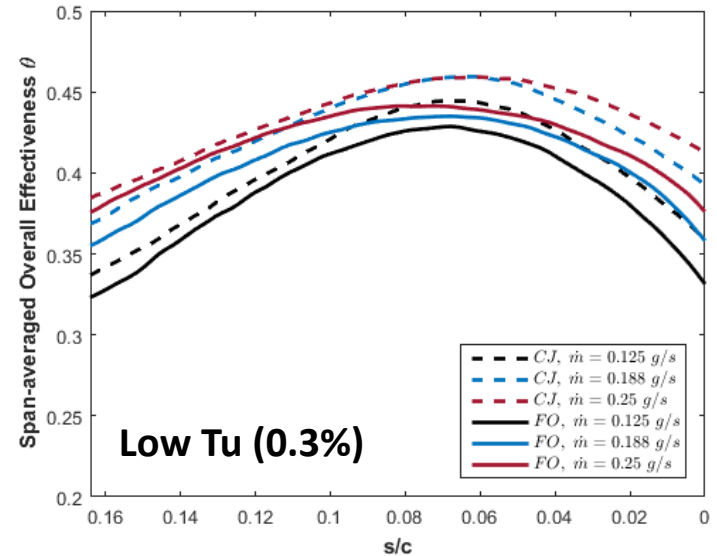
Overall Cooling Effectiveness

- Span-averaged θ profiles show the circular jet cools the surface more effectively
- Sweeping jet has a broader, more uniform cooling profile
- Increasing freestream turbulence has a similar effect on both circular and sweeping jets

Area averaged effectiveness



Span averaged effectiveness

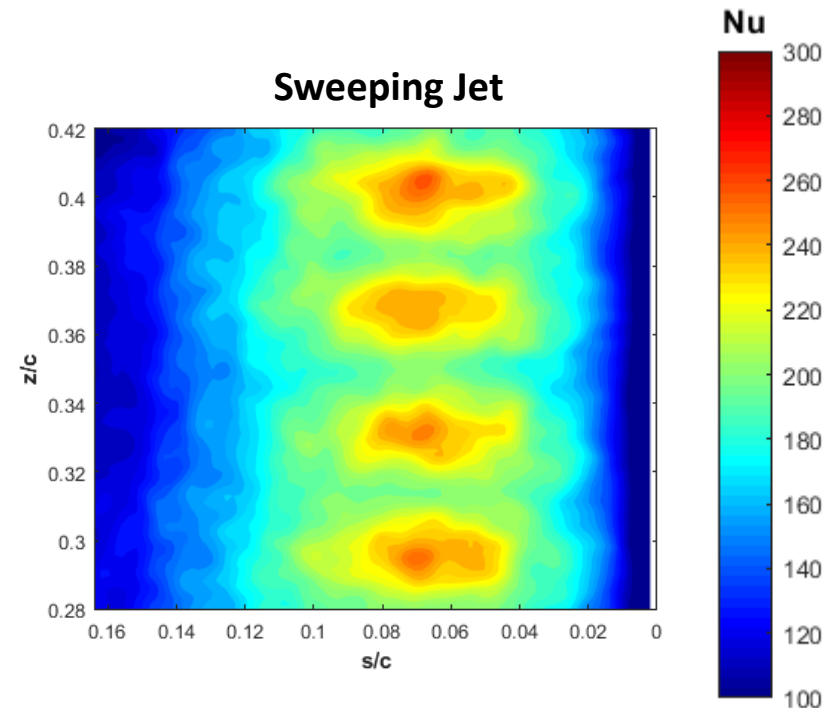
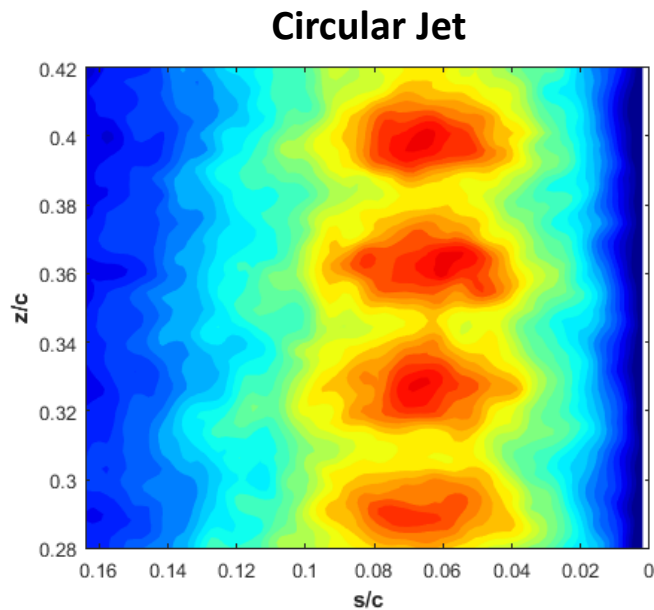




Internal Nusselt Number

- ❑ Calculated with a computational thermal inertia method
 - ❑ Driving coolant temperature, external temperature, and external heat transfer coefficient are known
 - ❑ Measured external surface temperature is applied as a boundary condition on the solid model
 - ❑ Internal heat transfer coefficient is guessed, and updated based on how accurate the predicted external temperature is compared to the measured temperature

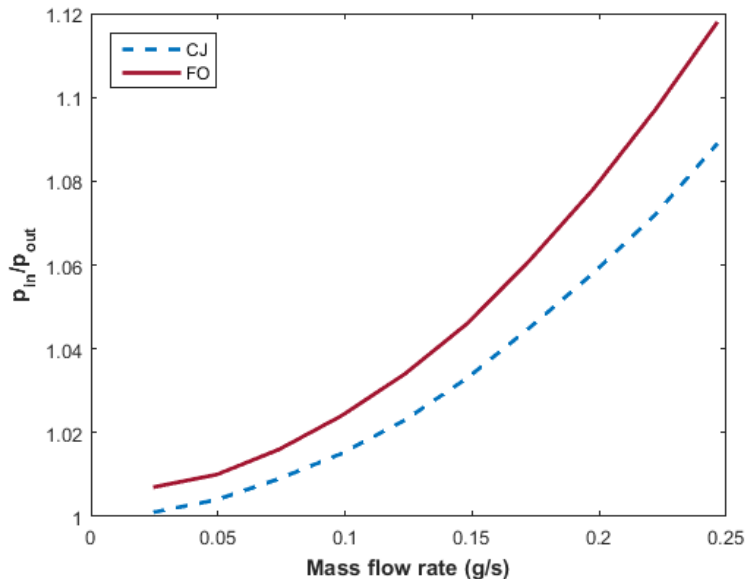
Low Tu (0.3%)



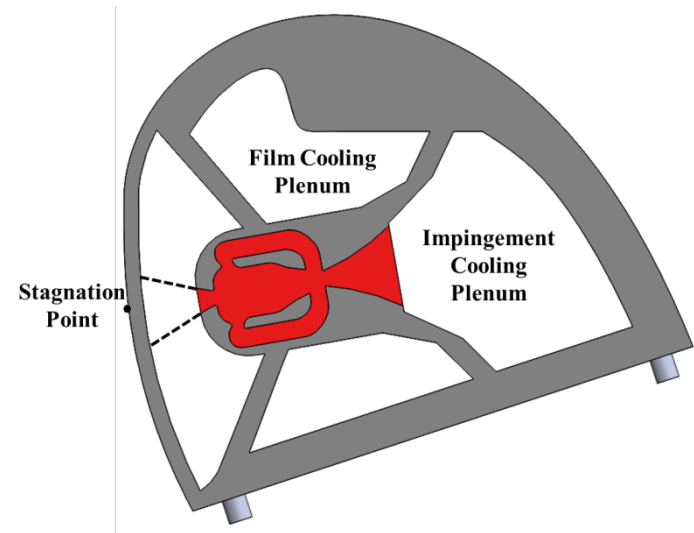


Pressure Drop

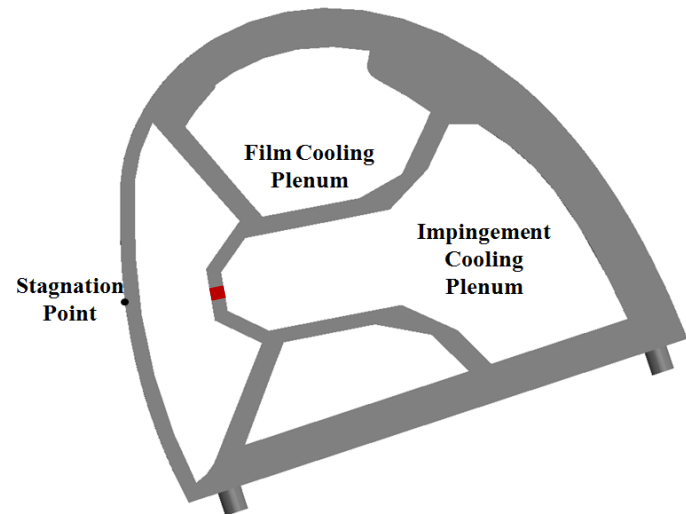
- ❑ Sweeping jet has **HIGHER** pressure drop than circular jets
- ❑ **Opposite of cylinder result**
- ❑ Could be solved with **improved plenum design**, enabled by additive manufacturing



Sweeping jet module



Steady jet module

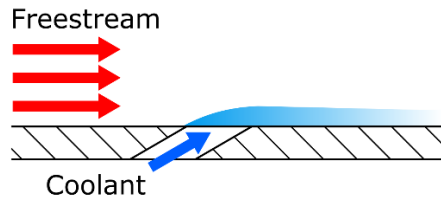




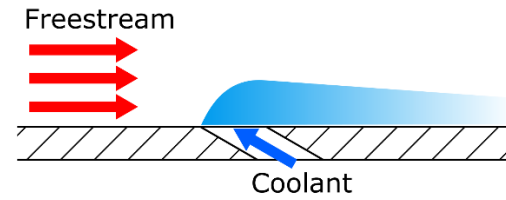
Reverse Film Cooling



Reverse-oriented Film Cooling



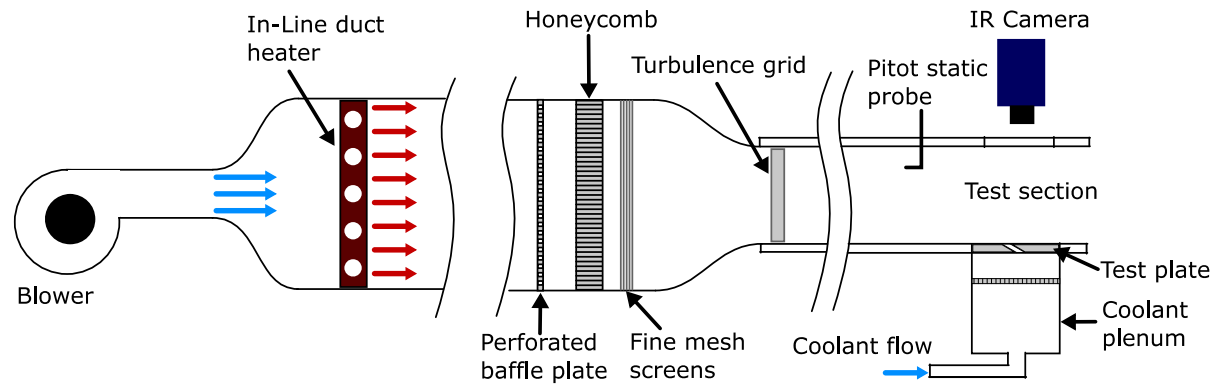
Conventional



Reverse

- ❑ Reverse film cooling has potential to provide a more uniform coolant spread due to the redirection of the coolant flow by the main flow
- ❑ Reverse cooling was studied experimentally and numerically to gain an understanding of the physics behind the interaction in attempt to increase net heat flux benefit

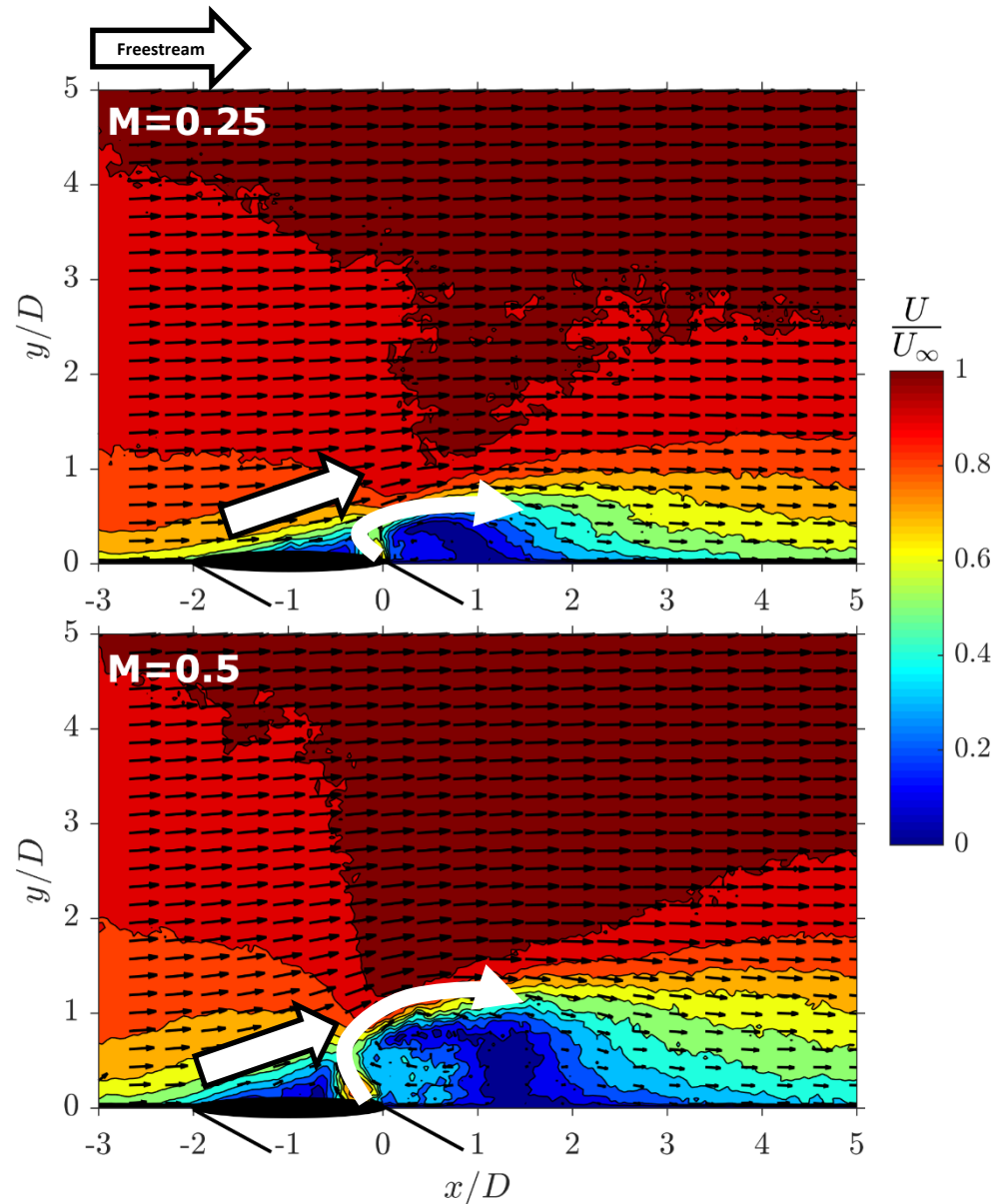
- ❑ Flat plate wind tunnel testing was performed in an open loop wind tunnel





Mid-hole PIV Measurements

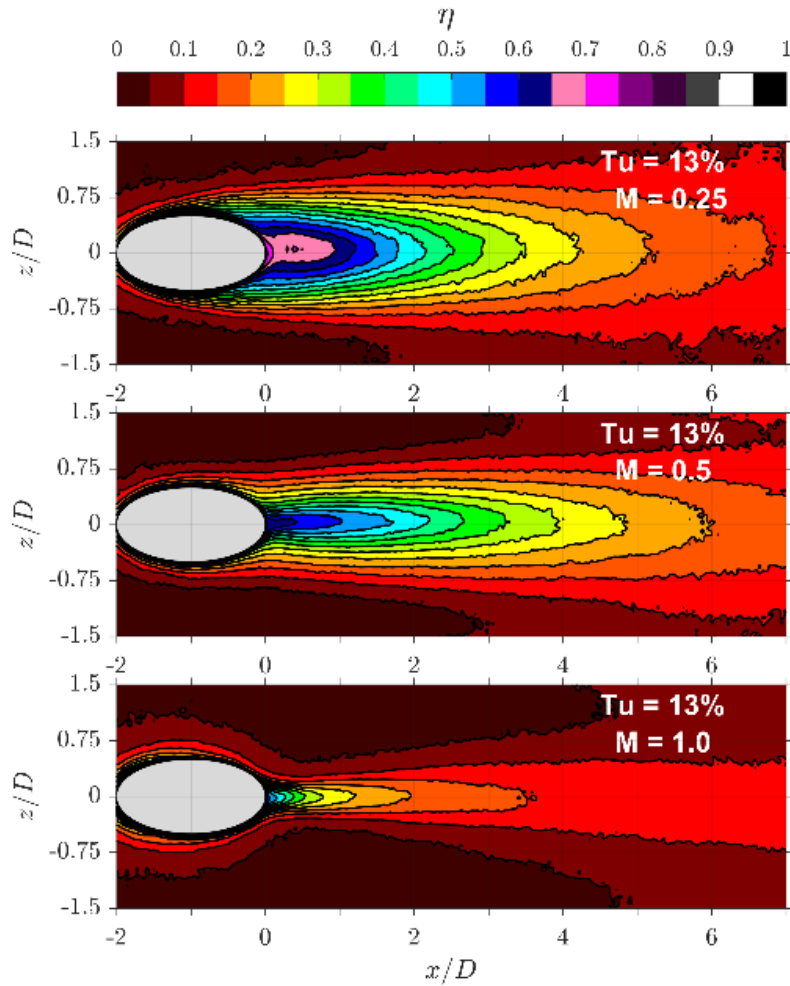
- ❑ Clear high-velocity jetting from the leeward edge of the hole
- ❑ Jetted fluid creates a blockage, accelerating the freestream over the hole
- ❑ Low velocity fluid above the hole, and large recirculation zone downstream of the hole



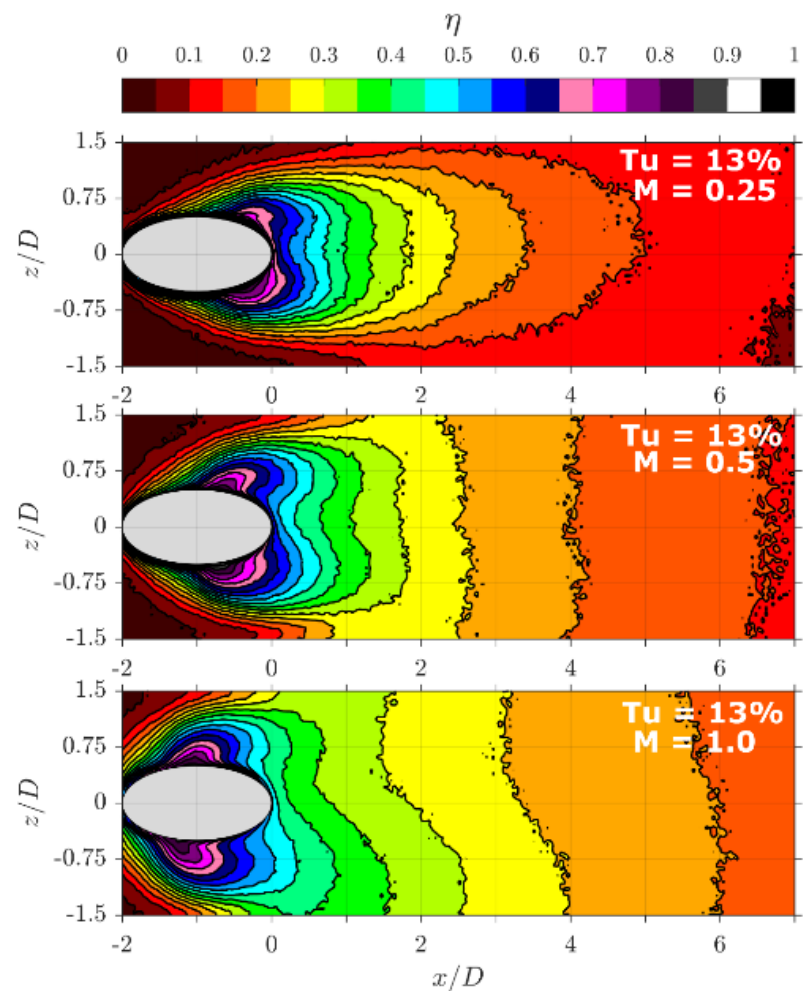


Adiabatic Cooling Effectiveness – High Turbulence

Conventional Cylindrical Cooling



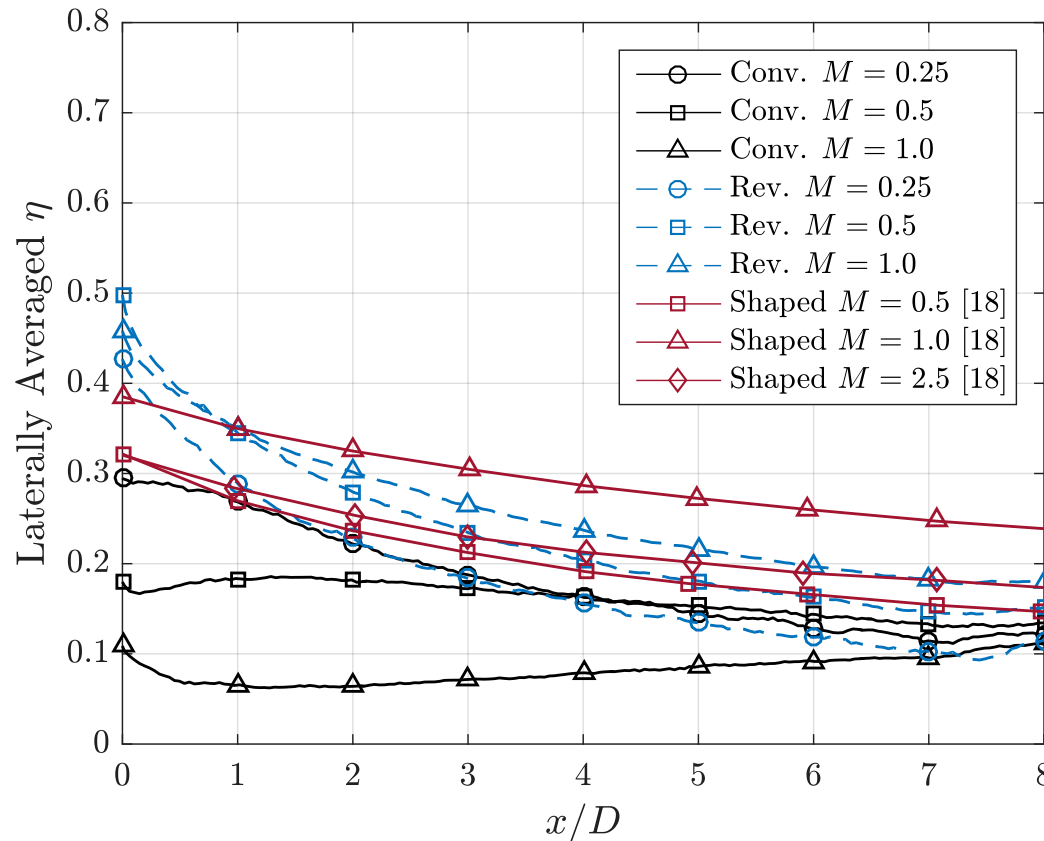
Reverse-oriented Cylindrical Cooling





Adiabatic Cooling Effectiveness

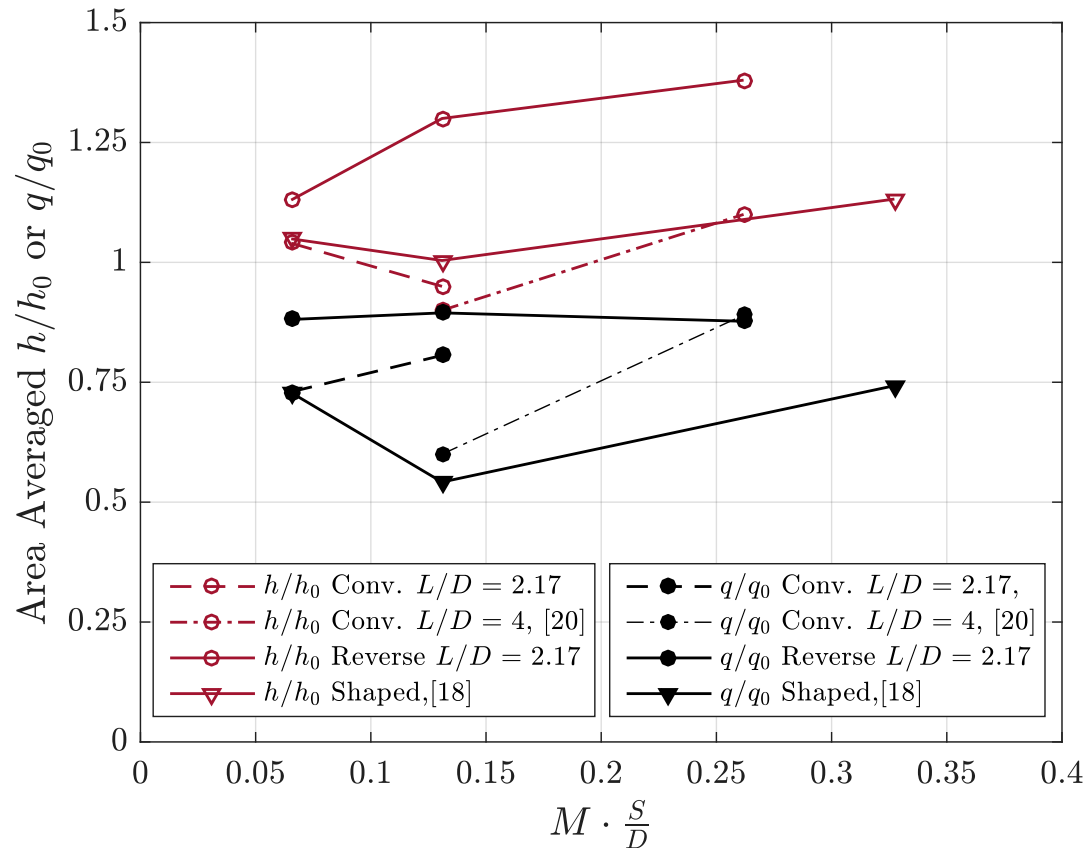
- ❑ Laterally averaged data compared with conventional cylindrical and 777-shaped holes
- ❑ **Reverse cooling shows better performance near the hole, with good coverage downstream**





Area-averaged Heat Transfer Values

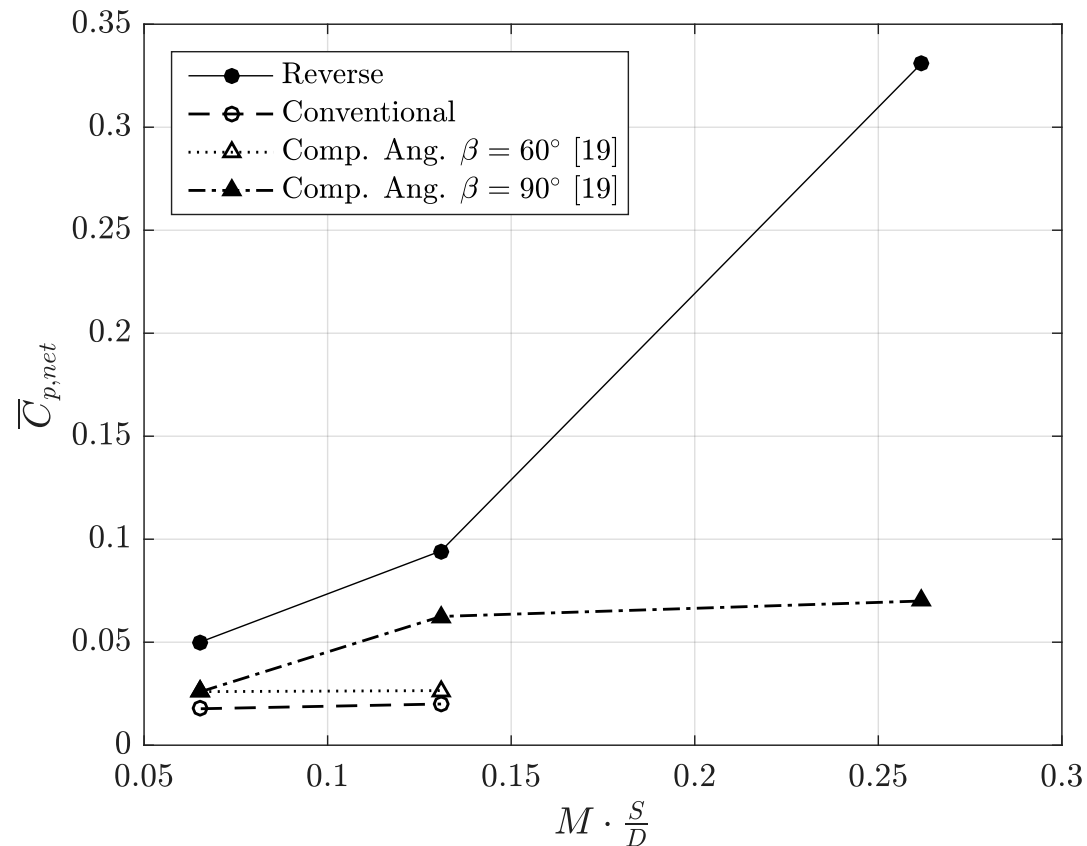
- ❑ Reverse cooling **augments heat transfer coefficient significantly** compared to conventional cooling cases
- ❑ Reverse cooling provides **net heat flux benefit**, but **less than the conventional holes** due to increased h





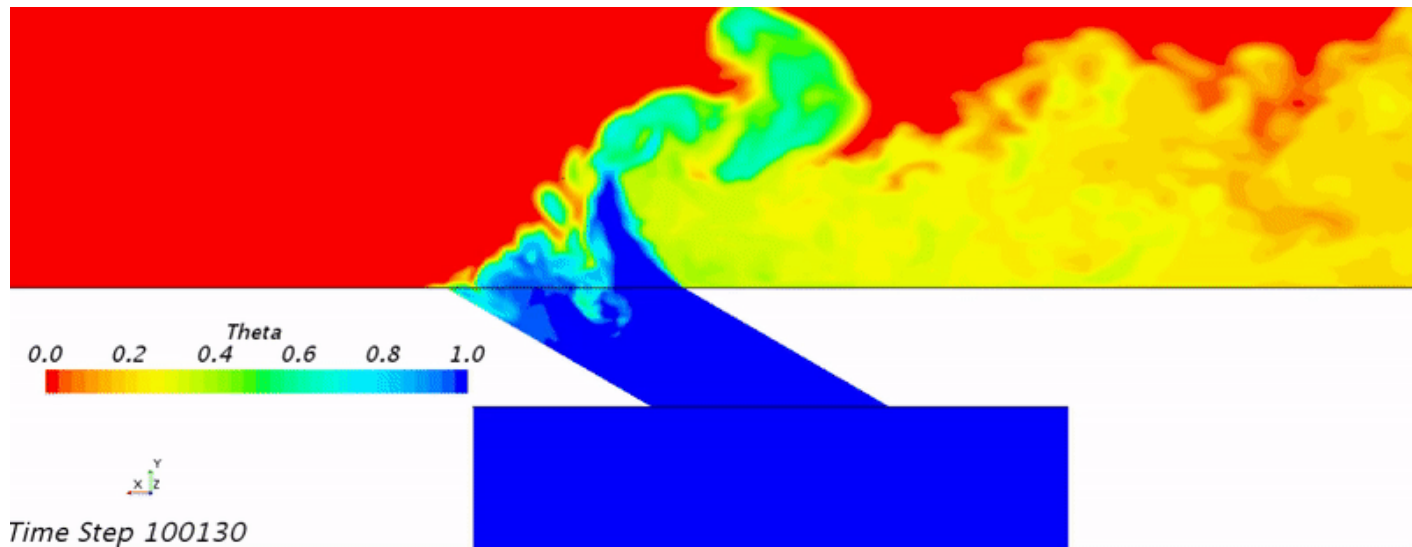
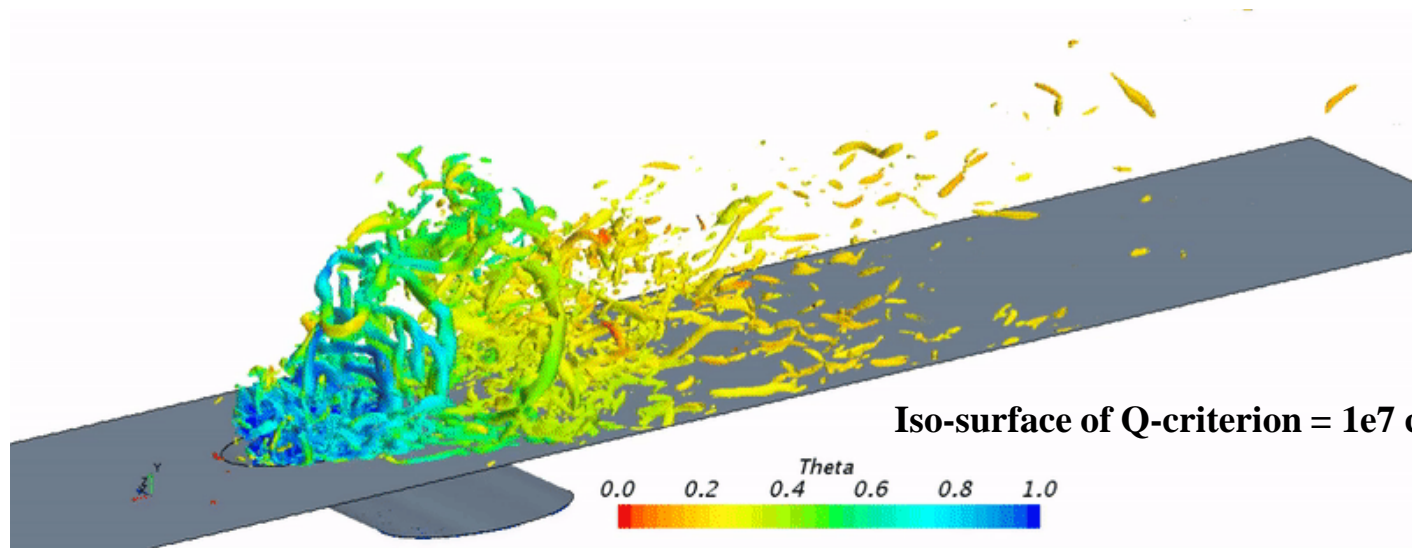
Pressure Loss

- ❑ Pressure loss created by reverse cooling holes was calculated with total pressure taps downstream
- ❑ Follows trend of increasing pressure loss with increasing compound angle





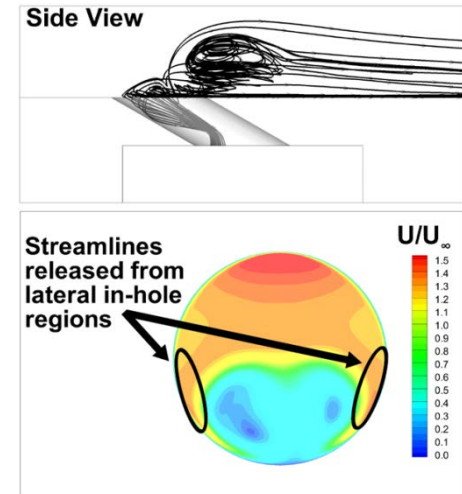
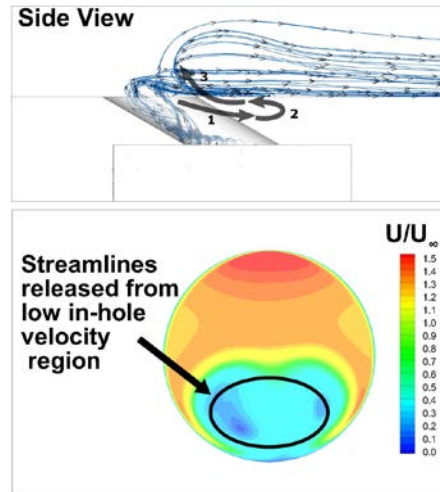
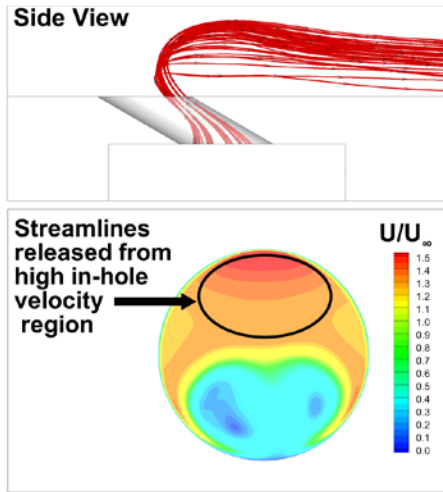
LES Computations – Flow Visualizations





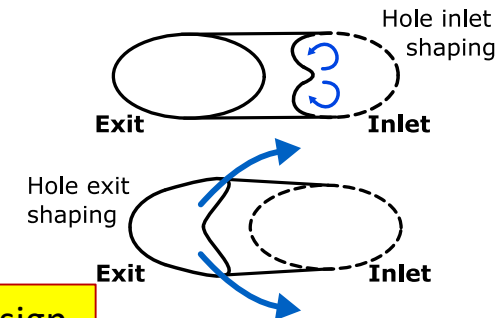
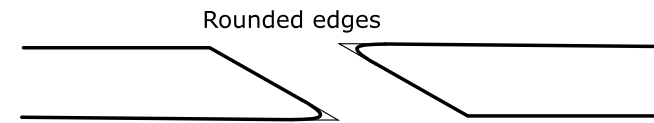
Physical Understanding

- ❑ Goal of the computations was to gain a better understanding of the hole flow physics so that design changes could be made to improve reverse cooling



Geometric Optimization Concepts

- ❑ Round hole edges to control separation
- ❑ Shape the inlet to induce vorticity to help spread coolant
- ❑ Shape the exit to guide coolant to better coverage



Some geometries may require reverse flow design

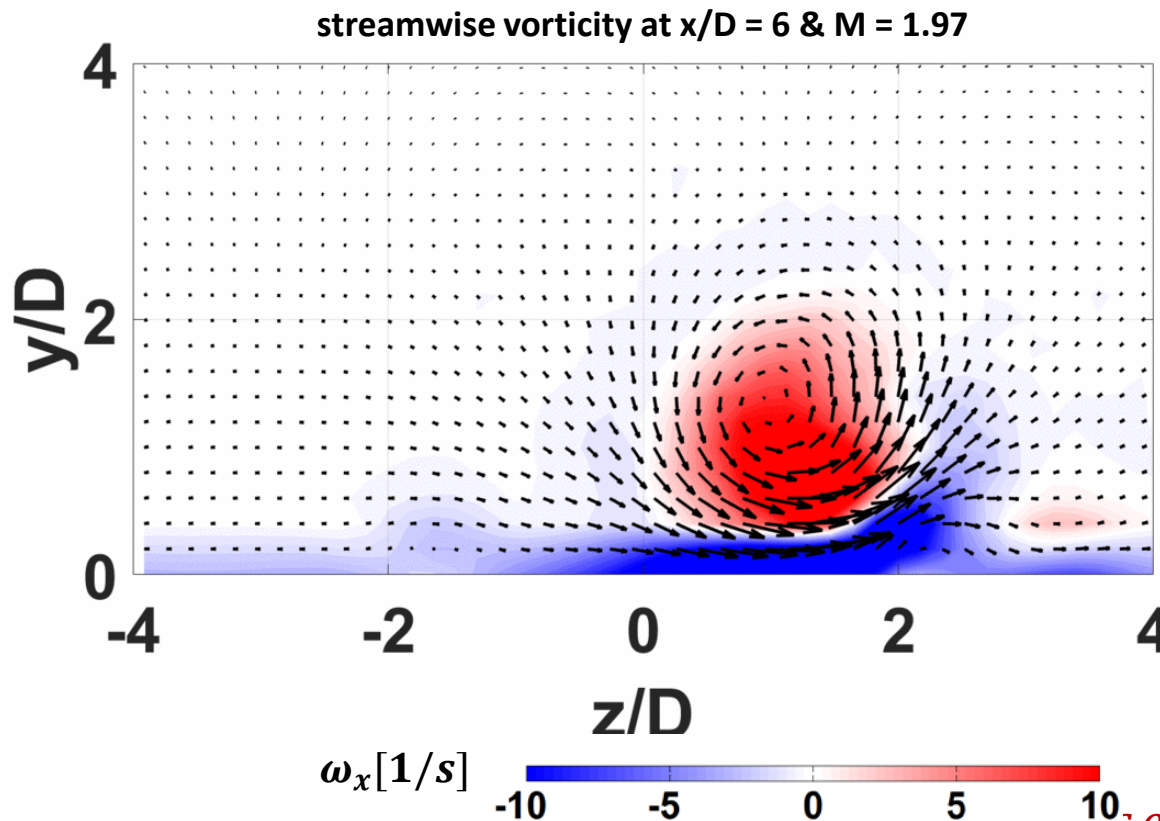


Sweeping Jet Film Cooling



Preliminary Flow Field Analysis (CFD)

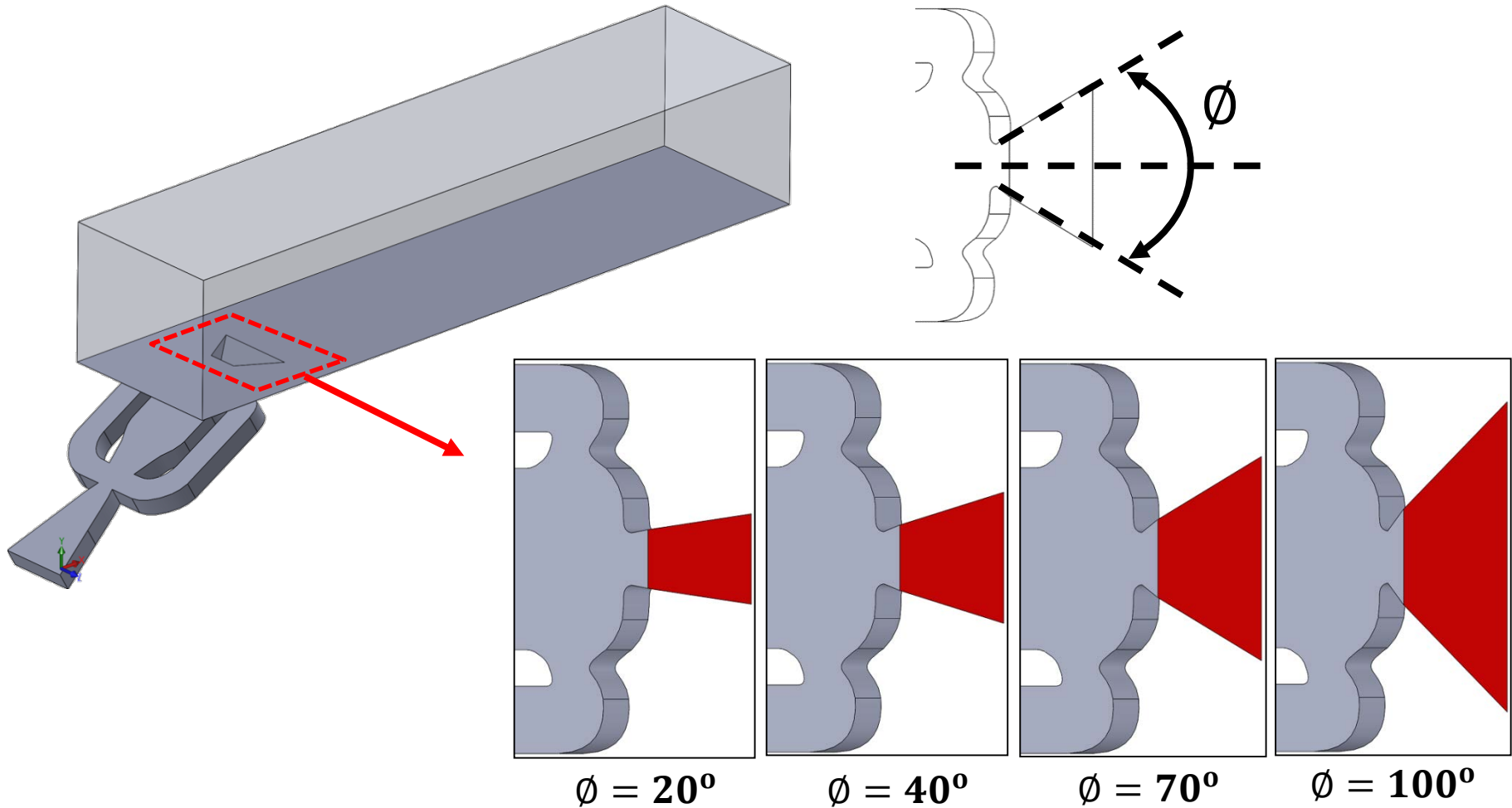
- ❑ Unsteady RANS simulation was performed to evaluate the time averaged and time accurate flow field at the down stream of the hole.
- ❑ The time averaged flow field is **deceiving** since it would suggest that the SJ vortices mutually induce each other to the wall.
- ❑ The jet acts as a **vortex generator** as it interacts with the freestream.





Effect of Exit Fan Angle for Film Cooling(CFD)

- ❑ Four different exit angles have been studied for sweeping jet film cooling hole.
- ❑ Distance between hole leading edge and trailing edge was kept constant.



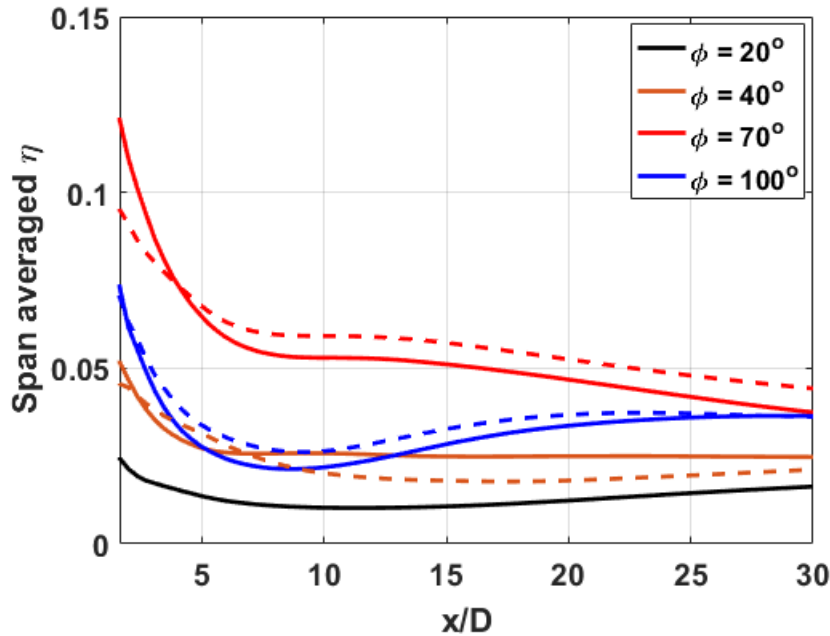


Effect of Exit Fan Angle for Film Cooling(CFD)

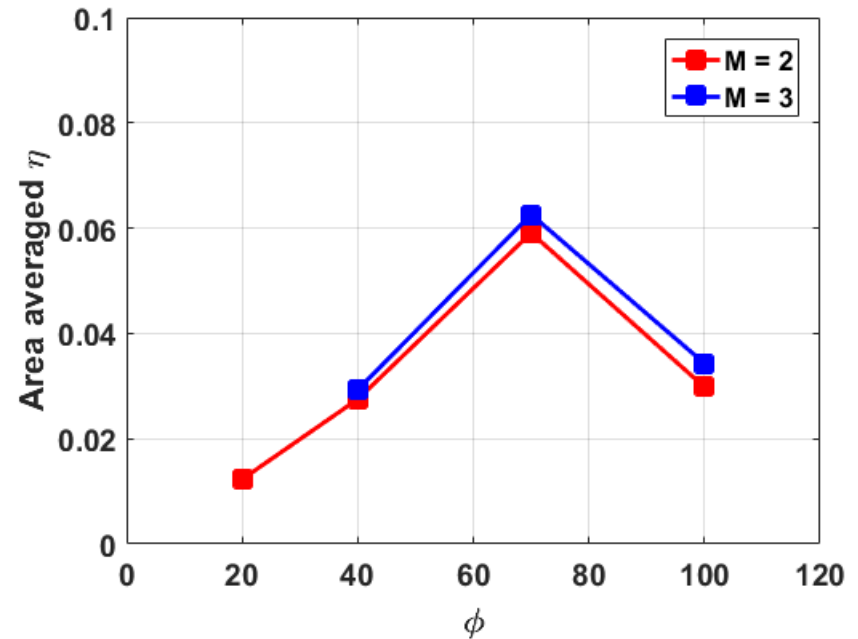
- ❑ Data were averaged over the hole pitch ($P/D = 8.5$).
- ❑ Hole with **70 degree fan angle shows the highest area averaged film effectiveness.**

Span averaged film effectiveness

— M = 2 - - M = 3



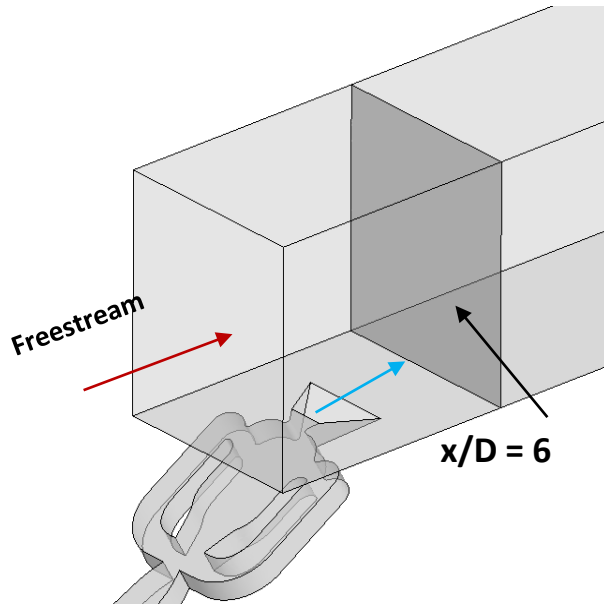
Area averaged film effectiveness



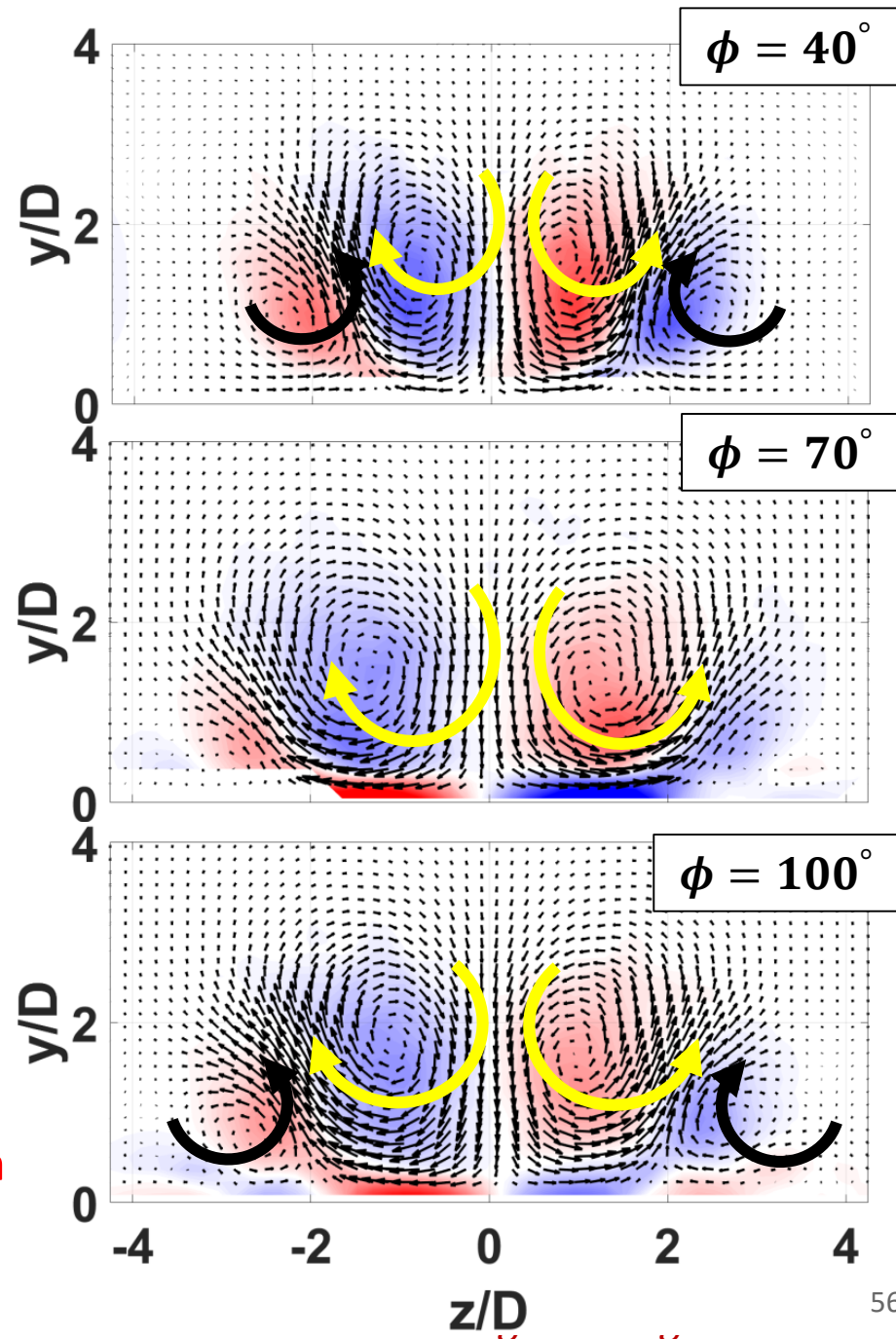


Effect of Exit Fan Angle (CFD)

- ❑ Cross plane velocity fields are shown at $x/D = 6$
- ❑ Two CRVPs have been observed for $\phi = 40^\circ$ and $\phi = 100^\circ$ case.



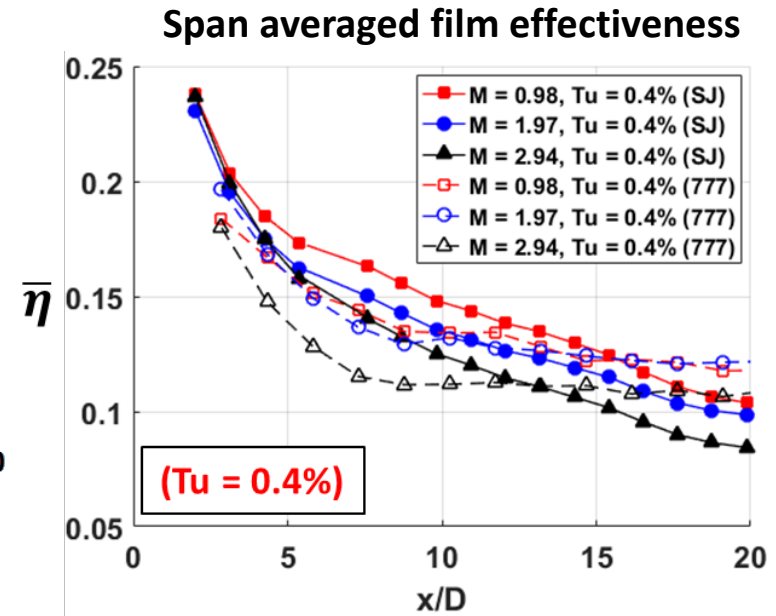
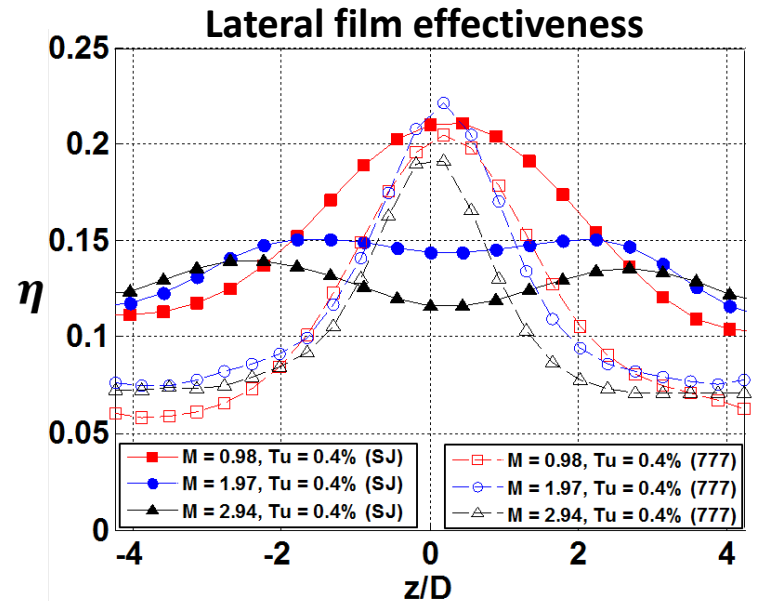
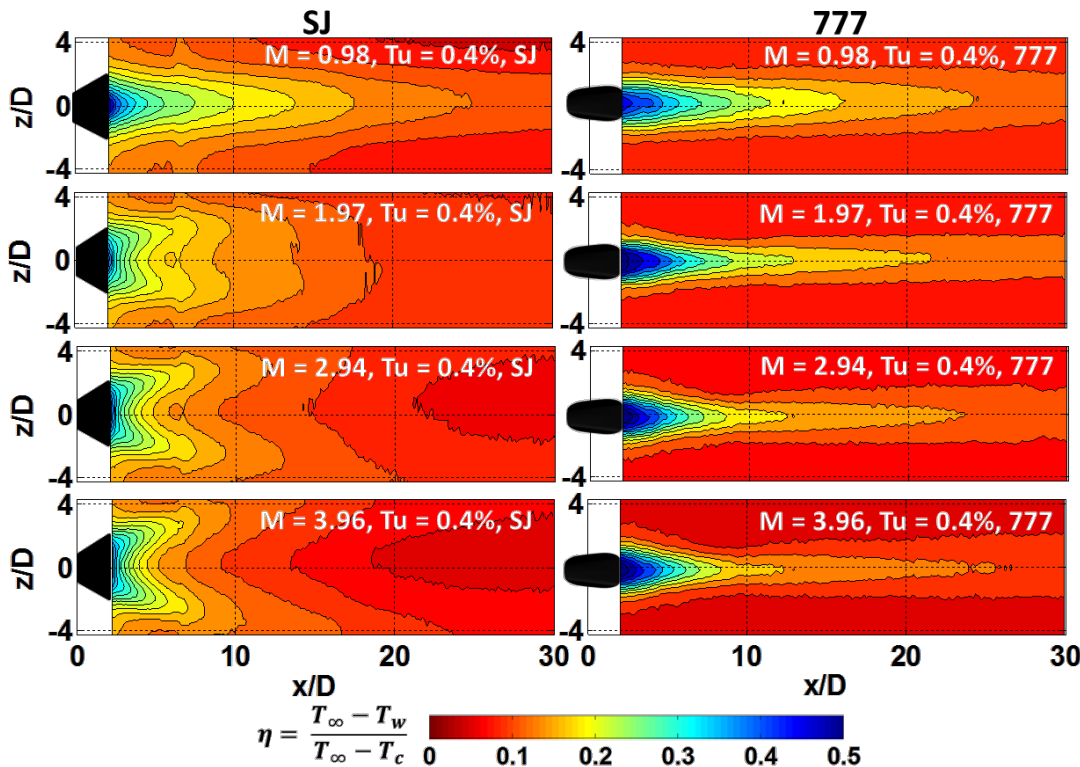
$\phi = 70^\circ$ was considered for final design





Preliminary Hole Design (Flat plate test)

- ❑ The SJ hole exhibits **higher** span averaged effectiveness at the **near hole region** ($x/D < 15$).
- ❑ SJ hole film effectiveness is more **uniform** along the span.





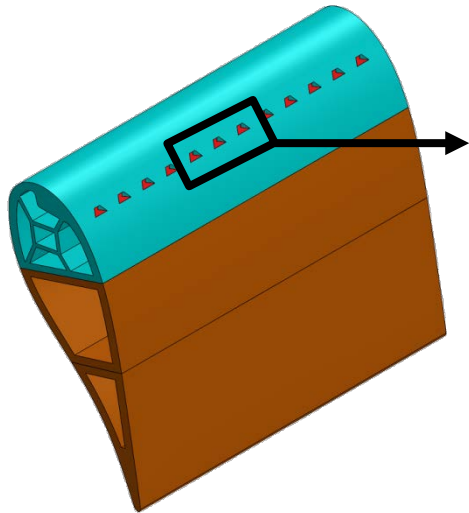
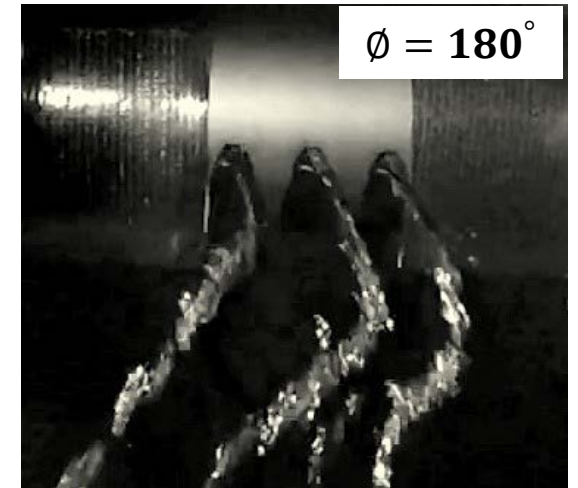
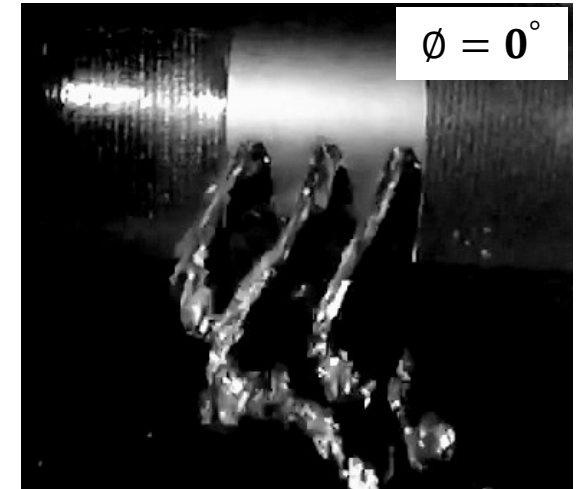
Vane Flow Visualization

- ❑ Water flow visualization shows uniform oscillation at each hole.

Time accurate



Instantaneous



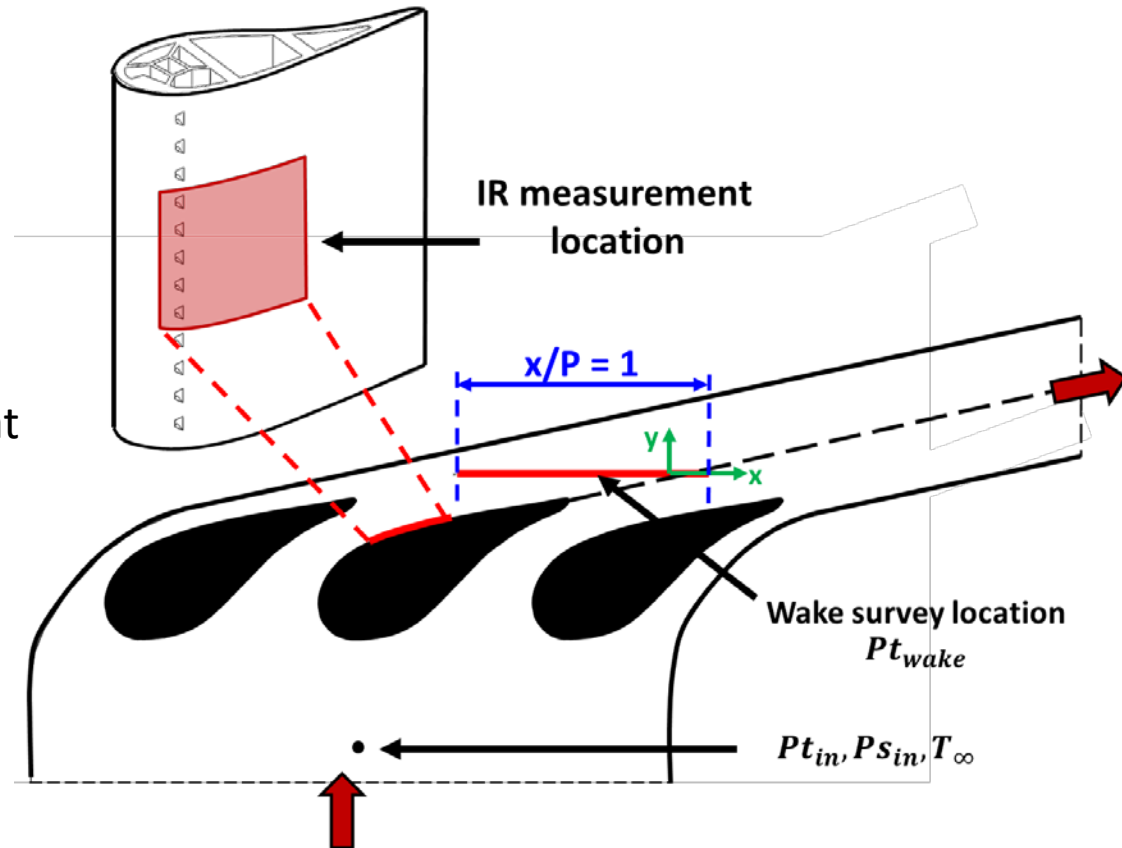
Measurement Location

- ❑ Transient IR measurements were taken at the mid-span of the vane. The measurement area covers five holes.

- ❑ Heat transfer measurement were taken at –
 - $Tu = 0.3\%$,
 - $M = 0, 0.5, 1.0, 1.5$.

- ❑ Wake survey was performed at $0.1C$ downstream of the vane over a single pitch.

- ❑ Wake survey was performed at –
 - $Tu = 0.3\%, 6.1\%$
 - $M = 0, 0.5, 1.0, 1.5$.



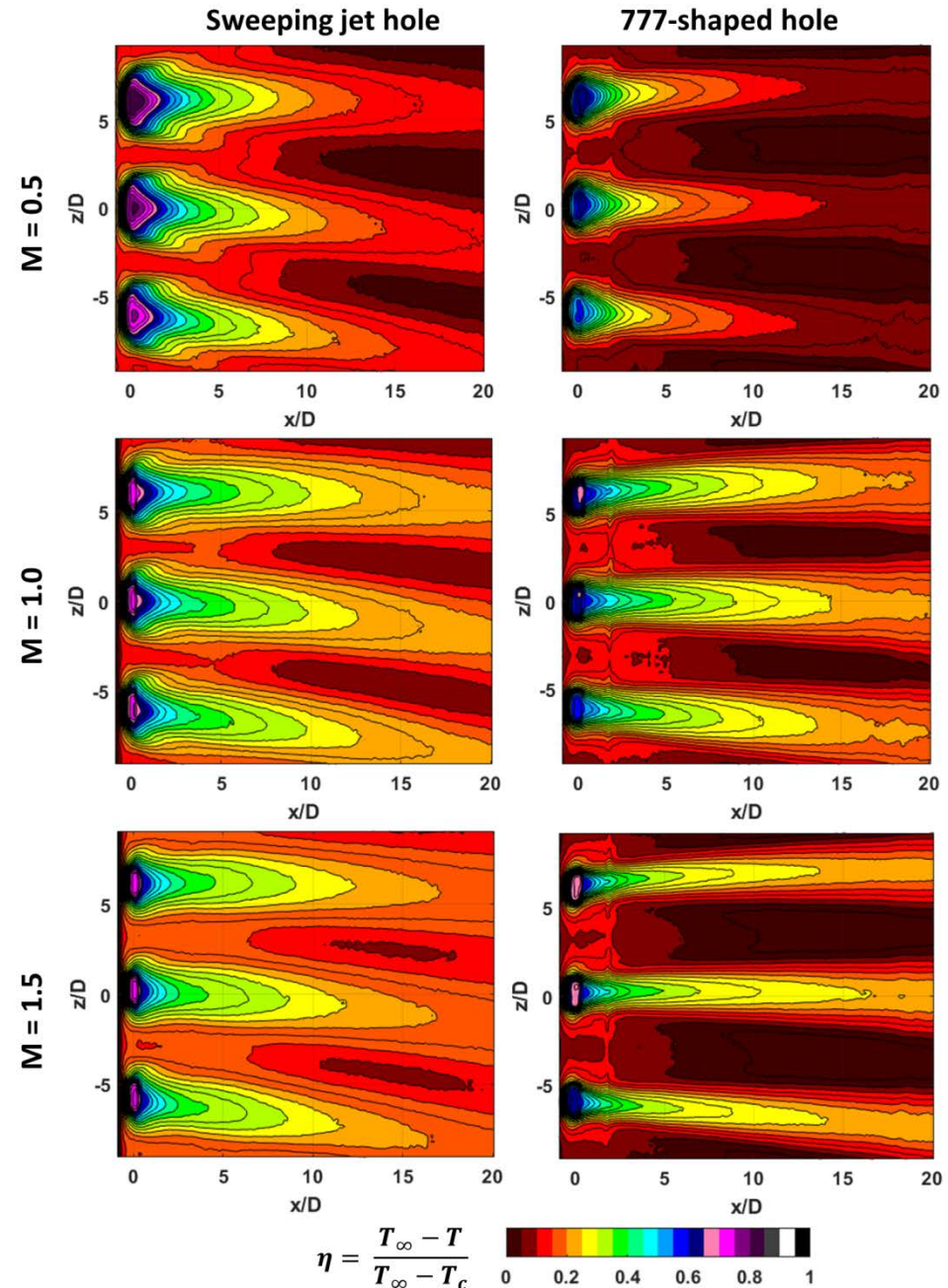


Cooling Effectiveness (η vs 777) at $Tu = 0.3\%$

- Cooling effectiveness was estimated at three different blowing ratios ($M = 0.5, 1.0, 1.5$)

$$\eta = \frac{T_\infty - T}{T_\infty - T_c}$$

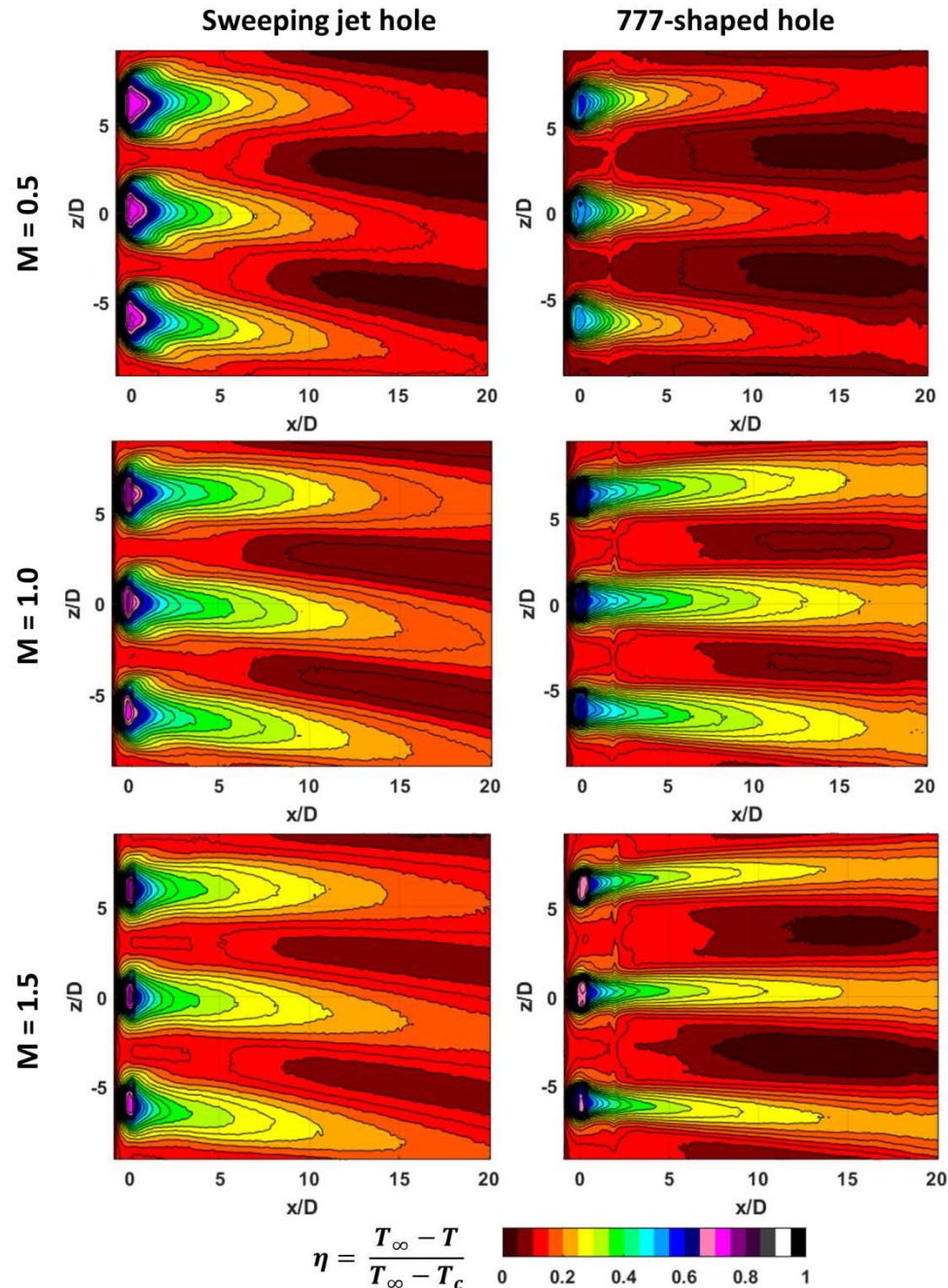
- At low blowing ratio ($M = 0.5$), a high cooling effectiveness was observed in the near hole region for SJ hole.
- As blowing ratio increases, the cooling effectiveness increases downstream and drops again at the highest blowing ratio ($M = 1.5$)
- Cooling performance of the 777-shaped hole similar to flat plate.





Cooling Effectiveness (η vs 777) at $Tu = 6.1\%$

- ❑ Turbulence increases lateral spreading of the coolant for 777 hole.
- ❑ Turbulence increases mixing, thus a reduced film effectiveness was observed at all blowing ratios for SJ hole.



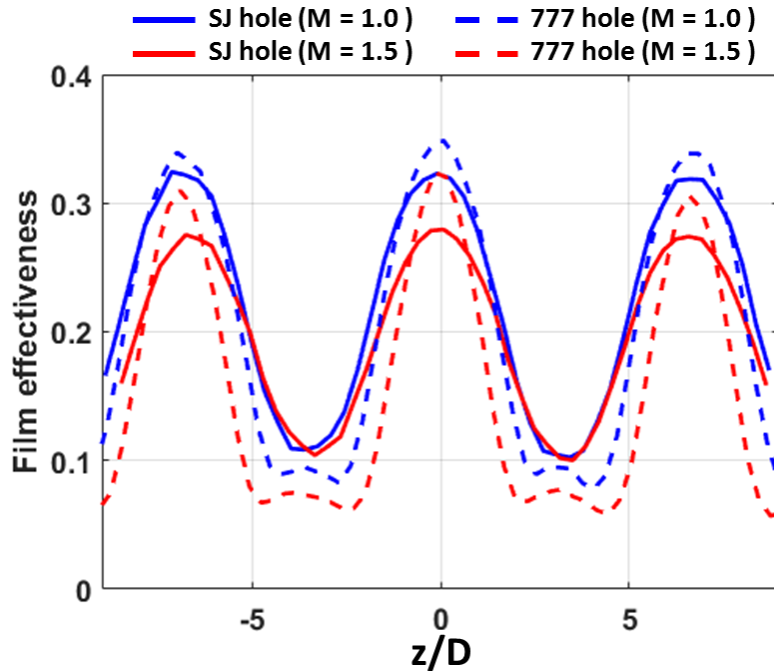
$$\eta = \frac{T_{\infty} - T}{T_{\infty} - T_c}$$



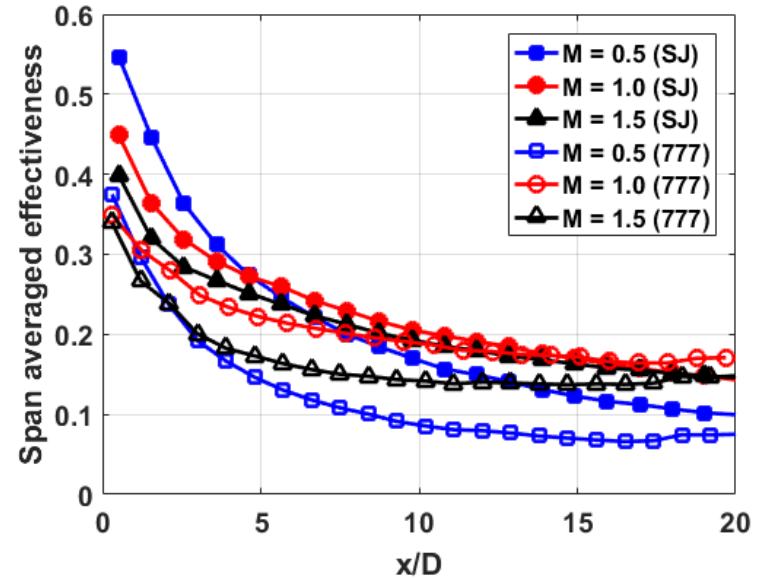
Span averaged Cooling Effectiveness

- Span averaged cooling effectiveness was estimated at three different blowing ratios ($M = 0.5, 1.0, 1.5$)
- Sweeping jet hole shows **higher cooling effectiveness** in the near hole region compared to 777-hole.

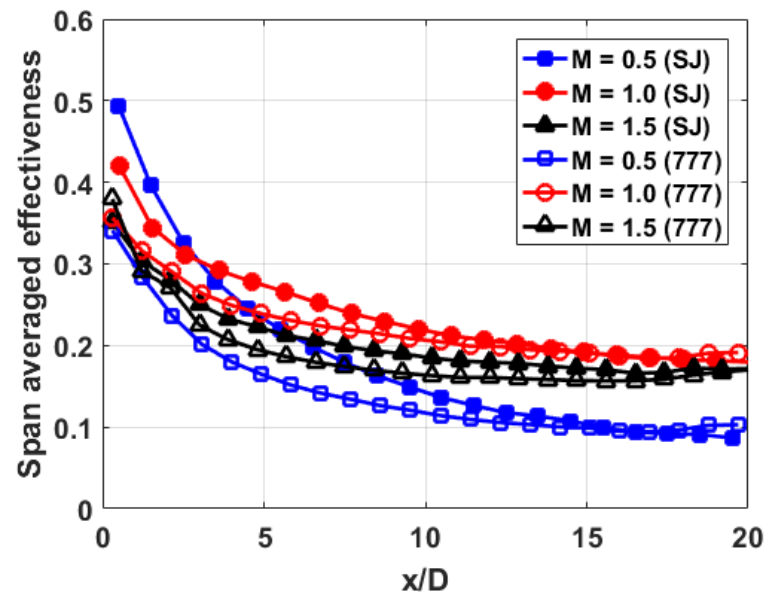
Lateral effectiveness



Span averaged ($Tu = 0.3\%$)



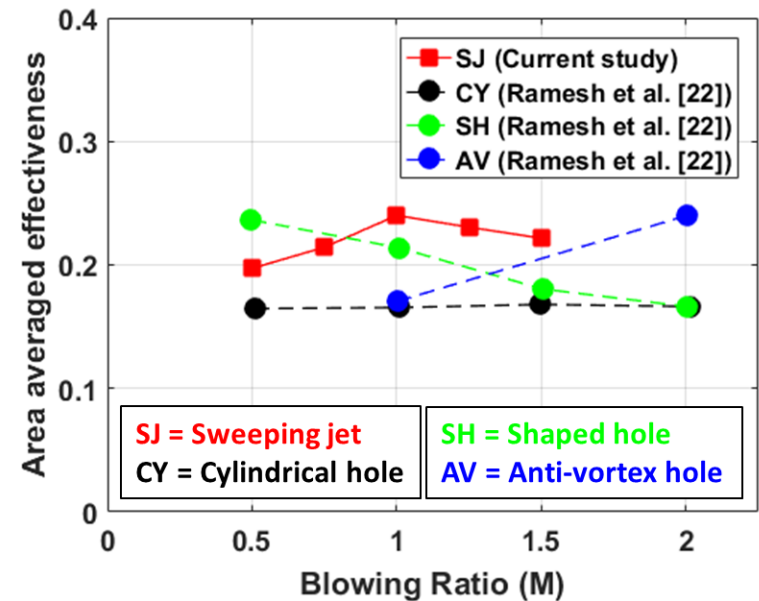
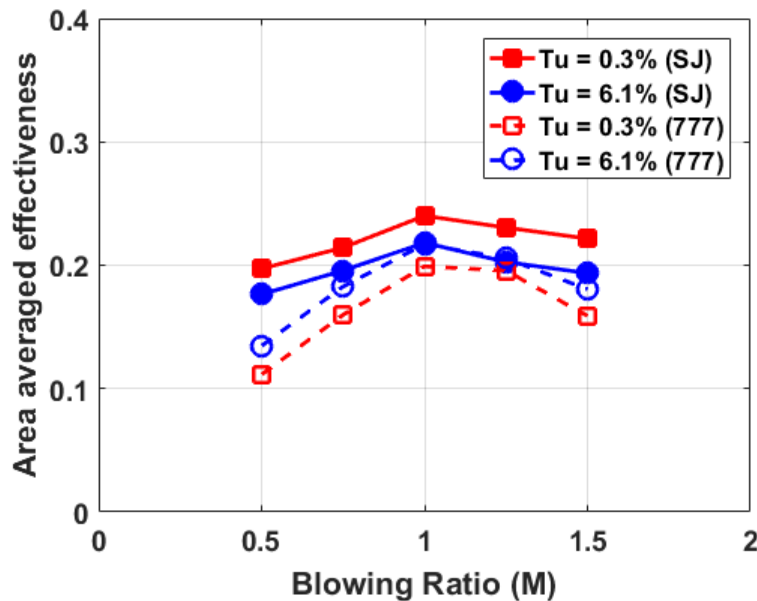
Span averaged ($Tu = 6.1\%$)





Area averaged Cooling Effectiveness

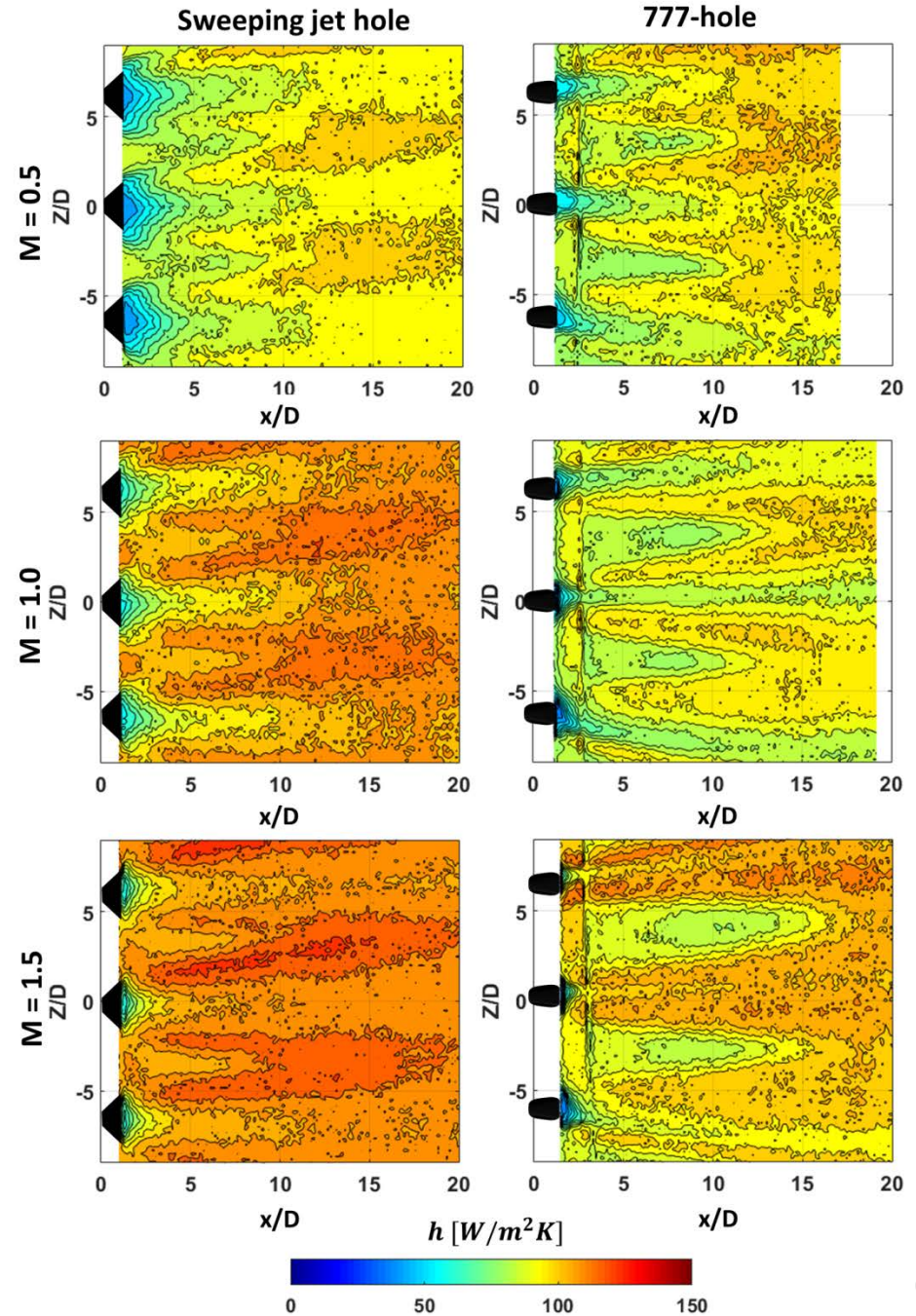
- ❑ Data were averaged over 20 hole diameter in the streamwise direction and three hole pitch (18D) in the spanwise direction.
- ❑ **Sweeping jet hole shows higher $\bar{\eta}$** compared to 777-holes at all blowing ratios
- ❑ The area averaged film effectiveness data for SJ are compared with cylindrical hole (CY), shaped hole (SH), and anti-vortex hole (AV) in a similar low speed cascade experiment performed by Ramesh et. al. [2017].
- ❑ Note that the vane geometry ($GE E^3$) used in their study is different from the current geometry





Heat Transfer Coefficient

- ❑ Transient experiments were performed at three different blowing ratios ($M = 0.5, 1$ and 1.5) and $Tu = 0.3\%$.
- ❑ The convective heat transfer coefficient was then estimated using Duhamel's superposition principle
- ❑ SJ shows a **high values of convective heat transfer coefficient** compared to 777-shaped hole.
- ❑ The unsteady interaction between the shear layers of two coolant streams probably causes this augmentation of h .



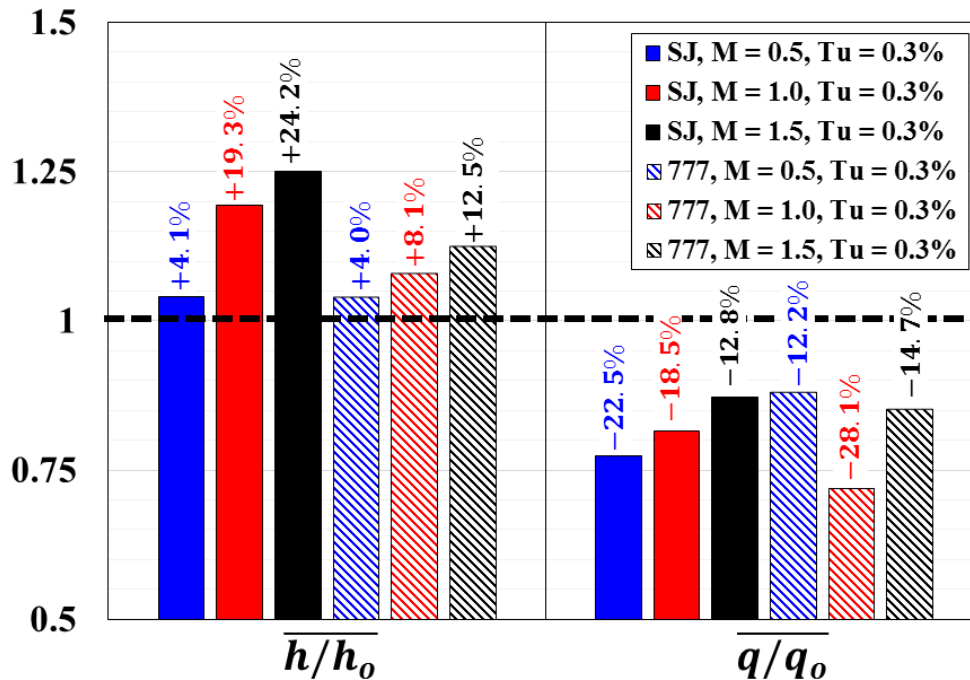
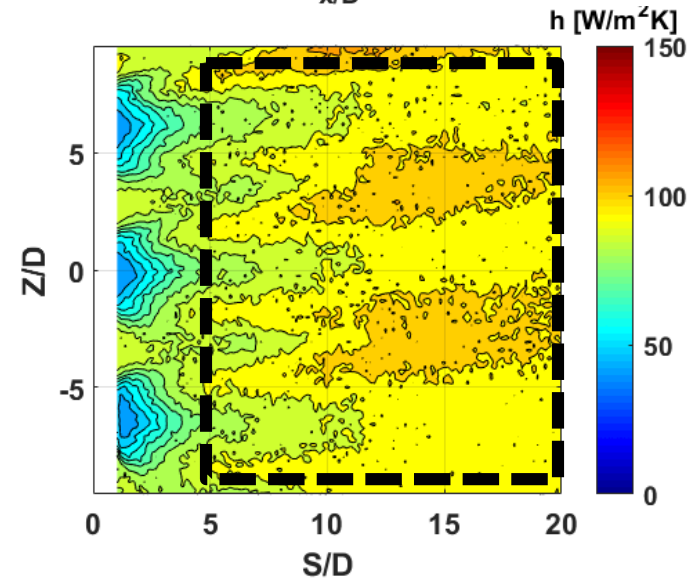
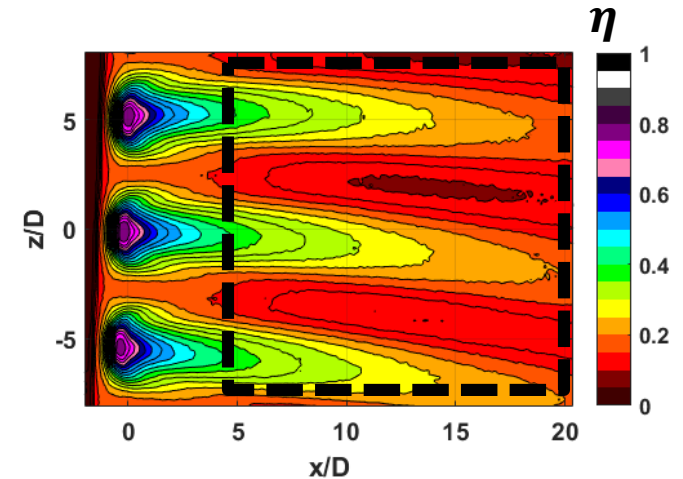


Net Heat Flux Reduction

- Heat transfer augmentation depends on both the heat transfer coefficient ratio and adiabatic film effectiveness.
- Results show approximately 18% improvement in overall cooling benefit at M = 1.0 for SJ hole.

$$\frac{q}{q_o} = \frac{h}{h_o} \left(1 - \frac{\eta}{\phi} \right)$$

Here, $\phi = 0.6$



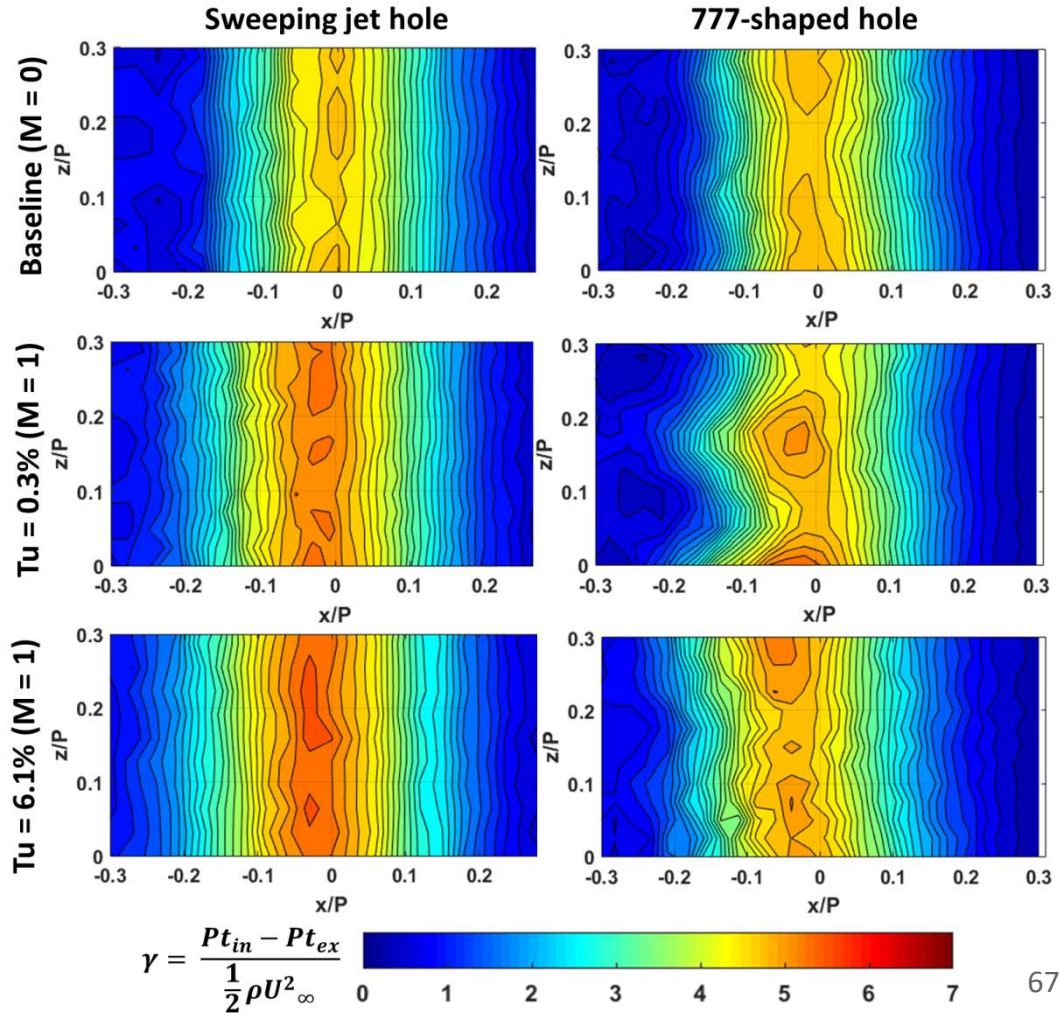
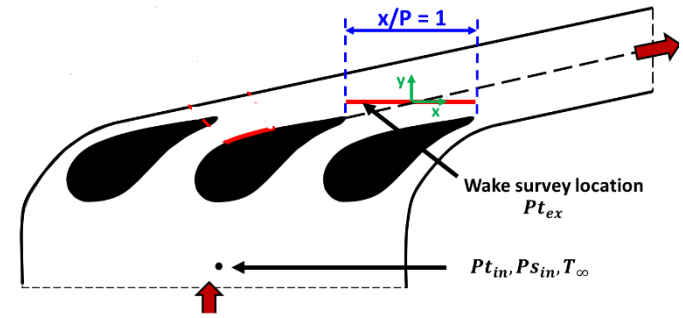


Total Pressure Loss Measurement (2D Grid)

- A wake survey was performed in a 127 mm x 51 mm plane normal to the vane span at 0.1C downstream of the vane trailing edge
- A wake total pressure loss coefficient (γ) was then estimated.

$$\gamma = \frac{Pt_{in} - Pt_{ex}}{\frac{1}{2} \rho U_{\infty}^2}$$

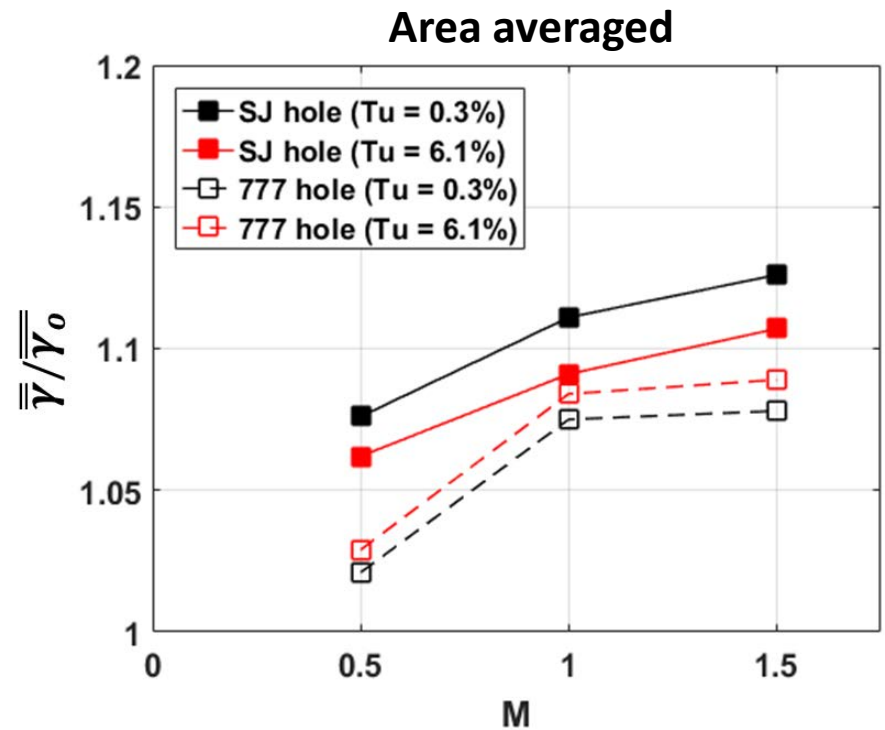
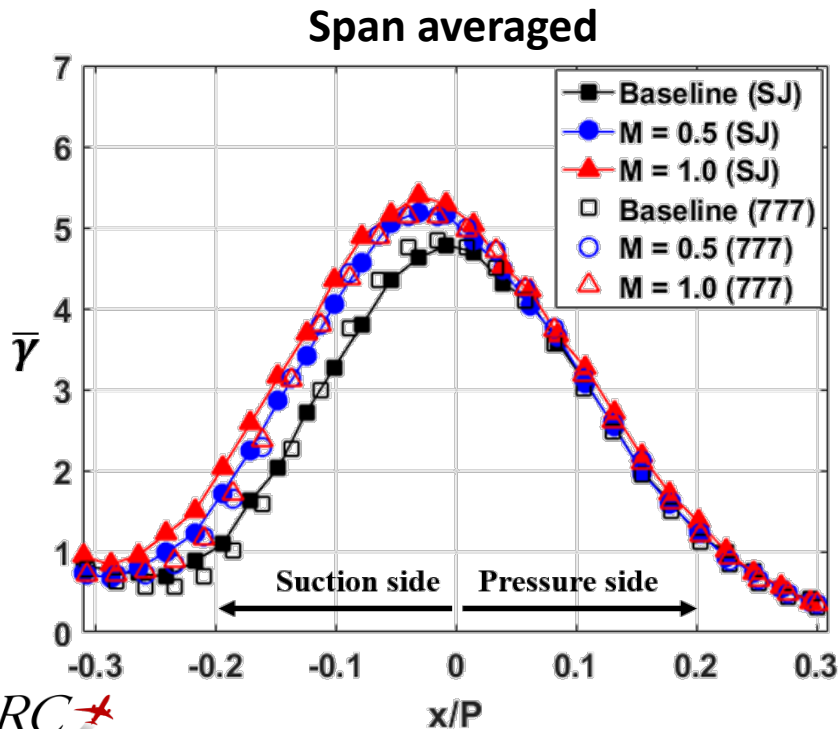
- SJ hole shows a uniform increase of γ along the span due to sweeping action of the coolant.





Total Pressure Loss Measurement

- Span averaged loss coefficient ($\bar{\gamma}$) for SJ and 777-shaped hole.
- The baseline data implies the span averaged loss coefficient ($\bar{\gamma}_0$) without any coolant flow.
- An increase in $\bar{\gamma}$ on the suction side implies additional aerodynamics loss due to coolant flow.
- It is also evident that SJ hole generates **more aerodynamic losses** compared to 777-hole at all blowing ratios.

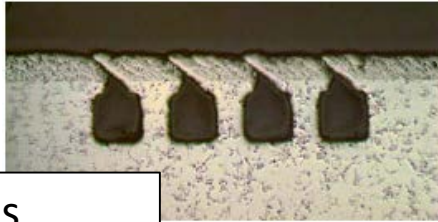




Trailing Edge Cooling

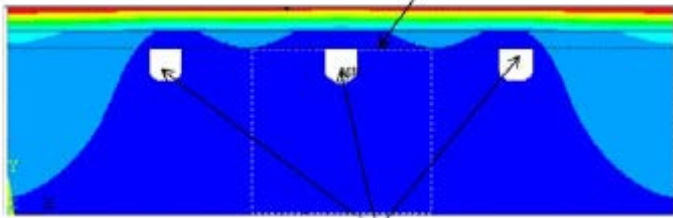


Trailing Edge Cooling



Microchannels provide unparalleled coverage.
Bunker (IGTI 2013)

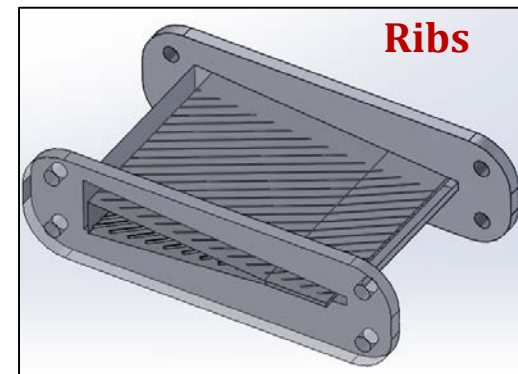
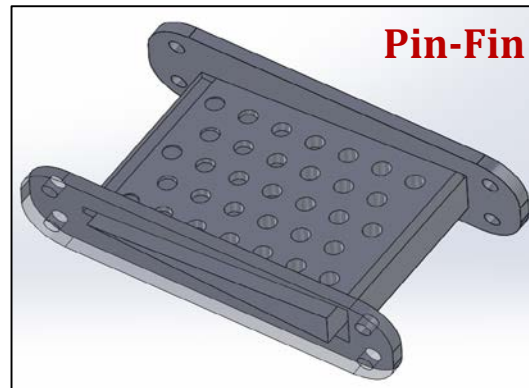
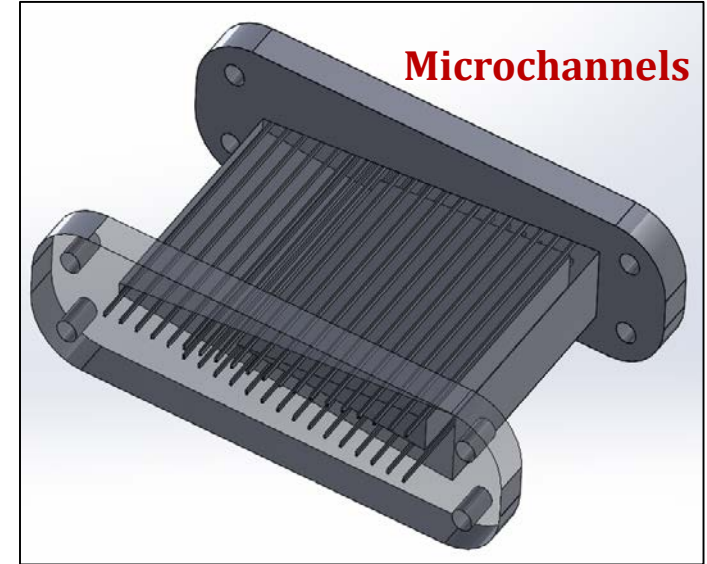
Substrate Bulk T averaging region inside box



0.51 mm TBC
0.38 mm NiCrAlY bondcoat
3.43 mm Ni alloy substrate

Keep the coolant where it is needed – at the surface!!

Concept to capitalize on AM



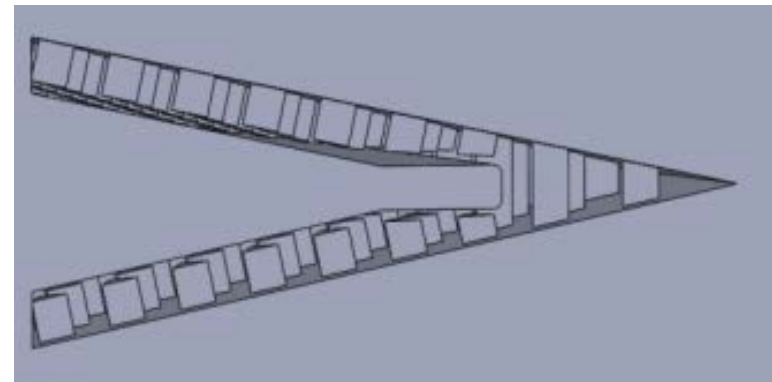
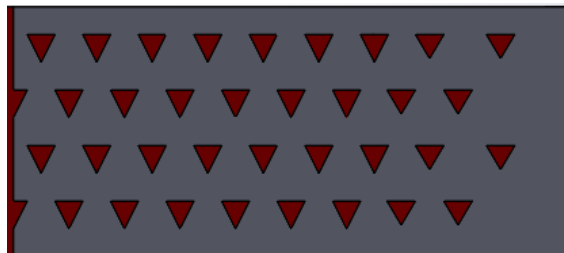
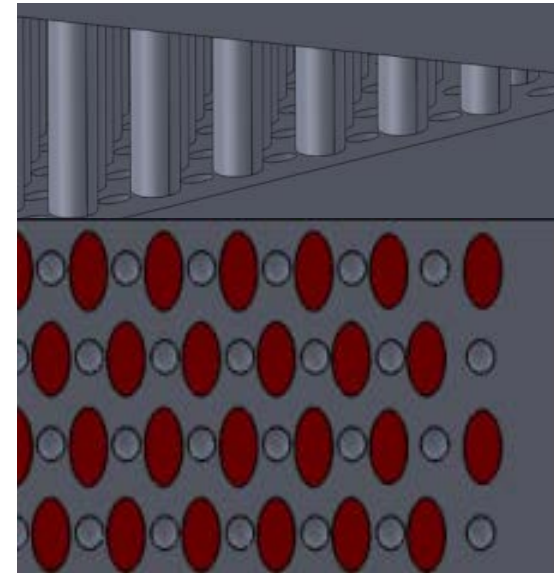
Excessive Pressure Drop and Mediocre Cooling ☹️



Trailing Edge Cooling AM Concepts

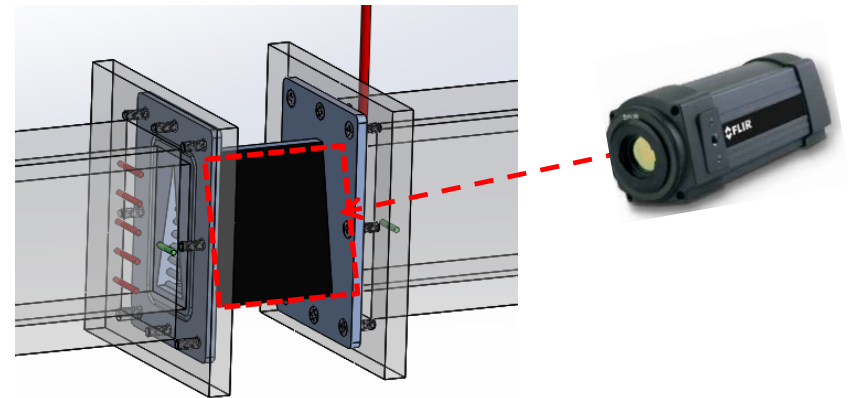
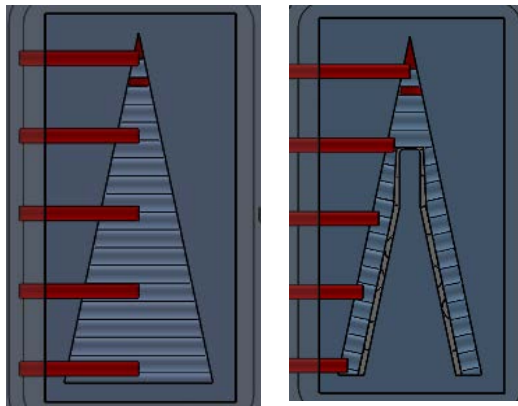
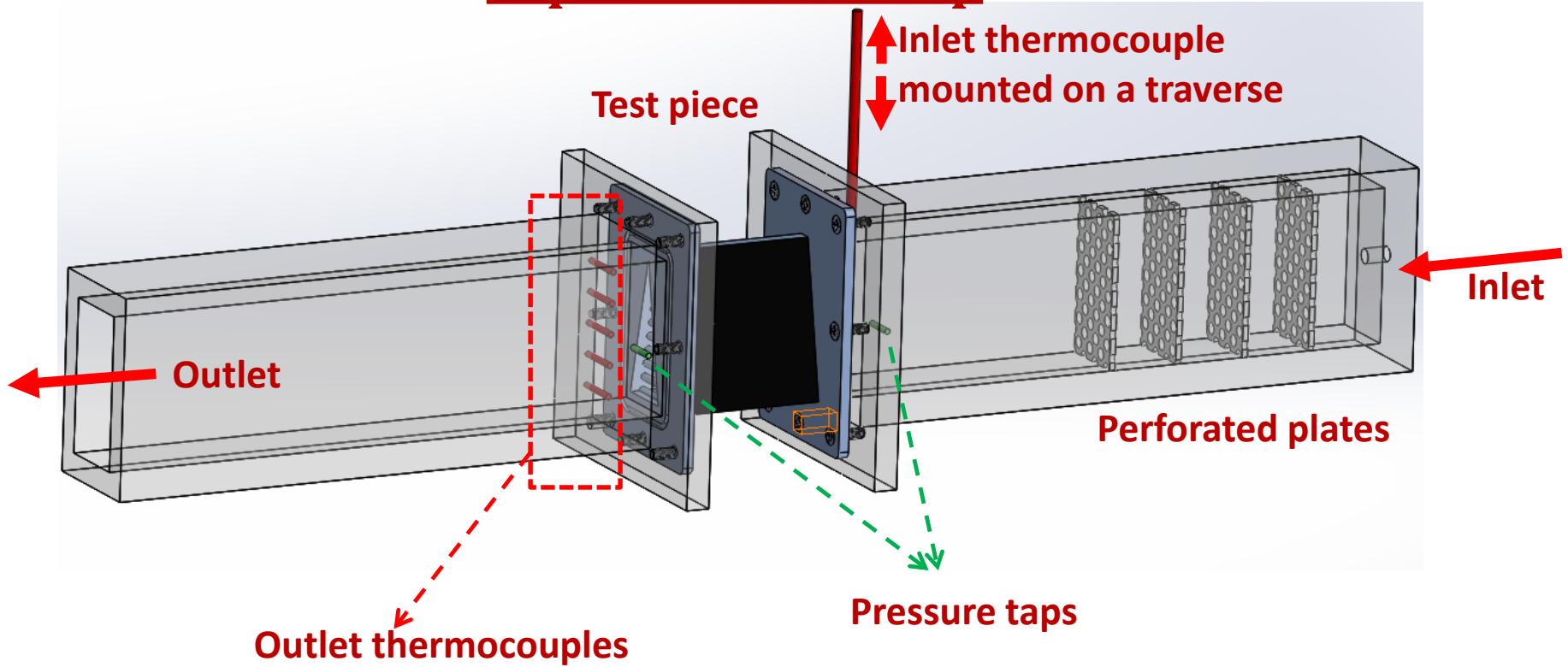
Can we decrease pressure drop without decreasing heat transfer?

- **Elliptical** pin fin decreases pressure loss with comparable thermal performance
- **Dimples** increase Nu while decreasing pressure loss
- **Centerbody** concentrates coolant at the wall
- **Tip clearance** decreases pressure drop and maintains Nu at the wall with the pins.
- **Triangular** pins increase heat transfer augmentation
- **Design concepts enabled by AM**



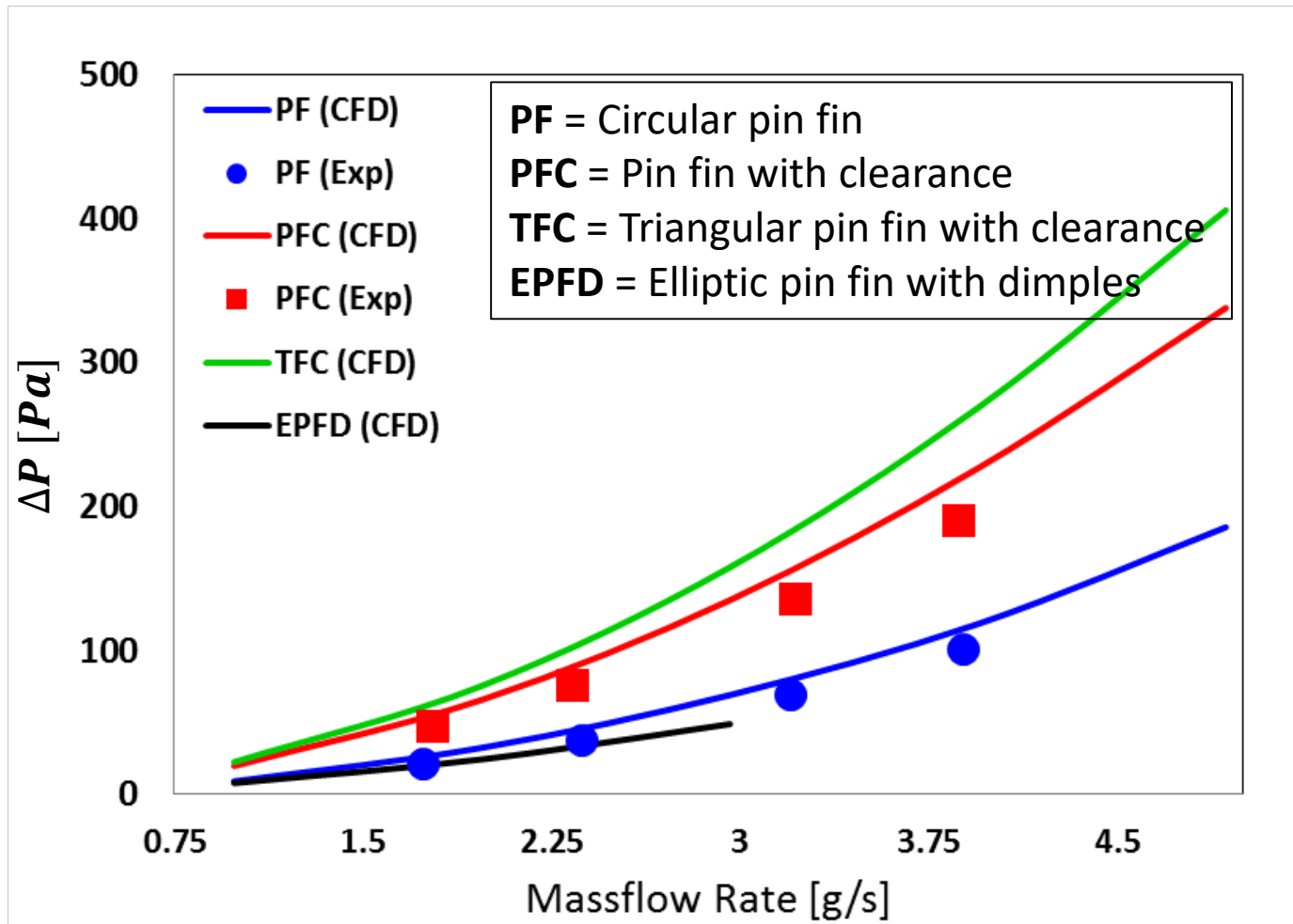


Experimental Setup





Preliminary Pressure Drop (CFD vs Exp)

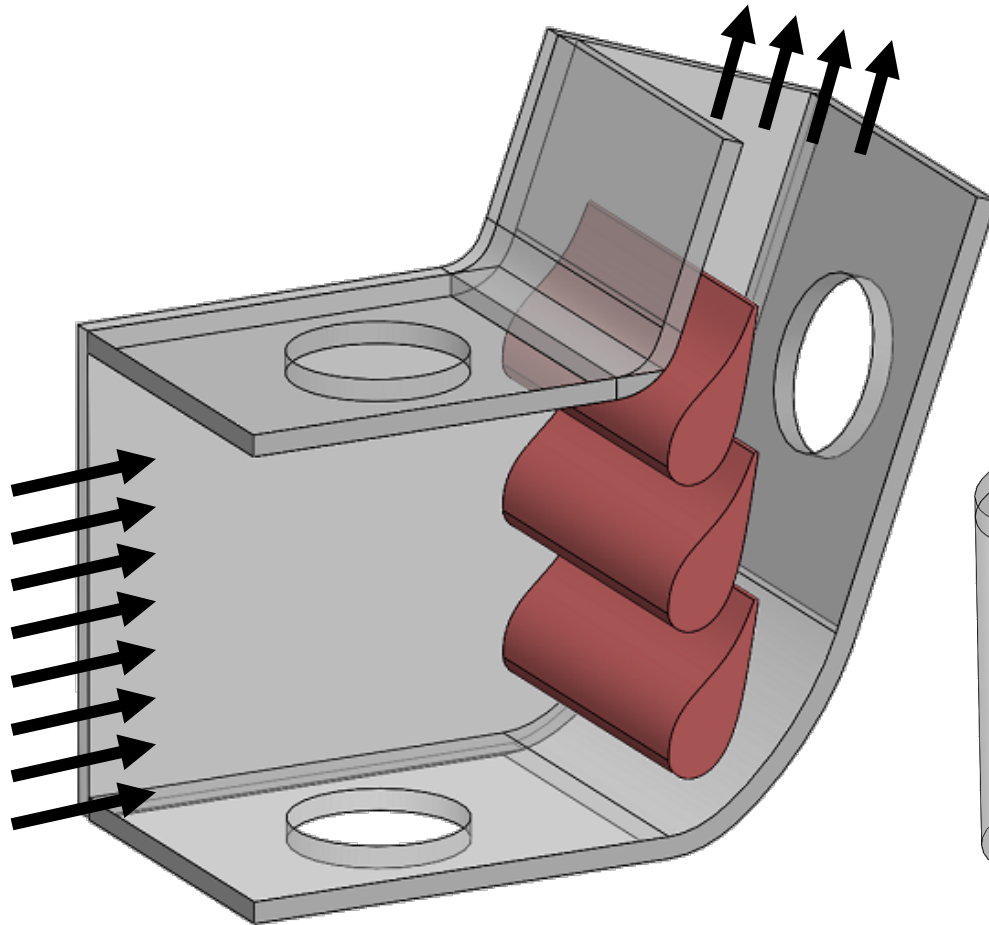




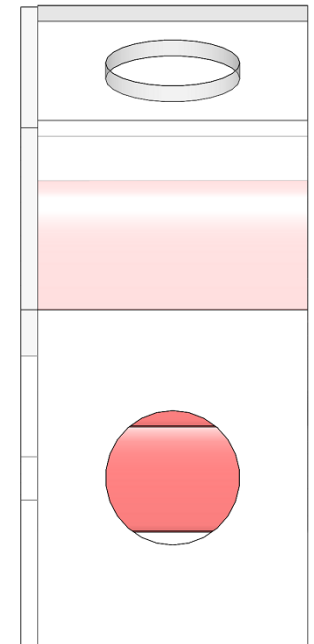
What's Next?



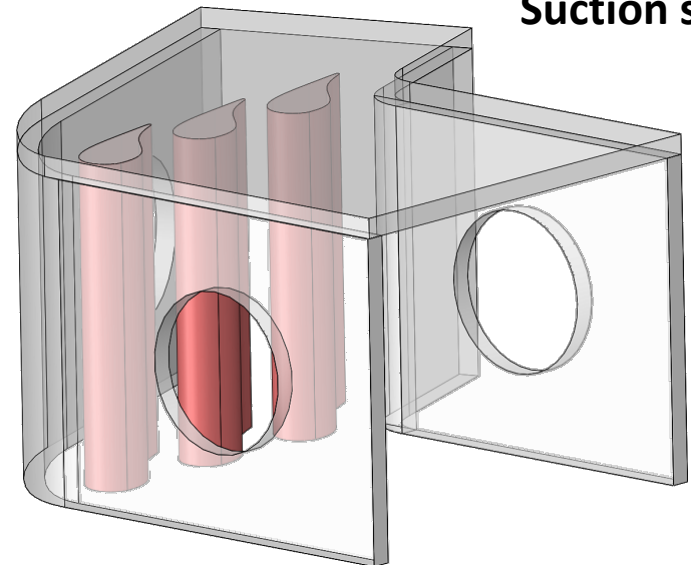
Transonic Cascade Design



Test section



Suction side

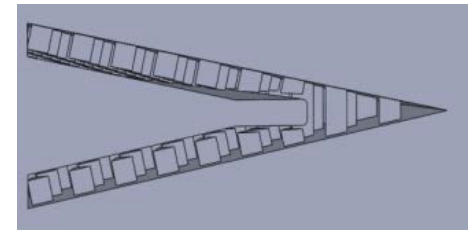
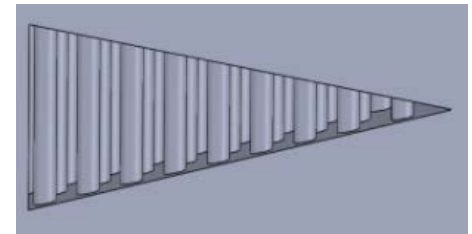
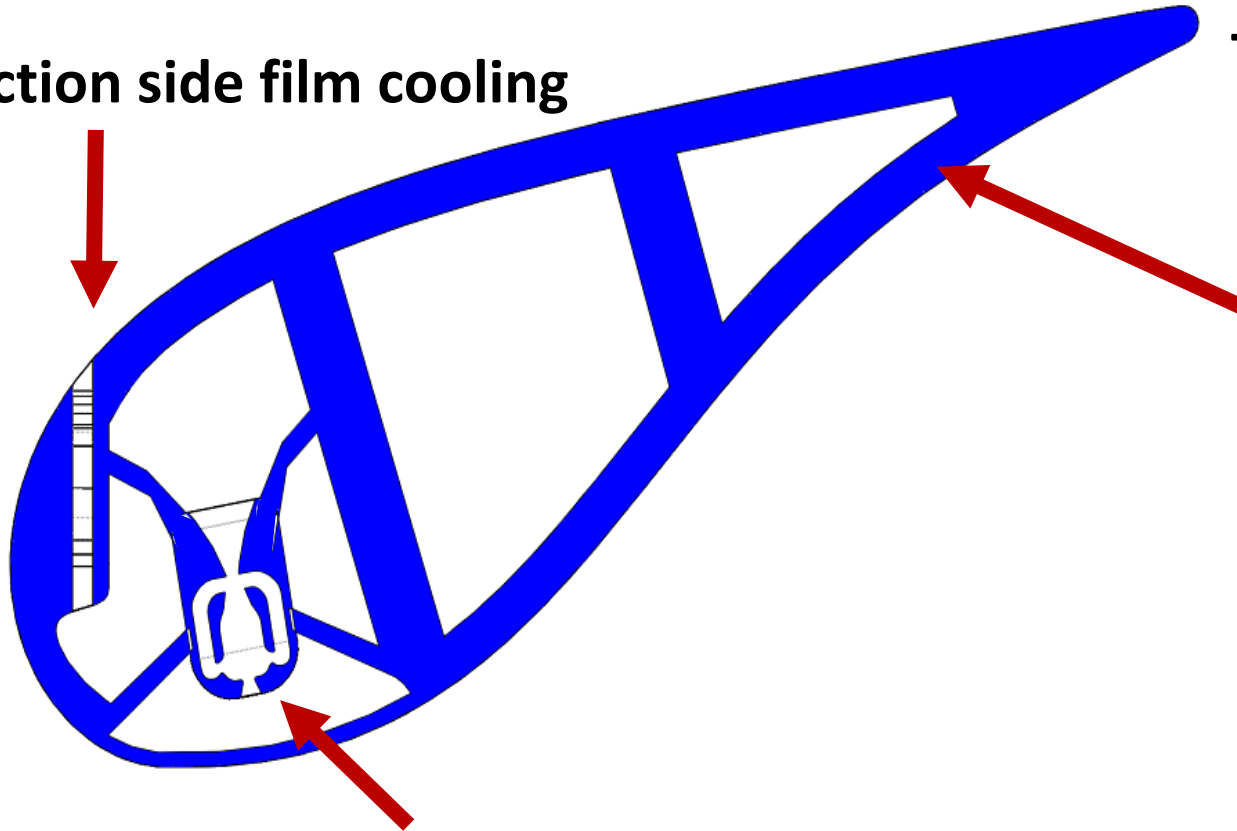


Leading edge and pressure side

Vane Integration (Trailing edge)

Suction side film cooling

Trailing edge design



Leading edge impingement



Questions?